NAVY DEPARTMENT

THE DAVID W. TAYLOR MODEL BASIN

AERODYNAMICS LABORATORY

WASHINGTON 7, D.C.

INTERACTION EFFECTS PRODUCED BY A SONIC JET EXHAUSTING FROM A CURVED TWO-DIMENSIONAL PLATE IN A SUPERSONIC STREAM

by

C. Carl Brindle and David W. Moxley, Jr.

Problem Assignment 1-34-14

April 1963

SYMBOLS

NF	normal force in pounds
C_N	coefficient of normal force
C_{N_I}	interaction force coefficient
C_p	coefficient of pressure $\left(\frac{p_r - p_\infty}{q}\right)$
p_∞	free-stream static pressure in pounds per square inch
p_r	pressure in pounds per square inch at orifice r
p_j	jet stagnation pressure in pounds per square inch
q	dynamic pressure in pounds per square inch ($\gamma p M^2/2$)
γ	ratio of specific heat at constant pressure to specific heat at constant volume
M	Mach number (V/a)
V	airspeed in inches per second
a	speed of sound in inches per second
R	Reynolds number ($\rho V \ell/\mu$)
ρ	mass density of air in slugs per cubic inch
ℓ	length of chord of model in inches
μ	absolute viscosity of air in pound-second per square inch
p_{t_2}/p_{t_1}	total pressure ratio across a shock wave
X	distance along the center line of the wind tunnel in inches
X_s	distance from leading edge of model to slot locations measured along the center line of the wind tunnel in inches
X_o	distance from leading edge of model to orifice locations measured along the center line of the wind tunnel in inches
Z	vertical distance in the wind tunnel in inches

TABLE OF CONTENTS

	Page
SYMBOLS	Preface
SUMMARY	1
INTRODUCTION	1
MODELS AND TEST APPARATUS	2
TEST CONDITIONS AND PROCEDURE	3
REDUCTION OF DATA AND ACCURACY	4
RESULTS	5
REFERENCES	8
BIBLIOGRAPHY	8
TABLES	
Table 1 - Coordinates for the Two-Dimensional Normal Jet Model	9
Table 2 - Test Program for Normal-Jet Investigation	10
Table 3 - Interaction Forces Produced by a Sonic Jet Exhausting Perpendicularly From a Curved Two-Dimensional Plate in a Supersonic Main Stream	11
Table 4 - Static Pressure Distribution Over Models With No Jet Exhausting	12
Table 5 - Static Pressure Distribution Over Model 1 at (M = 2.48) With Jet Exhausting	13
Table 6 - Static Pressure Distribution Over Model 2 at (M = 3.73) With Jet Exhausting	14
Table 7 - Static Pressure Distribution Over Model 3 at (M = 4.50) With Jet Exhausting	15
ILLUSTRATIONS	
Figure 1 - Photographs of the Curved Two-Dimensional Plate Models	16
Figure 2 - The Curved Two-Dimensional Plate Models	17-19
Figure 3 - The Normal Jet Model Mounting Strut With Air Passage	20
Figure 4 - Test Model Mounted in 9 1/2- by 9 1/2-Inch Wind Tunnel	21
Figure 5 - Exhausting Jet Penetration at a Main Stream Mach Number of 2.48	22-31
Figure 6 - Exhausting Jet Penetration at a Main Stream Mach Number of 3.73	32-41

TABLE OF CONTENTS (Concluded)

ILLUSTRATIONS (Concluded)

		Page
Figure 7 -	Exhausting Jet Penetration at a Main Stream Mach Number of 4.50	42-51
Figure 8 -	Schlieren Photographs of Models 1, 2, and 3 With No Jet Exhausting	52
Figure 9 -	Schlieren Photographs of Model 1 With Jet Exhausting. Main Stream Mach Number = 2.48	53-55
Figure 10 -	Schlieren Photographs of Model 2 With Jet Exhausting. Main Stream Mach Number = 3.73	56-58
Figure 11 -	Schlieren Photographs of Model 3 With Jet Exhausting. Main Stream Mach Number = 4.50	59-61
Figure 12 -	Pressure Distribution on the Upper and Lower Surfaces of Model 1 (M = 2.48)	62-69
Figure 13 -	Pressure Distribution on the Upper and Lower Surfaces of Model 2 (M = 3.73)	70-77
Figure 14 -	Pressure Distribution on the Upper and Lower Surfaces of Model 3 (M = 4.50)	78-86

Aero Report 1053

AERODYNAMICS LABORATORY
DAVID TAYLOR MODEL BASIN
UNITED STATES NAVY
WASHINGTON, D. C.

INTERACTION EFFECTS PRODUCED BY A SONIC JET EXHAUSTING FROM A CURVED TWO-DIMENSIONAL PLATE IN A SUPERSONIC STREAM

by

C. Carl Brindle and David W. Moxley, Jr.

SUMMARY

A wind-tunnel investigation was conducted to determine the effects of a sonic jet blowing perpendicularly from a curved two-dimensional plate. These tests were performed in the 9 1/2-Inch Supersonic Wind Tunnel of the Gas Dynamics Facility at Mach numbers of 2.48, 3.73, and 4.50. Experimental data are presented for (a) the interaction forces produced by the exhausting jet and the supersonic main stream and (b) the exhausting jet penetration into the supersonic main stream. Data were obtained for various slot locations and supply pressures.

INTRODUCTION

The use of jet reaction controls is a question of growing importance. It is essential to know how the jet penetration will occur in actual flight conditions, since such a jet could come in contact with stabilizing surfaces. In fact, even if the impinging jet happens to produce no adverse aerodynamic reactions when it encounters adjacent stabilizing surfaces, it could create serious problems of material protection if the jet was a hot or corroding stream.

It is not only necessary to know the forces which are generated on the body by reactions of the jet, but it is also necessary to know those forces created by the interaction of the exhausting jet and the supersonic main stream. Experience has already shown that such interaction forces can be of such magnitude that estimates of the forces produced by jet reaction controls on a supersonic vehicle will be substantially in error if the additional interaction forces are not properly accounted for.

In view of this fact, the Bureau of Naval Weapons requested, in Reference 1, that a wind-tunnel investigation be conducted to contribute to the current knowledge on the use of jet reaction controls near the nose of a supersonic vehicle in relatively dense atmosphere. These tests were conducted in the 9 1/2-Inch Supersonic Wind Tunnel of the Gas Dynamics Division to investigate the interaction effects produced by a sonic jet exhausting perpendicularly from a curved two-dimensional plate in a supersonic stream. These interaction effects were investigated at Mach numbers of 2.48, 3.73, and 4.50, with various jet slot locations and jet supply pressures.

MODELS AND TEST APPARATUS

The curved two-dimensional plate models used in this test are shown in Figure 1. Each model was constructed to be used at a specific Mach number. Model 1 was used at Mach number 2.48, model 2 at Mach number 3.73, and model 3 at Mach number 4.50. The model coordinates are shown in Table 1.

Each model was constructed so that there were three possible jet slot locations for each model (Figure 2). Since only one jet slot location was used at any one time, there was provided for each location a nozzle plate and a blank cover plate. Although the width of each slot was adjustable, the width for this test was maintained at 0.01 inch. The jet slot had a sonic nozzle throat.

On each model, seven 0.049-inch-diameter static pressure orifices were installed on the center line - four on the top surface and three on the bottom surface. Exact pressure orifice locations are shown in Figure 2. The plenum chamber of each model was also instrumented with a pressure orifice.

A special strut, provided with an air passage, was built to mount the models in the 9 1/2- by 9 1/2-inch wind tunnel. A sketch of this strut is shown in Figure 3, and a photograph of the model mounted in the wind tunnel is shown in Figure 4.

Filtered pressurized house air, controlled by a pressure-regulating valve, was directed through a passage in the mounting strut to the plenum chamber of each model. The plenum chamber pressure was measured with a 200-psi pressure gage.

Model surface pressures and survey rake pressures above the model were obtained with a solenoid-driven Scanivalve pressure switch and a Statham pressure transducer. A 5-psia transducer was installed at M = 3.73 and 4.50 and a 10-psia transducer was installed at M = 2.48. High-speed data readout from the Scanivalve pressure transducer was obtained with a Beckman 210, which senses, measures, digitizes, and records on magnetic tape the test data for direct entry into the UNIVAC computer.

The supersonic flow was obtained by using fixed converging-diverging laval-type nozzle blocks.

TEST CONDITIONS AND PROCEDURE

The tests were performed in the 9 1/2-Inch Supersonic Wind Tunnel at Mach numbers of 2.48, 3.73, and 4.50. The dew point of the testing air did not exceed -15°F, but no attempt was made to dry the compressed air that was blown through the sonic jet nozzle. The atmospheric supply pressure (p_t) for the air stream varied from 14.409 to 14.936 psi. The average Reynolds numbers, based on the chord length of the models, were as follows:

M	R x 10^{-6}
2.48	1.11
3.73	0.36
4.50	0.26

The wind-tunnel test program is shown in Table 2. The jet slot locations designated A, B, and C are shown on Figure 2. For each test run, surface pressure data on the model were obtained, and a total pressure survey above the model was made with a seven-tube total-pressure rake at various X and Z locations, as noted on the data plots. In addition to these data, a schlieren photograph was taken to study the interaction effects visually.

REDUCTION OF DATA AND ACCURACY

The interaction force produced by a sonic jet exhausting into a supersonic main stream is defined as the normal force coefficient calculated from pressure measurements on the model with the jet blowing minus the normal force coefficient calculated from pressure measurements on the model without the jet.

The normal force coefficient, C_N, of the curved two-dimensional plate model was determined by the mechanical integration of the static pressure over the model. The static pressure coefficients for the upper and lower surfaces were plotted perpendicular to the chord of the model; for the upper surface, $-C_p$ was plotted. The area under the curve will yield the normal force coefficient for the model; i.e.,

$$C_N = \frac{1}{l} \int_0^l C_p \, dl$$

The total normal force coefficient is equal to the C_N of the upper surface plus the C_N of the lower surface. A positive C_N indicates a resultant force in the upward direction and a negative C_N indicates a resultant force in the downward direction.

The spanwise distance assumed for the integration was unity and included the pressure orifices, which were located along the center line of the model; i.e., the area of integration did not include the entire region of jet interaction.

The jet penetration into the supersonic main stream in terms of the total-pressure survey above the model was represented by $\Delta \frac{p_{t_2}}{p_{t_1}}$, where $\Delta \frac{p_{t_2}}{p_{t_1}}$ is defined as p_{t_2}/p_{t_1} of the total pressure survey minus p_{t_2}/p_{t_1} of the free stream. The following free-stream total-pressure ratios were used.

M	$\frac{p_{t_2}}{p_{t_1}}$
2.48	0.5071
3.73	0.1746
4.50	0.0917

The following data are believed to be repeatable within the defined limits:

Data	Limits
C_p	±0.01
p_{t_2}/p_{t_1}	±0.005

The following is believed to be the Mach number variation in that part of the test section occupied by the model:

Mach Number	Variation
2.48	±0.02
3.73	±0.04
4.50	±0.10

The accuracy of the computed interaction forces is discussed in the following section, since it is based on assumptions set forth there.

RESULTS

The interaction effects of a sonic jet exhausting perpendicularly from a curved two-dimensional plate in a supersonic main stream are presented in Table 3 and Figures 5, 6, and 7. Schlieren photographs taken to study the interaction effects visually are shown in Figures 8 through 11.

Table 3 presents the interaction forces, in coefficient form, at main stream Mach numbers of 2.48, 3.73, and 4.50 for various jet slot locations and jet supply pressures. These interaction forces were determined by the mechanical integration of static pressure distribution curves shown in Figures 12, 13, and 14. These curves were plotted from data presented in Tables 4, 5, 6, and 7.

Figures 5, 6, and 7 present the penetration of the exhausting jet into the supersonic main stream in terms of the change in total pressure ratio from free-stream conditions to test conditions. A positive change in total pressure ratio represents a region of compression and a negative change in total pressure ratio represents a region of expansion.

Because of technical difficulties in the construction of the models, the number of pressure orifices on the models was limited. Of course, this scarcity of data points affects the accuracy of the interaction forces in Table 3. The accuracy of the static pressure distribution over that portion of the model lacking pressure orifices depends on the validity of the assumptions that were used to determine the static pressure distribution. Since most of the assumptions were based on accepted principles or experimental results, the accuracy of the interaction forces is believed to be good enough so that general trends will be evident.

The important considerations used in determining the static pressure distribution over the models are the following:

1. Only those effects that will take place in a perfect nonviscous fluid are considered. Reference 2 indicates that the effect of the boundary layer on the interaction field is negligible except for perhaps immediately upstream of the jet, where the boundary layer separates. Even in this region, it is found that the pressure which is capable of being sustained in the boundary layer is relatively weak. According to References 3 and 4, the state of the boundary layer does not matter in the region where it separates. Although the laminar boundary-layer separation covers a larger area of the model than does the turbulent separation, the pressure rise at separation is greater for a turbulent boundary layer than for a laminar one.

2. The schlieren photographs in Figures 8, 9, 10, and 11 show that for a specific model, the shocks standing in front of each jet sheet are similar for every jet slot location and jet supply pressure.

3. In the region before the shock standing in front of the jet sheet, the pressure distribution is displaced by a constant positive pressure difference from the pressure distribution of the initial test conditions of no jet. This constant positive pressure difference is due to the negative change in angle of attack of the model, which is induced by the force of the jet. From Figures 12, 13, and 14 it can be seen that the jet slot locations closer to the leading edge produce the greatest change in angle of attack, since the moment arms are the greatest at these locations.

4. In the region between the shock standing in front of the jet sheet to the first orifice after the jet slot, a linear expansion is assumed to

take place. This assumption was made, since there was no evidence as to the exact manner of expansion. Although this assumption may contribute to the inaccuracy of the absolute results, it should not affect the qualitative results.

5. In the region from the first orifice after the jet slot to the base of the model, initially overexpansion takes place because of the jet pump action. After the overexpansion, there is a return to a pressure distribution which is similar to the pressure distribution obtained under the initial test condition of no jet.

In describing the flow phenomena, the jet can be imagined to be frozen into a rigid sheet. This obstruction would cause a detached shock upstream of the sheet. In the actual case, horizontal momentum is imparted to the jet sheet which bends rapidly toward the direction of the free-stream flow.

Upstream of the jet, the impingement of the detached shock wave on the boundary layer creates an adverse pressure gradient in the boundary layer, which tends to separate the flow from the surface of the body, whether it is laminar or turbulent.

After the jet, an overexpansion takes place, with a gradual return to normal no-jet conditions.

Aerodynamics Laboratory
David Taylor Model Basin
Washington, D. C.
April 1963

REFERENCES

1. BUAER ltr Aer-AD-311/537 of 2 Sep 1959
2. Morkovin, Mark V., C. A. Pierce, Jr., and C. E. Craven. Interaction of a Side Jet With a Supersonic Main Stream. Ann Arbor, Sep 1952. 34 p. incl. illus. (Michigan Univ. Engineering Research Bulletin 35)
3. Romeo, David J. and James R. Sterrett. Aerodynamic Interaction Effects Ahead of a Sonic Jet Exhausting Perpendicularly From a Flat Plate Into a Mach Number 6 Free Stream. Wash., Apr 1961. 26 p. incl. illus. (National Aeronautics & Space Administration. TN D-743)
4. Vinson, P. W., James L. Amick, and Hans Peter Liepman. Interaction Effects Produced by Jet Exhausting Laterally Near Base of Ogive-Cylinder Model in Supersonic Main Stream. Wash., Feb 1959. 37 p. incl. illus. (National Aeronautics & Space Administration. Memo 12-5-58W)

BIBLIOGRAPHY

1. Ferrari, Carlo. Interference Between a Jet Issuing Laterally From a Body and the Enveloping Supersonic Stream. Silver Spring, Md., Apr 1959. 112 p. incl. illus. (Johns Hopkins Univ. Applied Physics Lab. Bumblebee Rpt 286. Contract NOrd 7386)
2. Hayman, Lovick O., Jr. and Russell W. McDearmon. Jet Effects on Cylindrical Afterbodies Housing Sonic and Supersonic Nozzles Which Exhaust Against a Supersonic Stream at Angles of Attack From 90° to 180°. Wash., Mar 1962. 49 p. incl. illus. (National Aeronautics & Space Administration. TN D-1016)
3. Janos, Joseph J. Loads Induced on a Flat-Plate Wing by an Air Jet Exhausting Perpendicularly Through the Wing and Normal to a Free-Stream Flow of Mach Number 2.0. Wash., Mar 1961. 21 p. incl. illus. (National Aeronautics & Space Administration. TN D-649)

Table 1

Coordinates for the Two-Dimensional Normal Jet Model

Model 1 (M = 2.48)			
x	y	x	y
0	0	2.312	0.774
0.250	0.104	2.842	0.887
0.503	0.204	3.377	0.974
0.756	0.299	3.917	1.028
1.012	0.391	4.459	1.045
1.268	0.477	4.999	1.015
1.787	0.636		

Model 2 (M = 3.73)			
x	y	x	y
0	0	2.256	0.996
0.305	0.171	2.599	1.084
0.615	0.333	2.946	1.153
0.935	0.486	3.296	1.198
1.254	0.629	3.646	1.213
1.583	0.772	3.994	1.183
1.917	0.891		

Model 3 (M = 4.50)			
x	y	x	y
0	0	2.917	1.337
0.417	0.242	3.333	1.454
0.833	0.471	3.750	1.542
1.250	0.679	4.167	1.617
1.667	0.871	4.583	1.646
2.083	1.046	5.000	1.642
2.500	1.204		

Table 2

Test Program for Normal-Jet Investigation

Series	Model	Slot Position	Supply Pressure in psi	Mach Number
1	1	None	None	2.48
2	1	A	75, 85, 95	2.48
3		B		
4		C		
5	2	None	None	3.73
6	2	A	75, 85, 95	3.73
7		B		
8		C		
9	3	None	None	4.50
10	3	A	25, 35, 45	4.50
11		B		
12		C		

All data were taken at an angle of attack of 0°

Table 3

Interaction Forces Produced by a Sonic Jet Exhausting Perpendicularly From a Curved Two-Dimensional Plate in a Supersonic Main Stream

M	$(C_N)_{p_j=0}$	p_j, psig	$\frac{p_j}{p_\infty}$	Slot Location	C_{N_I}
2.48	-0.2868	95	126	A	-0.3424
			124	B	-0.3211
			126	C	-0.2661
		85	114	A	-0.3424
			112	B	-0.2223
			114	C	-0.2164
		75	103	A	-0.3992
			101	B	-0.2223
			103	C	-0.2661
3.73	0.1631	95	784	A	-0.4118
			788	B	-0.4998
			789	C	-0.3383
		85	712	A	-0.4118
			717	B	-0.4288
			717	C	-0.2818
		75	641	A	-0.4118
			645	B	-0.3852
			645	C	-0.2778
4.50	0.8592	45	1174	A	-0.5020
			1153	B	-0.4096
			1171	C	-0.1124
		35	977	A	-0.5020
			960	B	-0.3650
			975	C	-0.0930
		25	781	A	-0.6008
			768	B	-0.3198
			779	C	-0.0582

Table 4

Static Pressure Distribution Over the Models
With No Jet Exhausting

Orifice Number	C_p
a. Model 1 (M = 2.48)	
1	0.57
2	0.47
3	0.25
4	0.03
5	0.00
6	0.00
7	0.10
b. Model 2 (M = 3.73)	
1	0.64
2	0.58
3	0.55
4	0.04
5	0.75
6	0.35
7	1.12
c. Model 3 (M = 4.50)	
1	0.63
2	0.97
3	0.97
4	0.65
5	1.08
6	0.50
7	2.55

Table 5

Static Pressure Distribution Over Model 1 at M = 2.48
With Jet Exhausting

Slot	p_j/p_∞	Orifice	C_p	Slot	p_j/p_∞	Orifice	C_p
A	126	1	1.61	C	114	1	0.62
		2	0.07			2	0.51
		3	0.23			3	0.89
		4	0.08			4	-0.03
		5	-0 02			5	0.00
		6	-0.03			6	-0.01
		7	0.00			7	0.10
B	124	1	0.71	A	103	1	1.85
		2	1.27			2	0.08
		3	0.19			3	0.26
		4	-0.03			4	0.08
		5	-0.02			5	-0.01
		6	-0.02			6	-0.01
		7	0.06			7	0.00
C	126	1	0.61	B	101	1	0.69
		2	0.54			2	1.14
		3	0.84			3	0.22
		4	0.00			4	-0.02
		5	0.00			5	-0.02
		6	0.00			6	-0.02
		7	0.02			7	0.17
A	114	1	1.62	C	103	1	0.62
		2	0.08			2	0.51
		3	0.24			3	0.85
		4	0.07			4	-0.02
		5	-0.02			5	0.00
		6	-0.02			6	-0.01
		7	0.00			7	0.10
B	112	1	0.71				
		2	1.22				
		3	0.21				
		4	-0.02				
		5	-0.01				
		6	-0.02				
		7	0.06				

Table 6

Static Pressure Distribution Over Model 2 at M = 3.73
With Jet Exhausting

Slot	p_j/p_∞	Orifice	C_p	Slot	p_j/p_∞	Orifice	C_p
A	784	1	1.71	C	717	1	0.67
		2	0.40			2	0.86
		3	0.46			3	1.10
		4	0.10			4	0.07
		5	0.68			5	0.73
		6	0.33			6	0.33
		7	1.11			7	1.10
B	788	1	1.08	A	641	1	1.71
		2	1.60			2	0.41
		3	0.52			3	0.47
		4	0.04			4	0.10
		5	0.77			5	0.68
		6	0.35			6	0.33
		7	1.17			7	1.11
C	789	1	0.68	B	645	1	1.00
		2	0.92			2	1.38
		3	1.12			3	0.52
		4	0.07			4	0.05
		5	0.74			5	0.77
		6	0.33			6	0.36
		7	1.10			7	1.17
A	712	1	1.71	C	645	1	0.65
		2	0.40			2	0.82
		3	0.46			3	1.07
		4	0.10			4	0.07
		5	0.68			5	0.73
		6	0.33			6	0.33
		7	1.11			7	1.10
B	717	1	1.06				
		2	1.43				
		3	0.52				
		4	0.04				
		5	0.77				
		6	0.35				
		7	1.17				

Table 7

Static Pressure Distribution Over Model 3 at M = 4.50

With Jet Exhausting

Slot	p_j/p_∞	Orifice	C_p	Slot	p_j/p_∞	Orifice	C_p
A	1174	1	1.87	C	975	1	0.64
		2	0.74			2	1.10
		3	0.89			3	1.39
		4	0.64			4	0.70
		5	0.92			5	1.24
		6	0.52			6	0.45
		7	2.31			7	2.57
B	1153	1	1.11	A	781	1	2.20
		2	1.87			2	0.75
		3	0.90			3	0.92
		4	0.63			4	0.66
		5	1.02			5	0.92
		6	0.46			6	0.52
		7	2.48			7	2.31
C	1171	1	0.64	B	768	1	0.99
		2	1.18			2	1.58
		3	1.43			3	0.94
		4	0.69			4	0.65
		5	1.24			5	1.03
		6	0.45			6	0.48
		7	2.56			7	2.41
A	977	1	1.83	C	779	1	0.65
		2	0.74			2	1.16
		3	0.90			3	1.27
		4	0.64			4	0.70
		5	0.92			5	1.24
		6	0.52			6	0.48
		7	2.31			7	2.57
B	960	1	1.03				
		2	1.72				
		3	0.91				
		4	0.64				
		5	1.02				
		6	0.47				
		7	2.40				

P-913 (a) Model 1

P-914 (b) Model 2

P-915 (c) Model 3

Figure 1 - Photographs of the Curved Two-Dimensional Plate Models

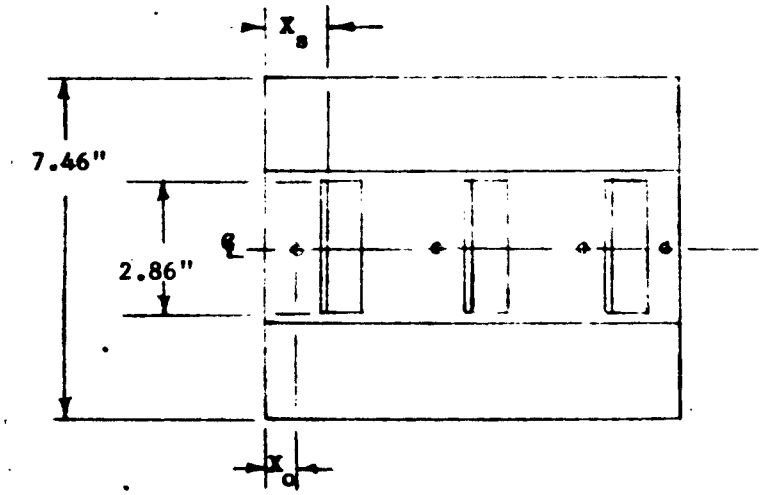

Note: Sketches not to scale

Slot Locations

Slot	X_s in in.
A	1.02
B	2.01
C	3.50

Orifice Locations

Upper		Lower	
Orifice	X_o in in.	Orifice	X_o in in.
1	0.81	5	1.25
2	1.88	6	2.51
3	3.35	7	3.75
4	4.48		

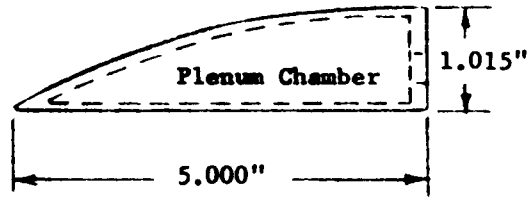

FIGURE 2a

Figure 2 - Sketches of Curved Two-Dimensional Plate Models

(a) Model 1

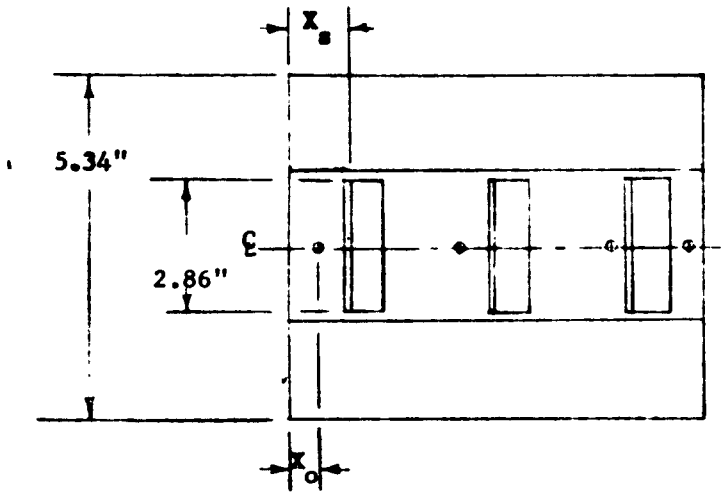

Note: Sketches are not to scale

Slot Locations

Slot	X_s in in.
A	1.00
B	2.02
C	3.02

Orifice Locations

Upper		Lower	
Orifice	X_o in in.	Orifice	X_o in in.
1	0.76	5	0.93
2	1.80	6	2.61
3	2.88	7	3.70
4	3.90		

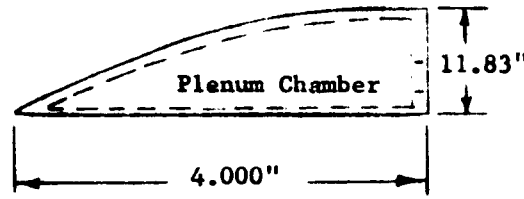

Figure 2 (Continued)

(b) Model 2

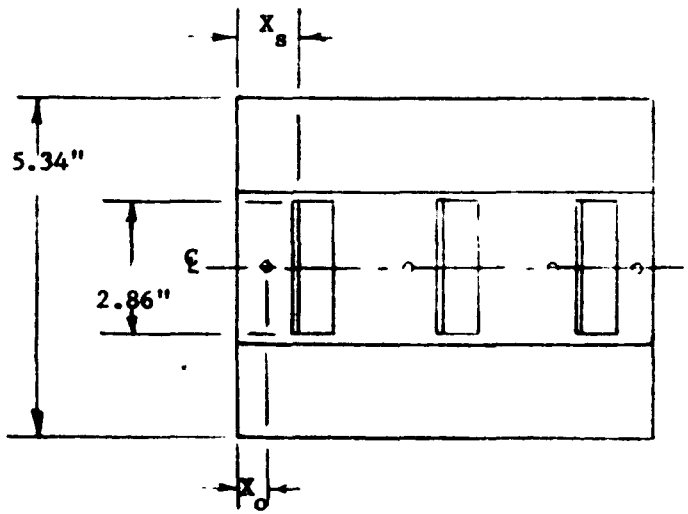

Note: Sketches are not to scale

Slot Locations

Slot	X_s in in.
A	1.02
B	2.02
C	3.50

Orifice Locations

Upper		Lower	
Orifice	X_o in in.	Orifice	X_o in in.
1	0.86	5	1.25
2	1.78	6	2.50
3	3.20	7	3.76
4	4.42		

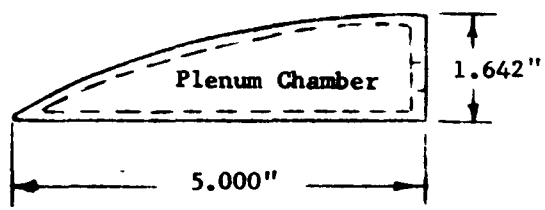

Figure 2 (Concluded)
(c) Model 3

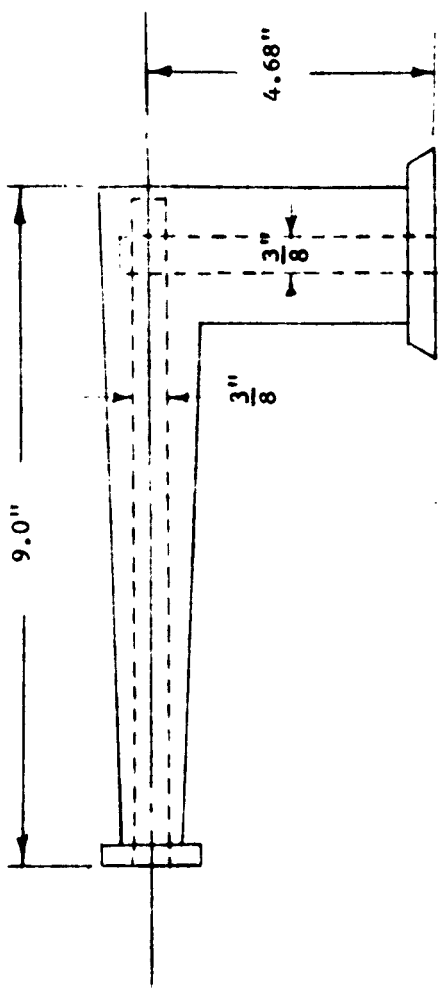

Figure 3 - The Normal Jet Model Mounting Strut With Air Passage

Figure 4 - Test Model Mounted in 9 1/2- by 9 1/2-Inch Wind Tunnel

Note: H P indicates that an undetermined high pressure reading above the range of the pressure transducer (0 - 10 psi) was obtained at the surveyed point.

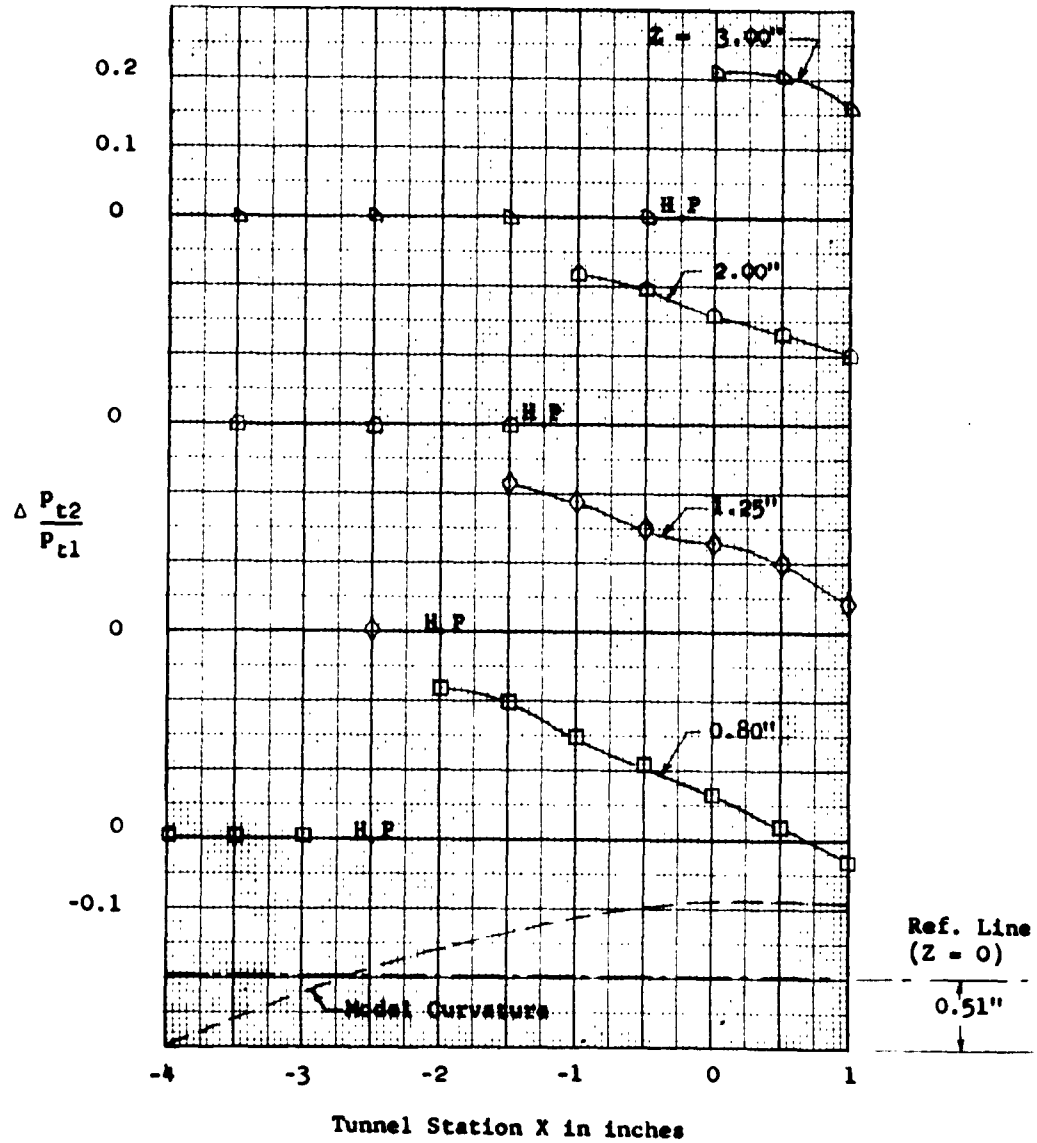

Figure 5 - Exhausting Jet Penetration at a Main Stream Mach Number of 2.48
(a) $p_j/p_\infty = 0$

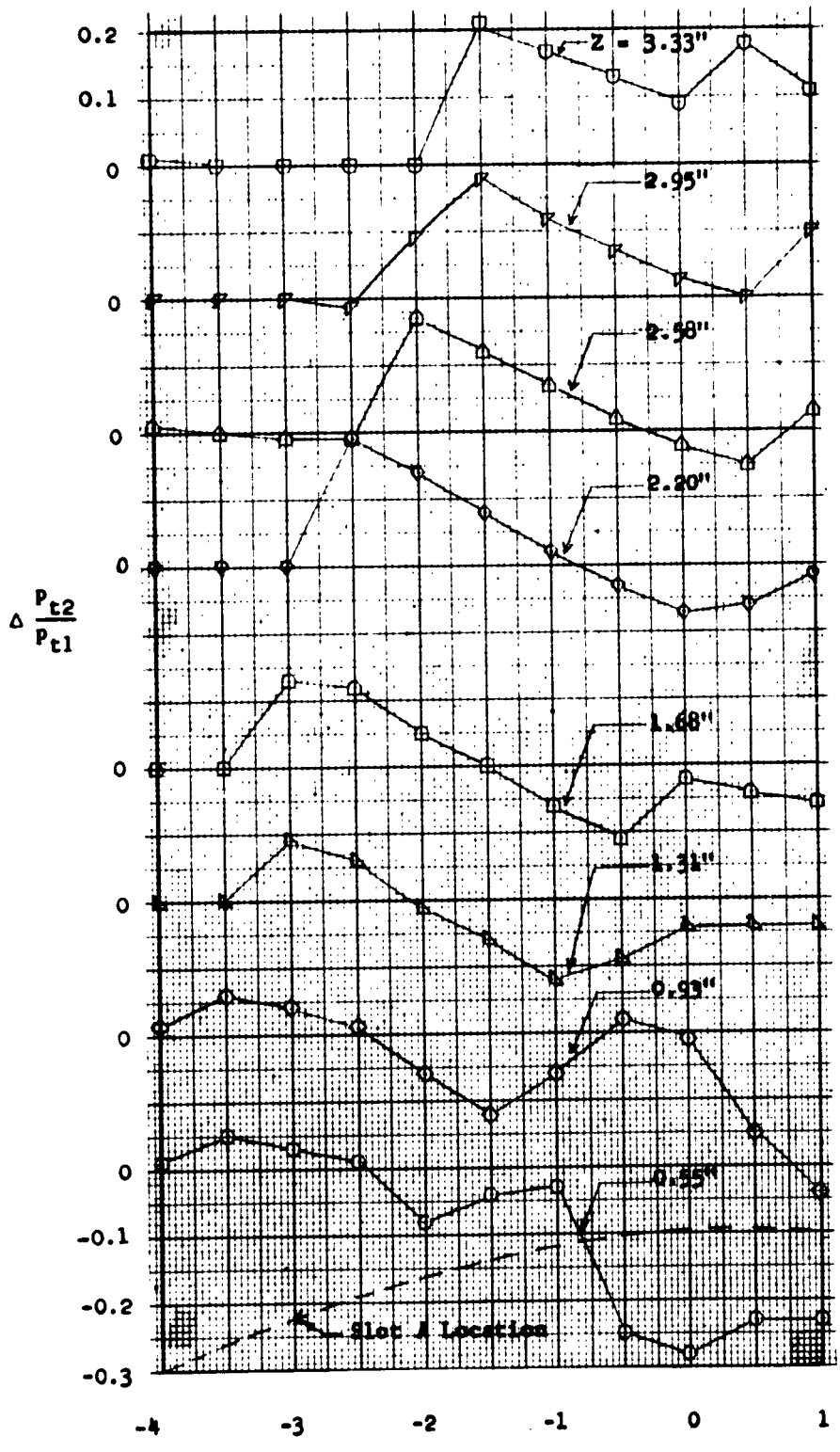

$\Delta \frac{P_{t2}}{P_{t1}}$

Figure 5 (Continued)
(b) p_j/p_∞ = 126; Slot A

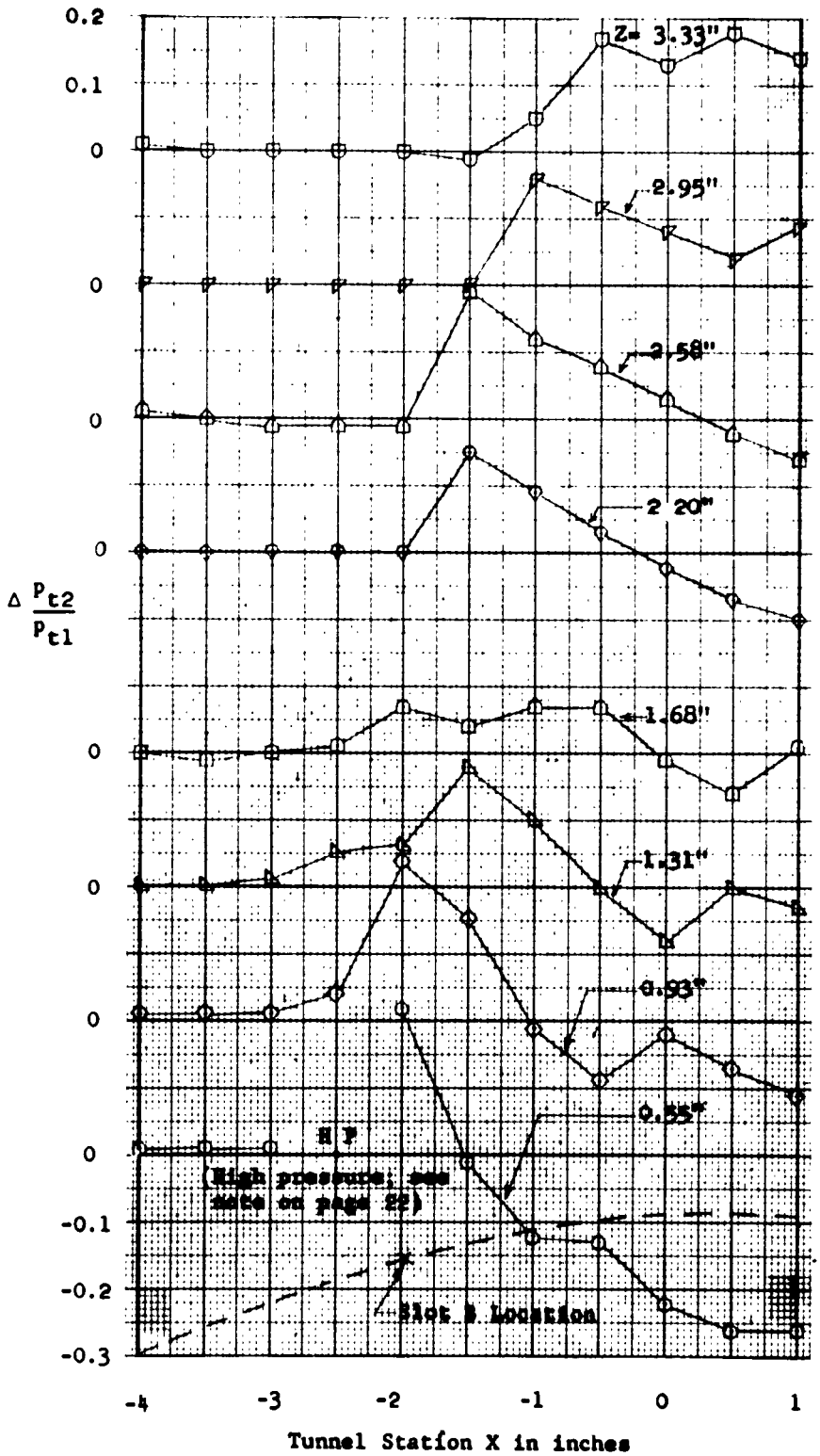

Figure 5 (Continued)

(c) p_j/p_∞ = 124; Slot B

See note on page 22 for explanation of H P

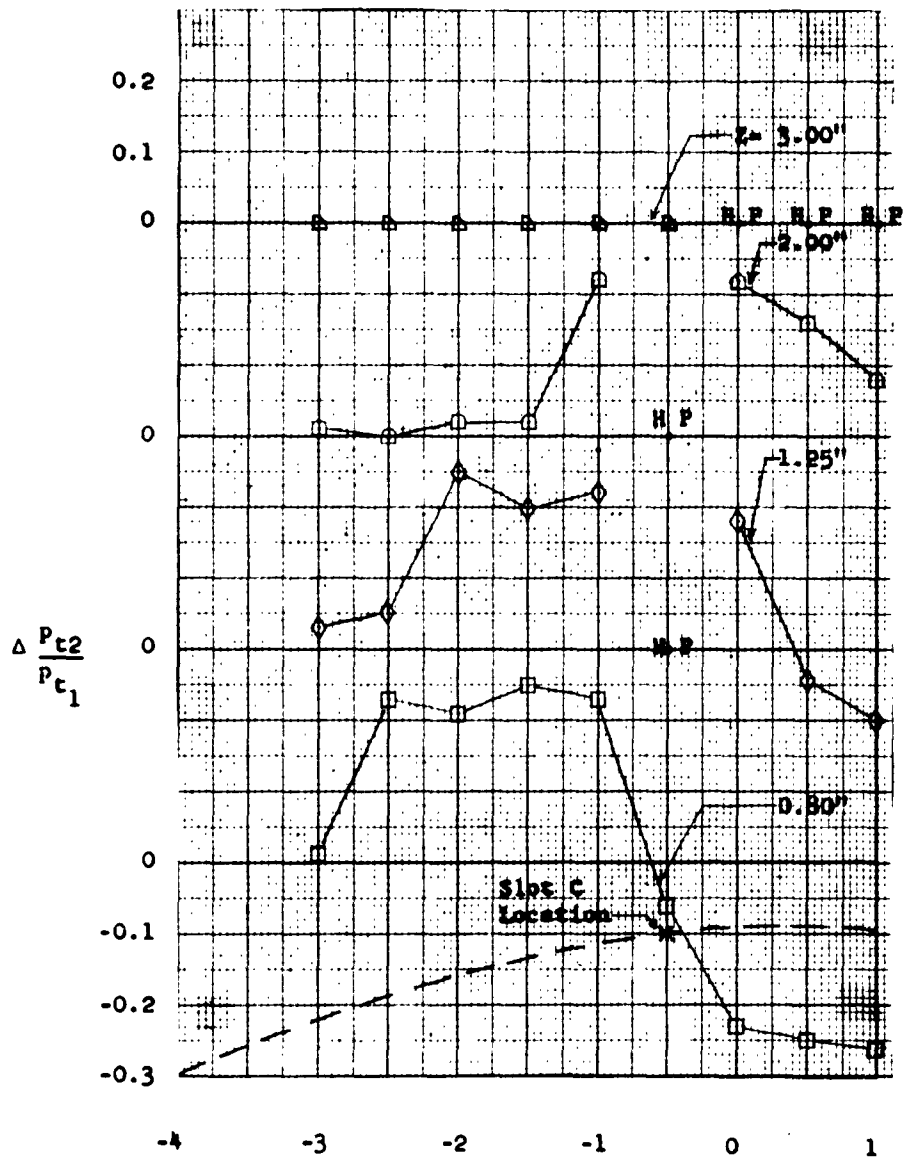

Figure 5 (Continued)
(d) p_j/p_∞ = 126; Slot C

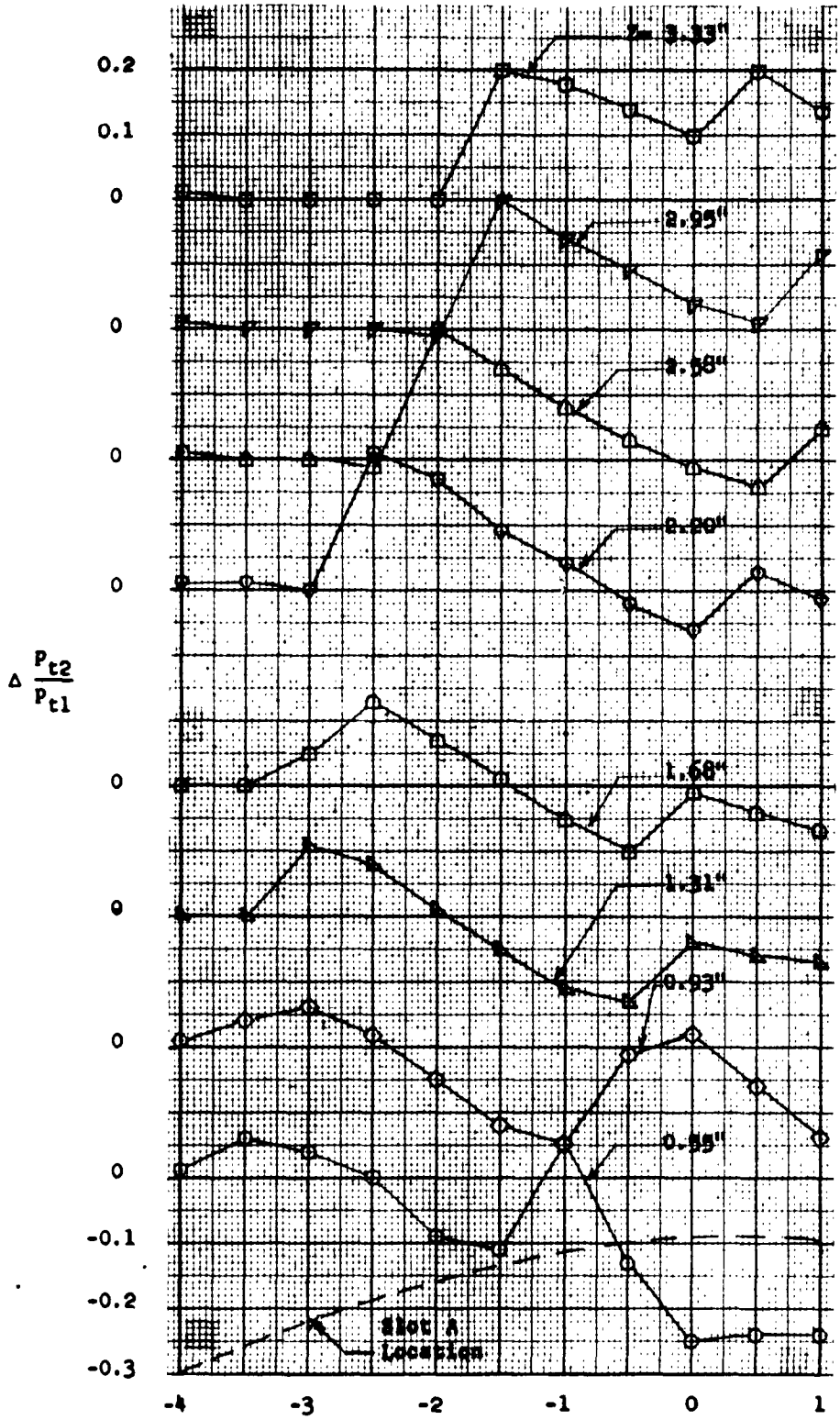

Figure 5 (Continued)

(e) p_j/p_∞ = 114; Slot A

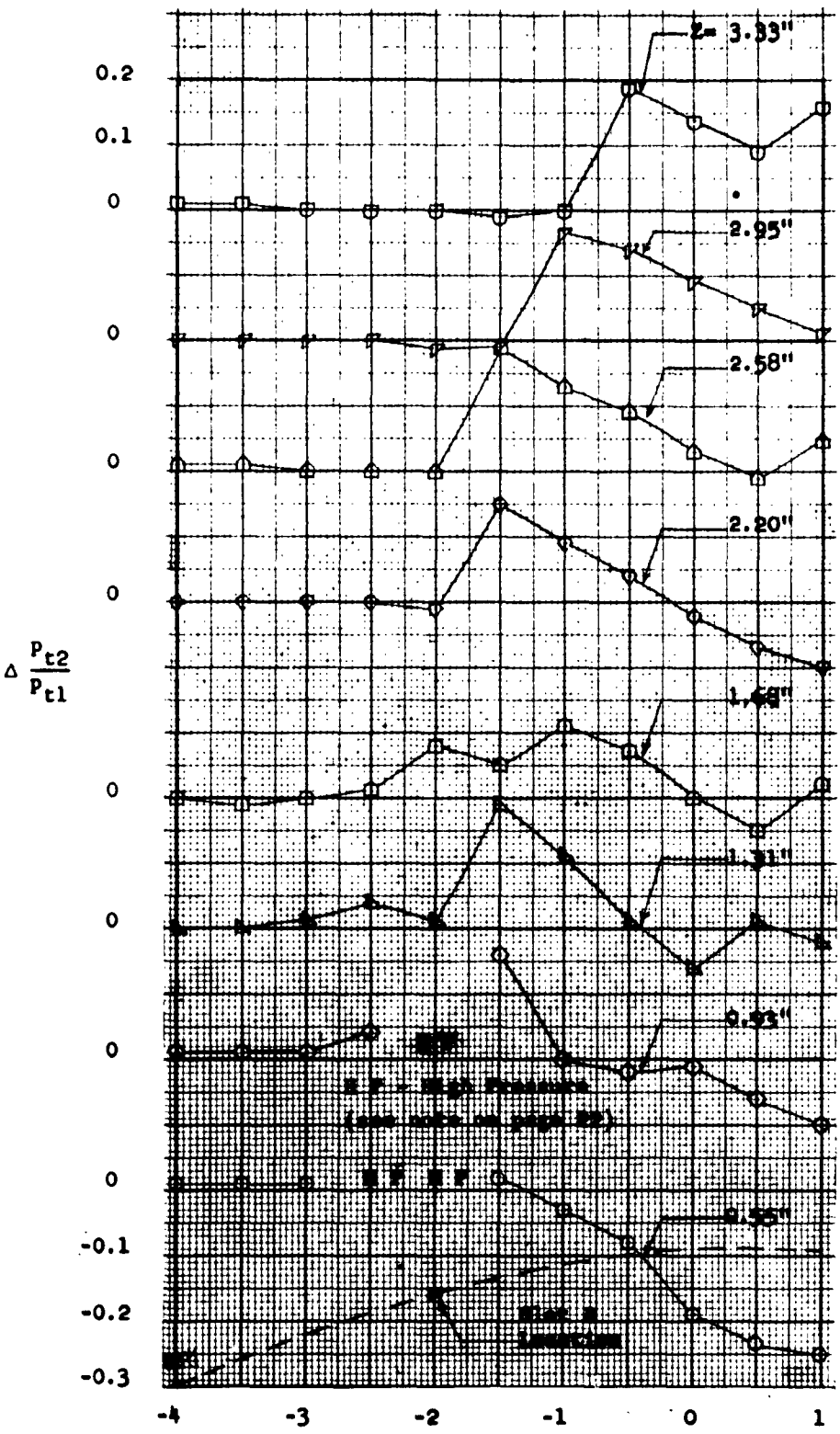

Figure 5 (Continued)

(f) p_j/p_∞ = 112; Slot B

H P - High Pressure (see note on page 22)

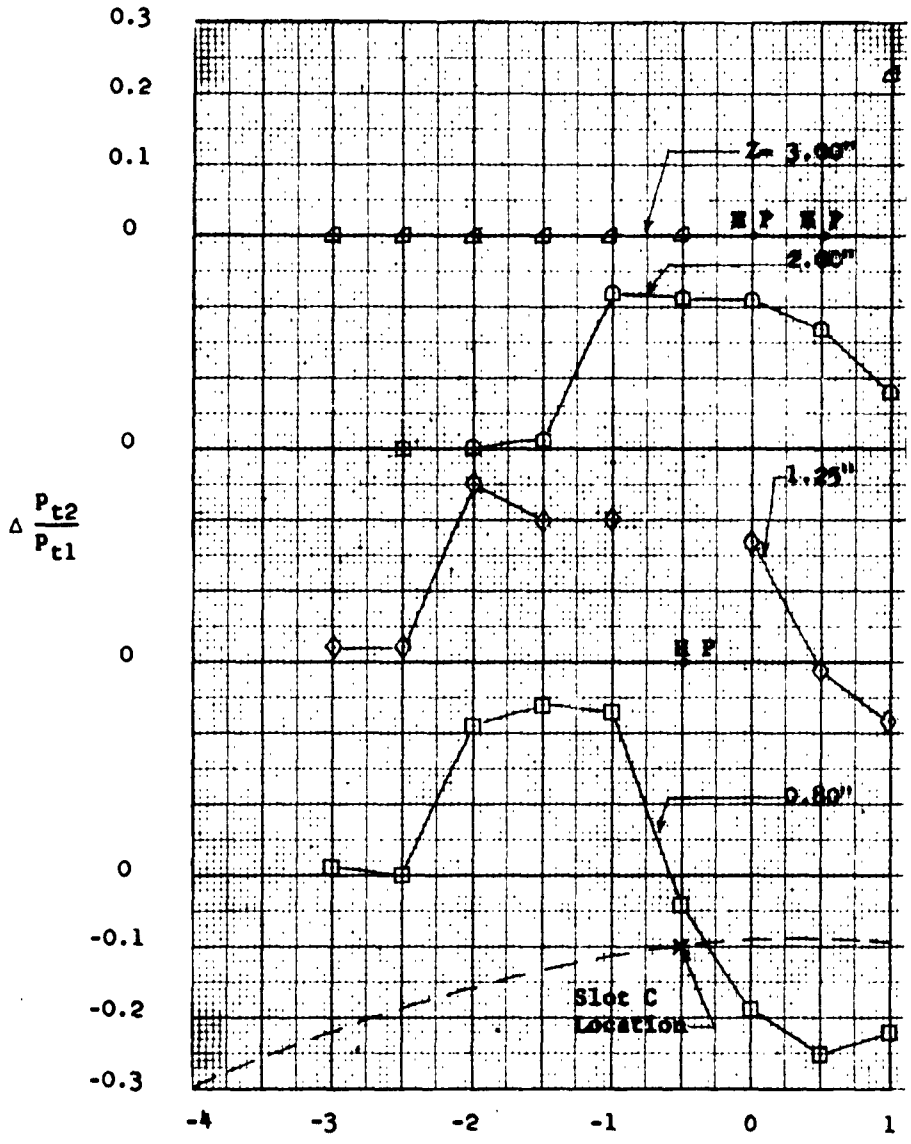

Figure 5 (Continued)

(g) p_j/p_∞ = 114; Slot C

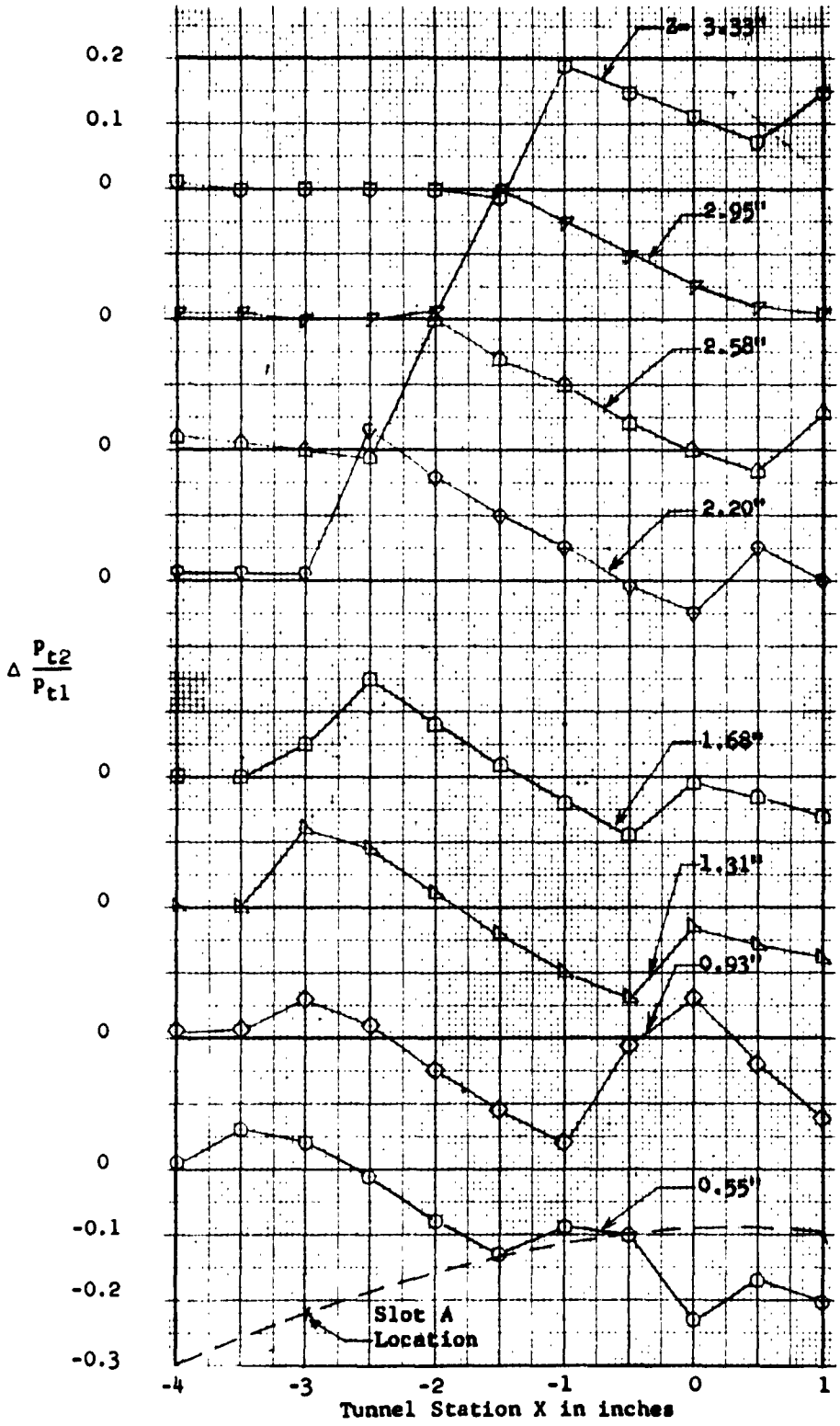

Figure 5 (Continued)

(h) p_j/p_∞ = 103; Slot A

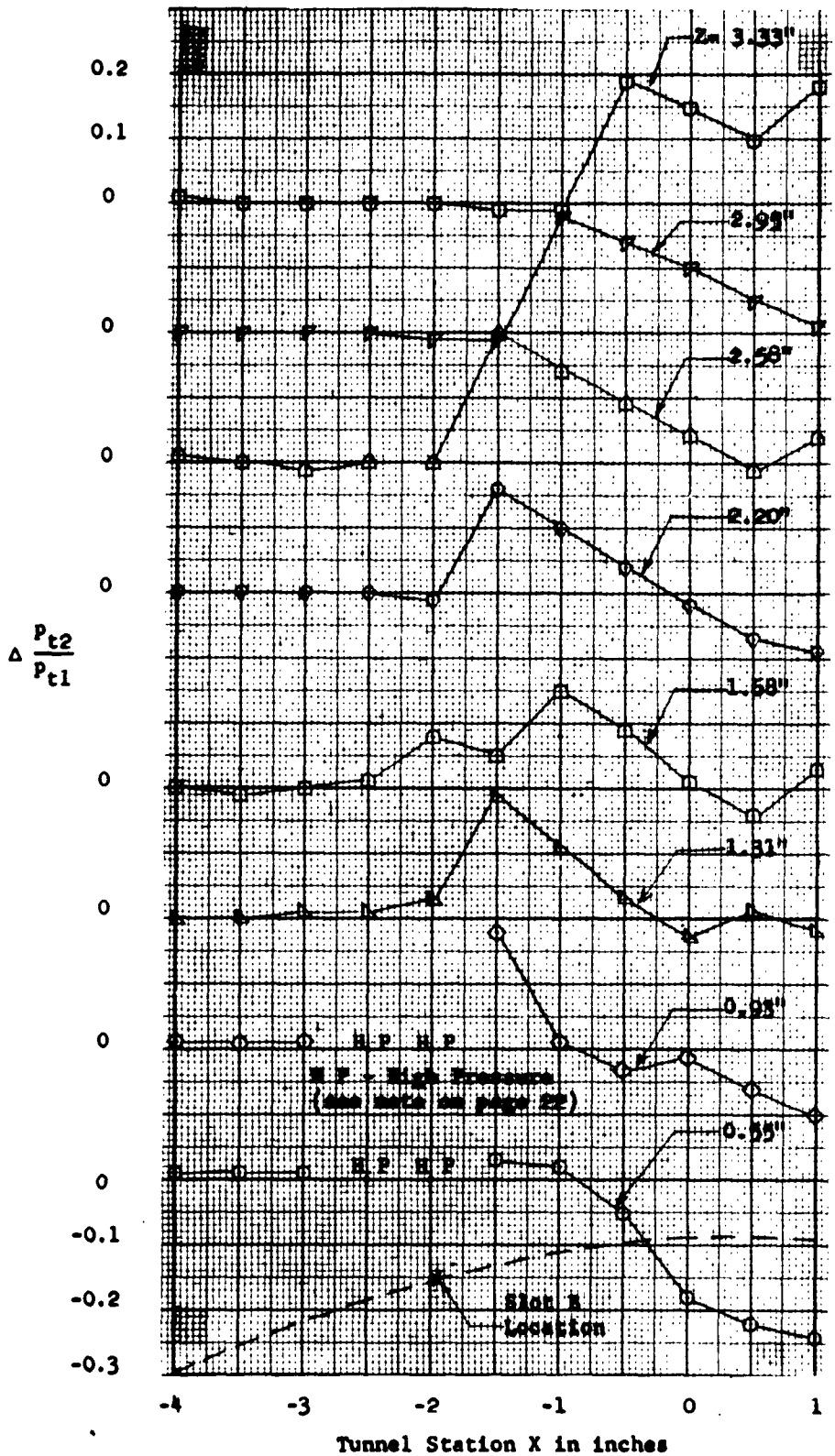

Figure 5 (Continued)

(i) p_j/p_∞ = 101; Slot B

H P - High pressure (see note on page 22)

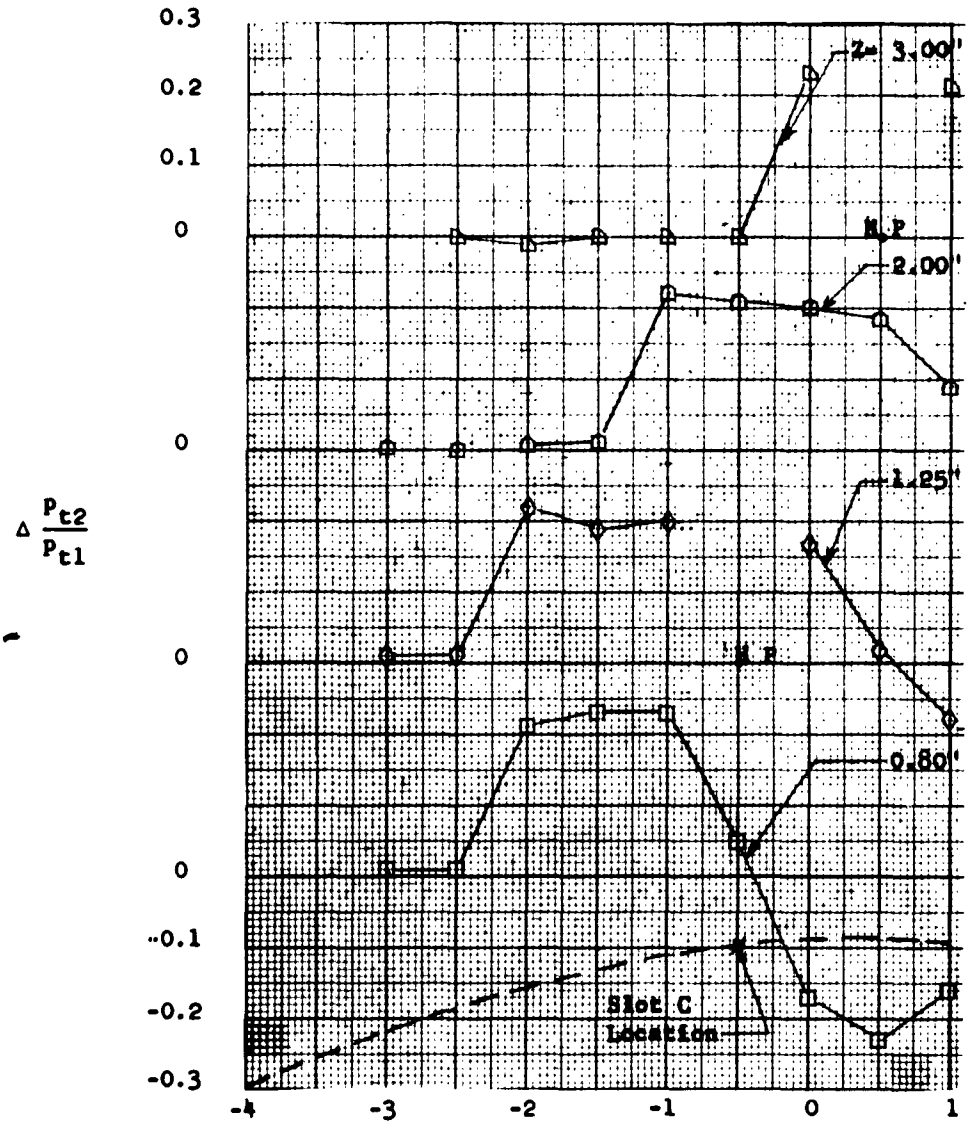

Figure 5 (Concluded)

(j) P_j/P_∞ = 103; Slot C

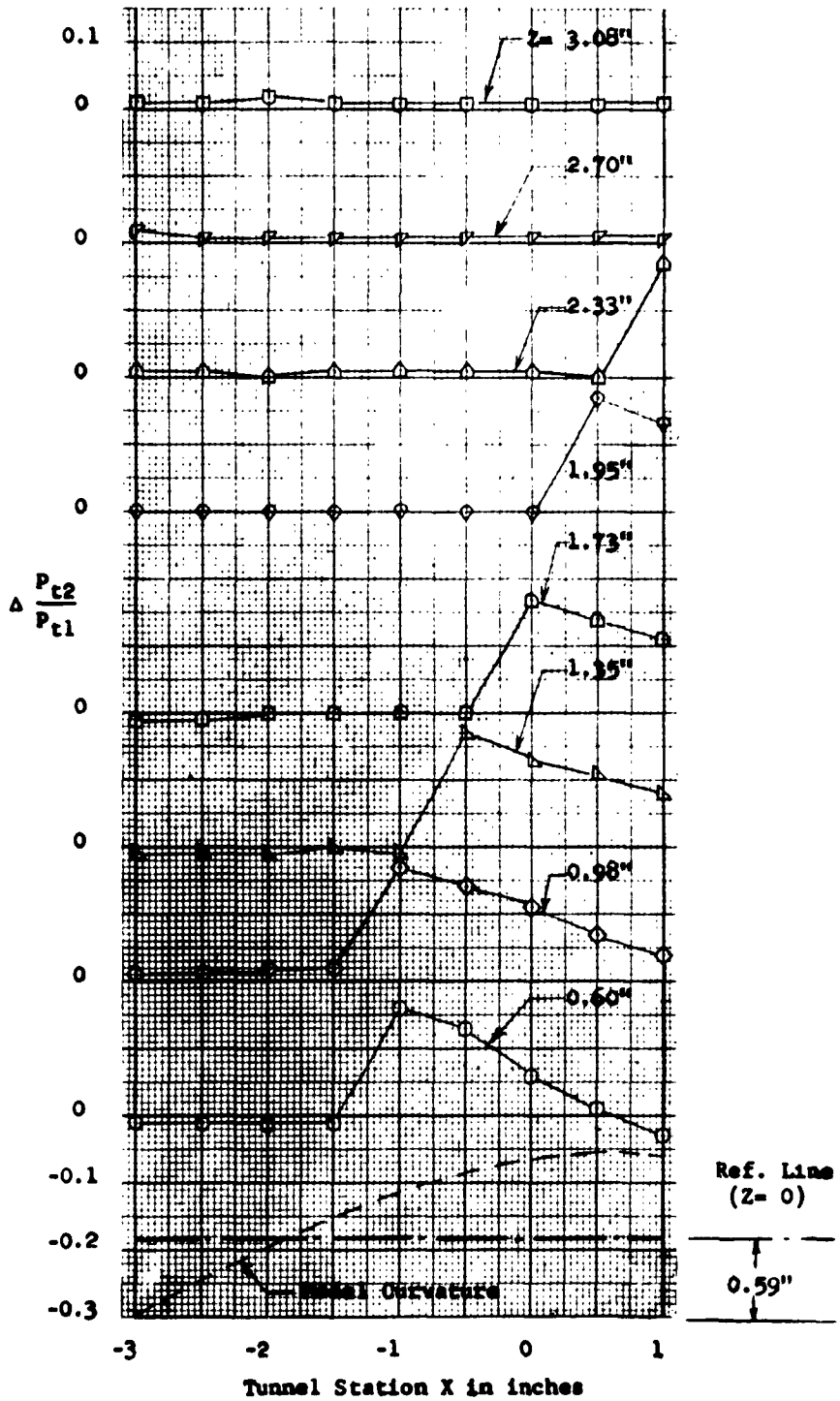

Figure 6 - Exhausting Jet Penetration at a Main Stream Mach Number of 3.73

(a) $P_j/P_\infty = 0$

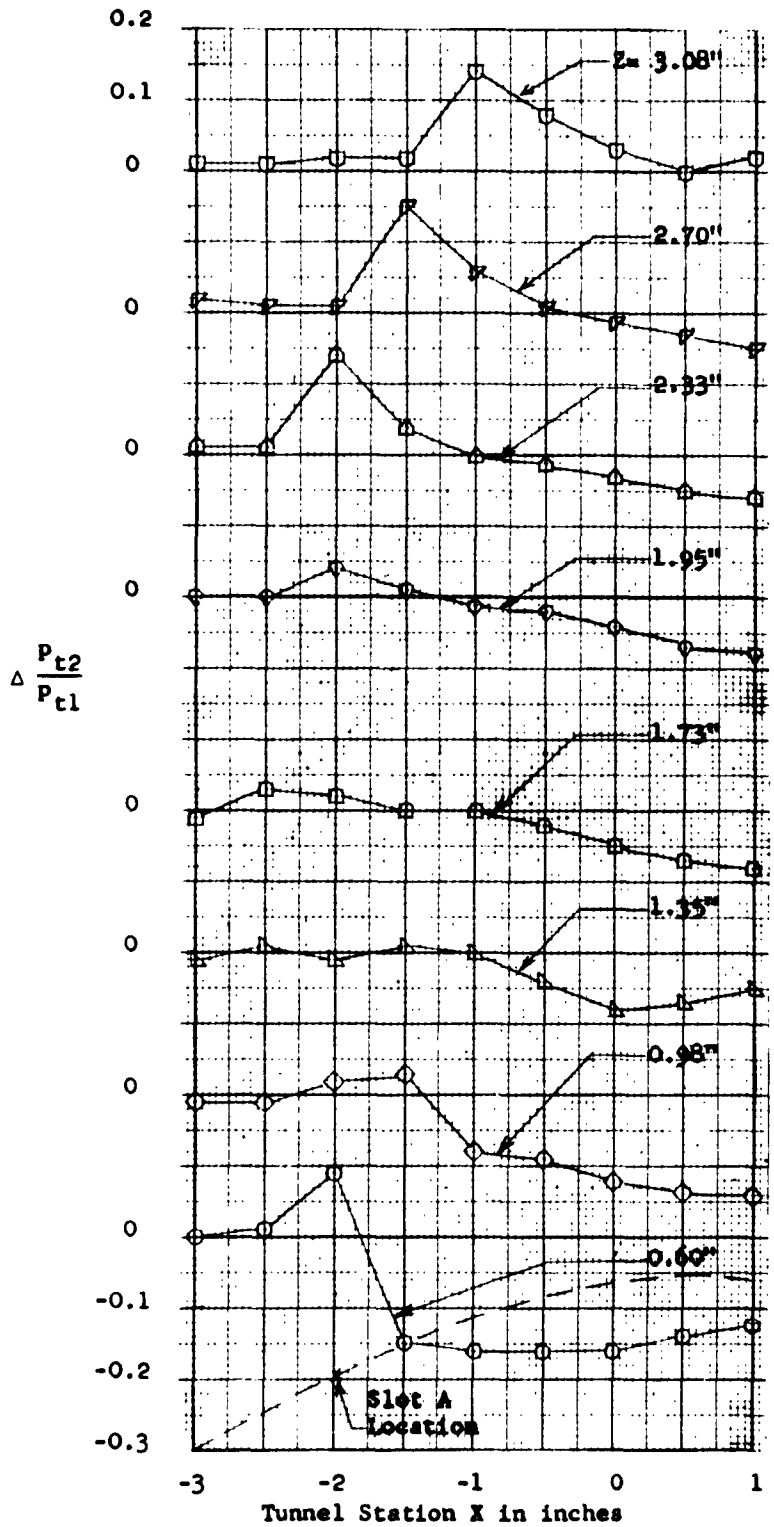

Figure 6 (Continued)

(b) p_j/p_∞ = 784; Slot A

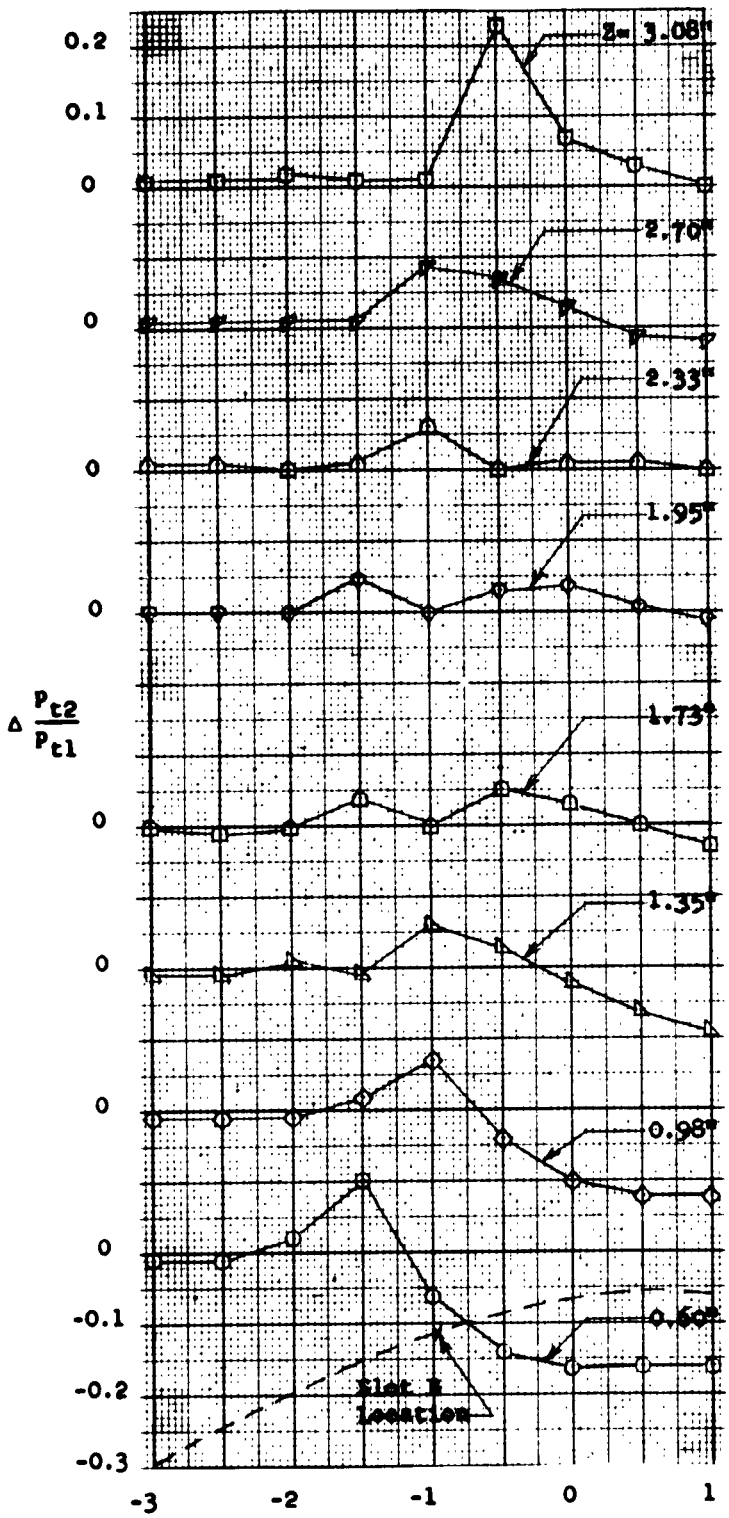

Figure 6 (Continued)

(c) p_j/p_∞ = 788; Slot B

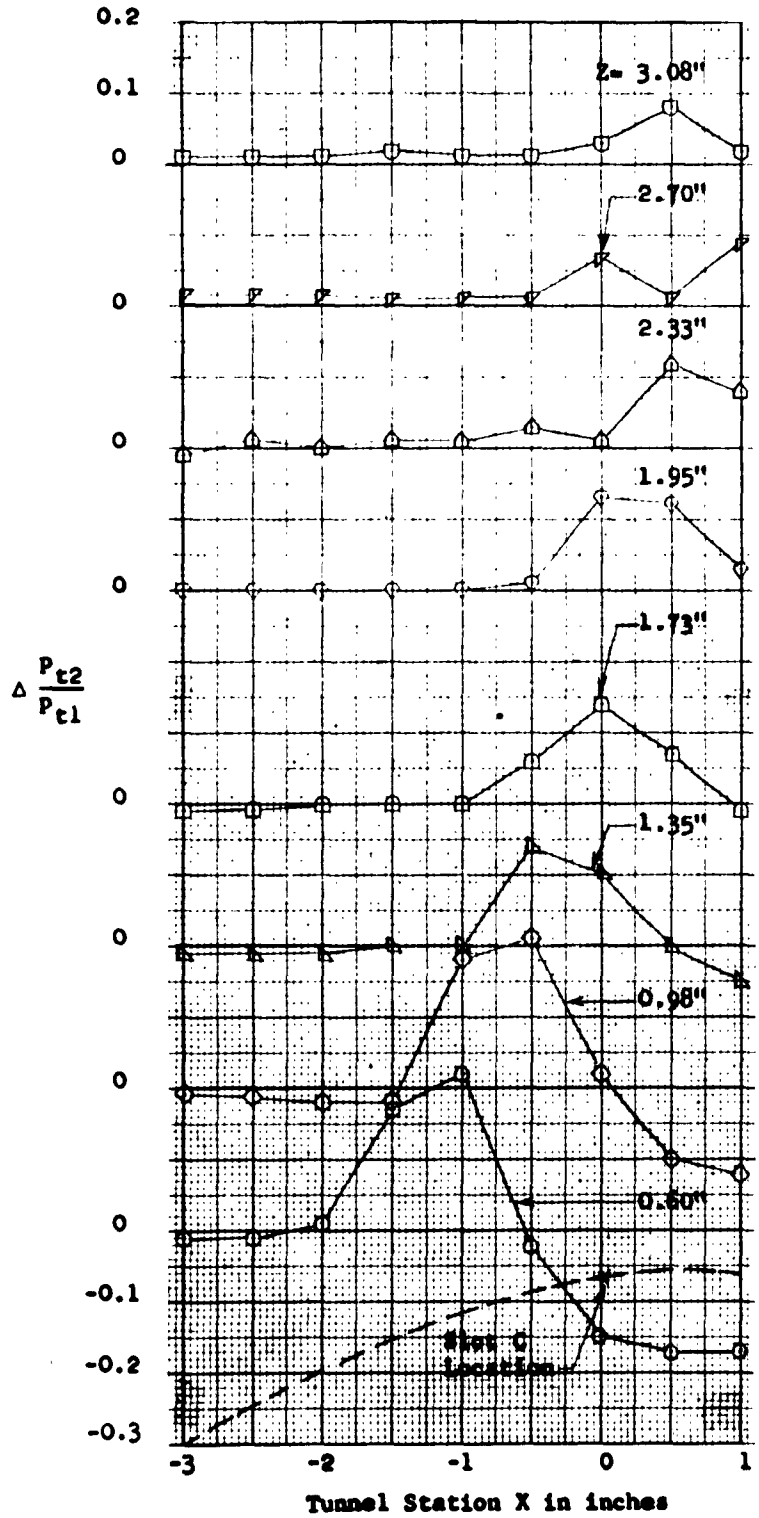

Figure 6 (Continued)

(d) p_j/p_∞ = 789; Slot C

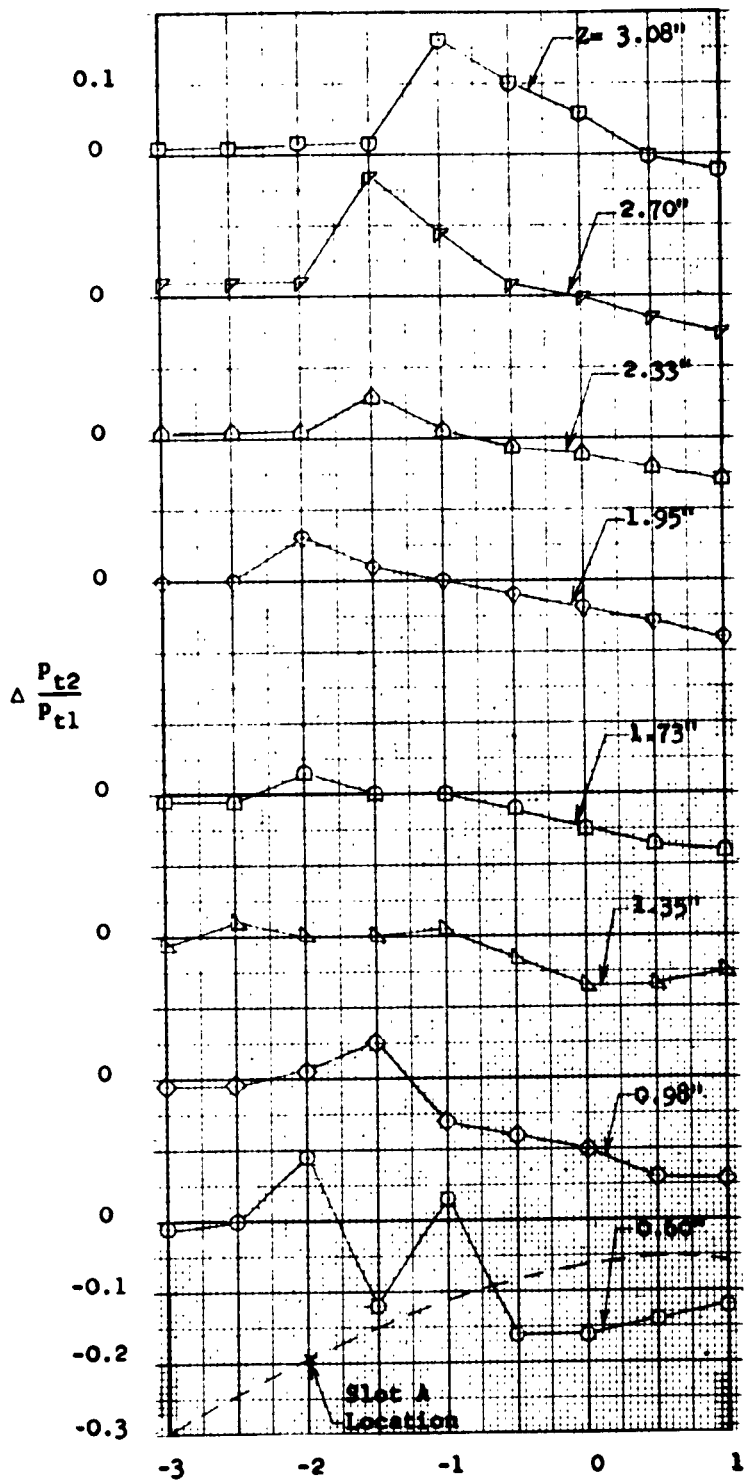

Figure 6 (Continued)

(e) P_j/P_∞ = 712; Slot A

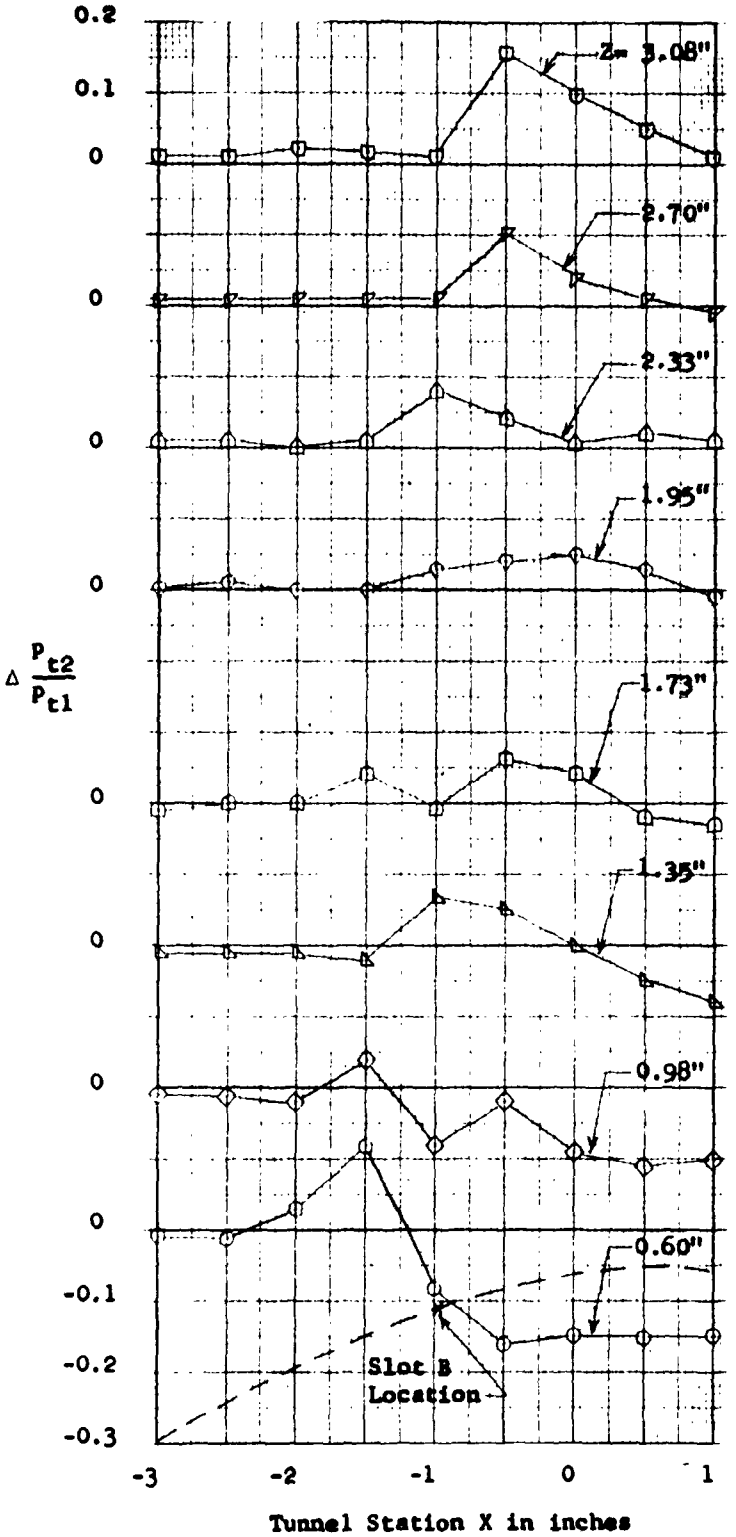

Figure 6 (Continued)

(f) p_j/p_∞ = 717; Slot B

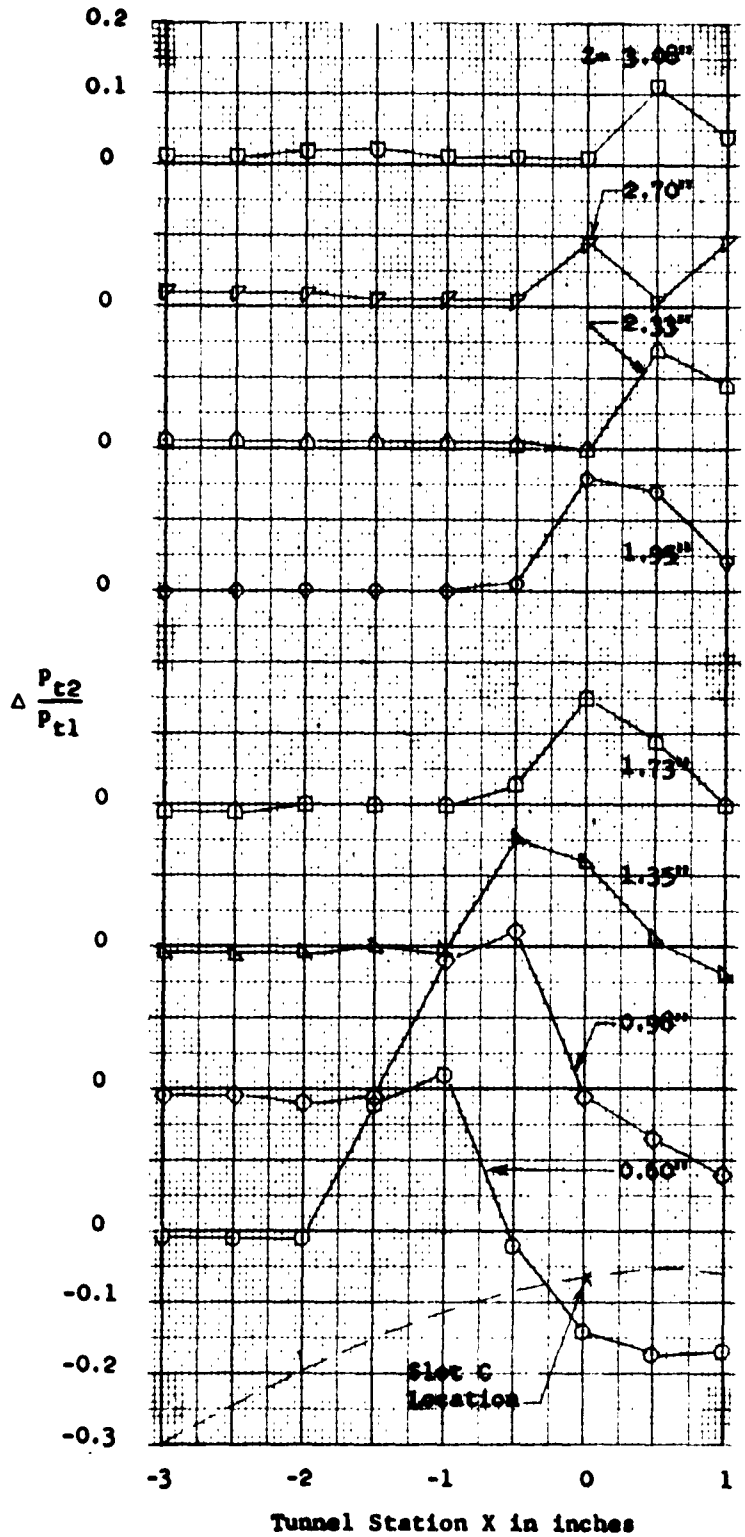

Figure 6 (Continued)

(g) P_j/P_∞ = 717; Slot C

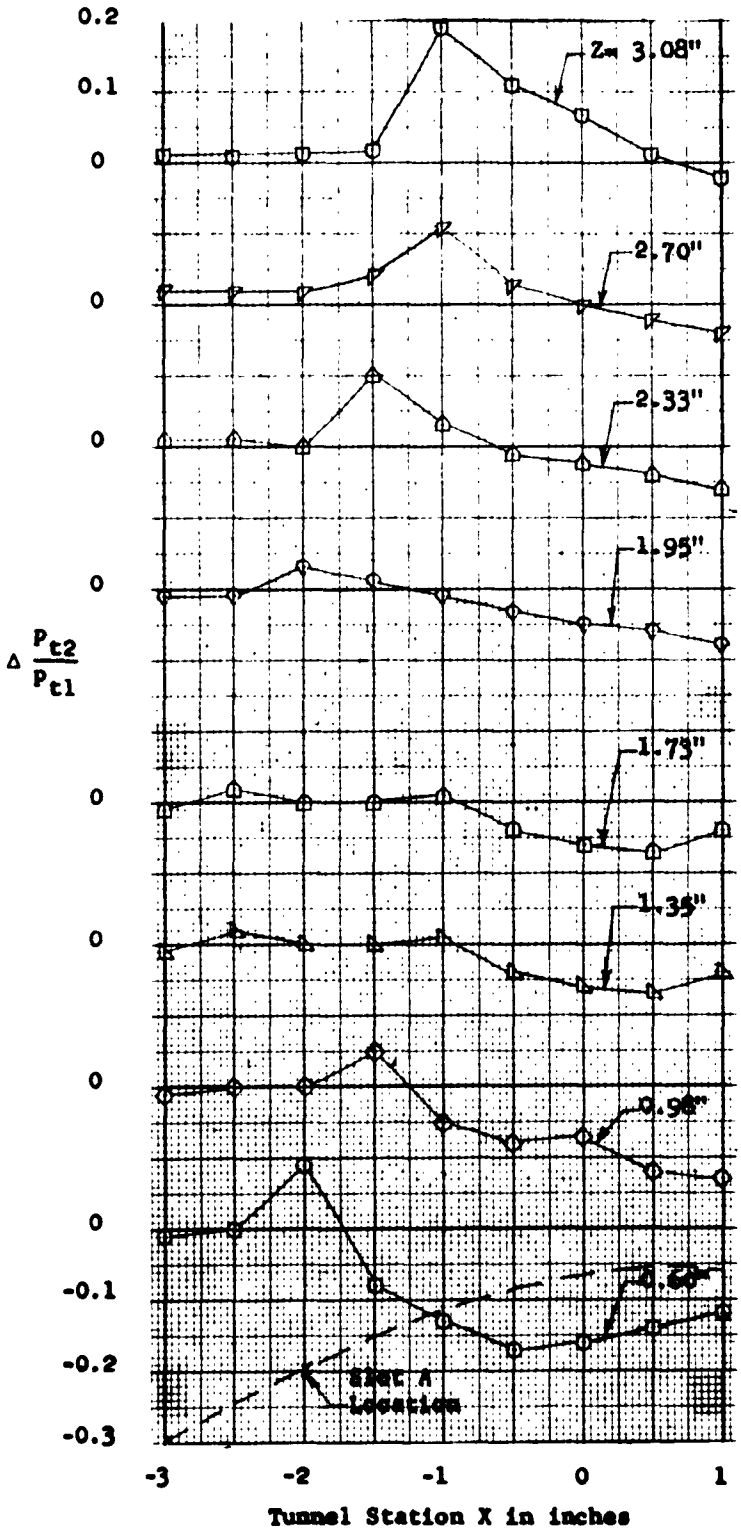

Figure 6 (Continued)

(h) p_j/p_∞ = 641; Slot A

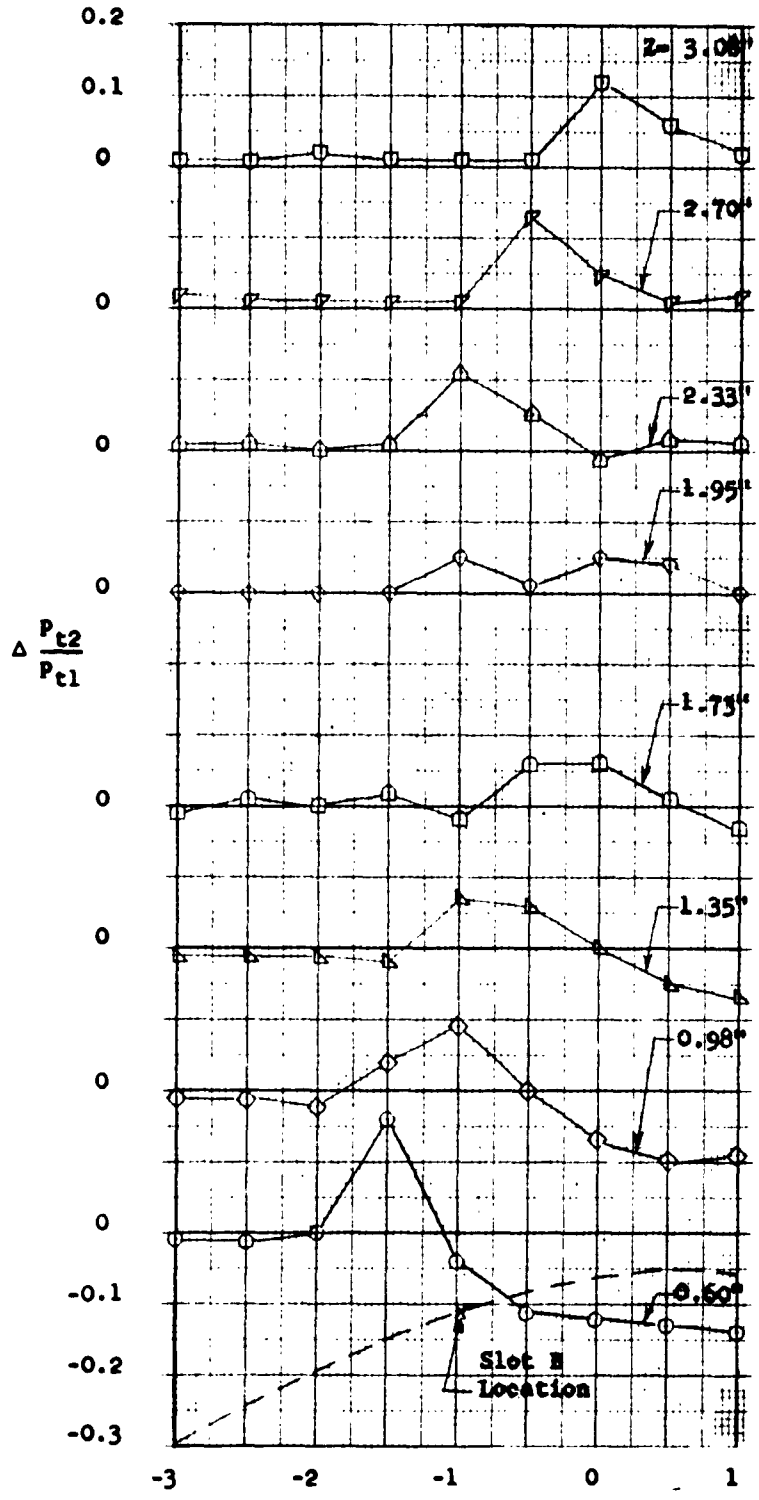

Figure 6 (Continued)

(i) p_j/p_∞ = 645; Slot B

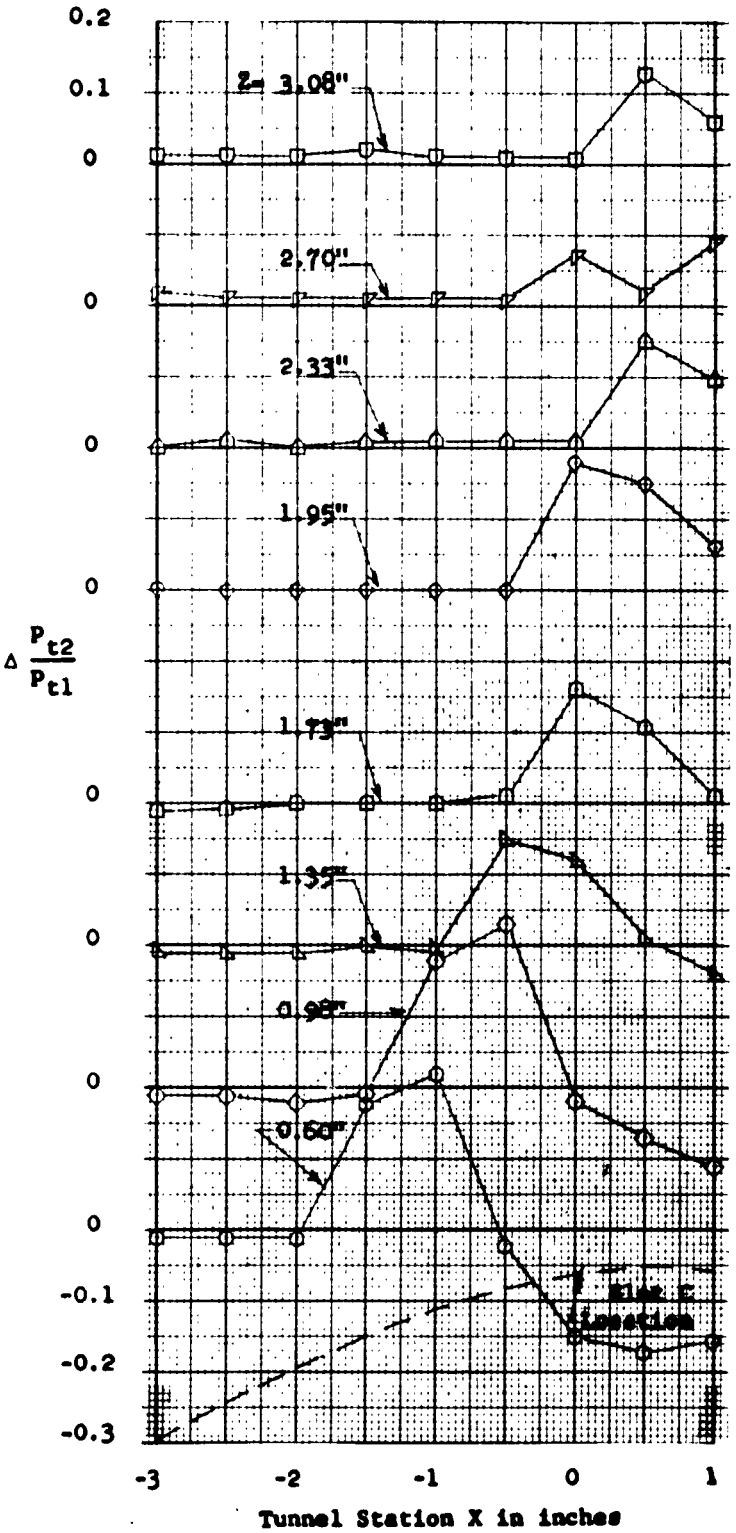

Figure 6 (Concluded)

(j) P_j/P_∞ = 645; Slot C

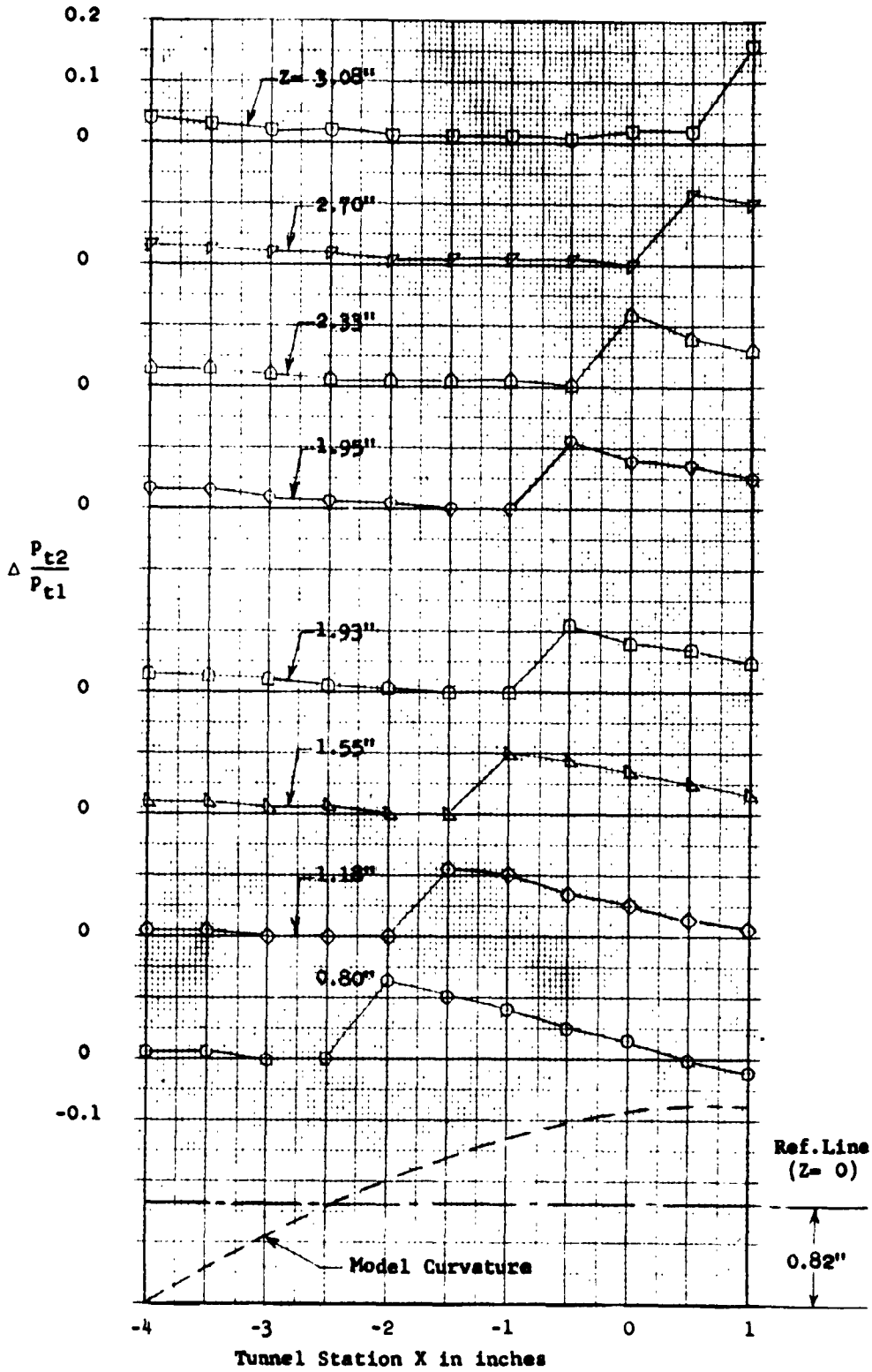

Figure 7 - Exhausting Jet Penetration at a Main Stream Mach Number of 4.50

(a) $P_j/P_\infty = 0$

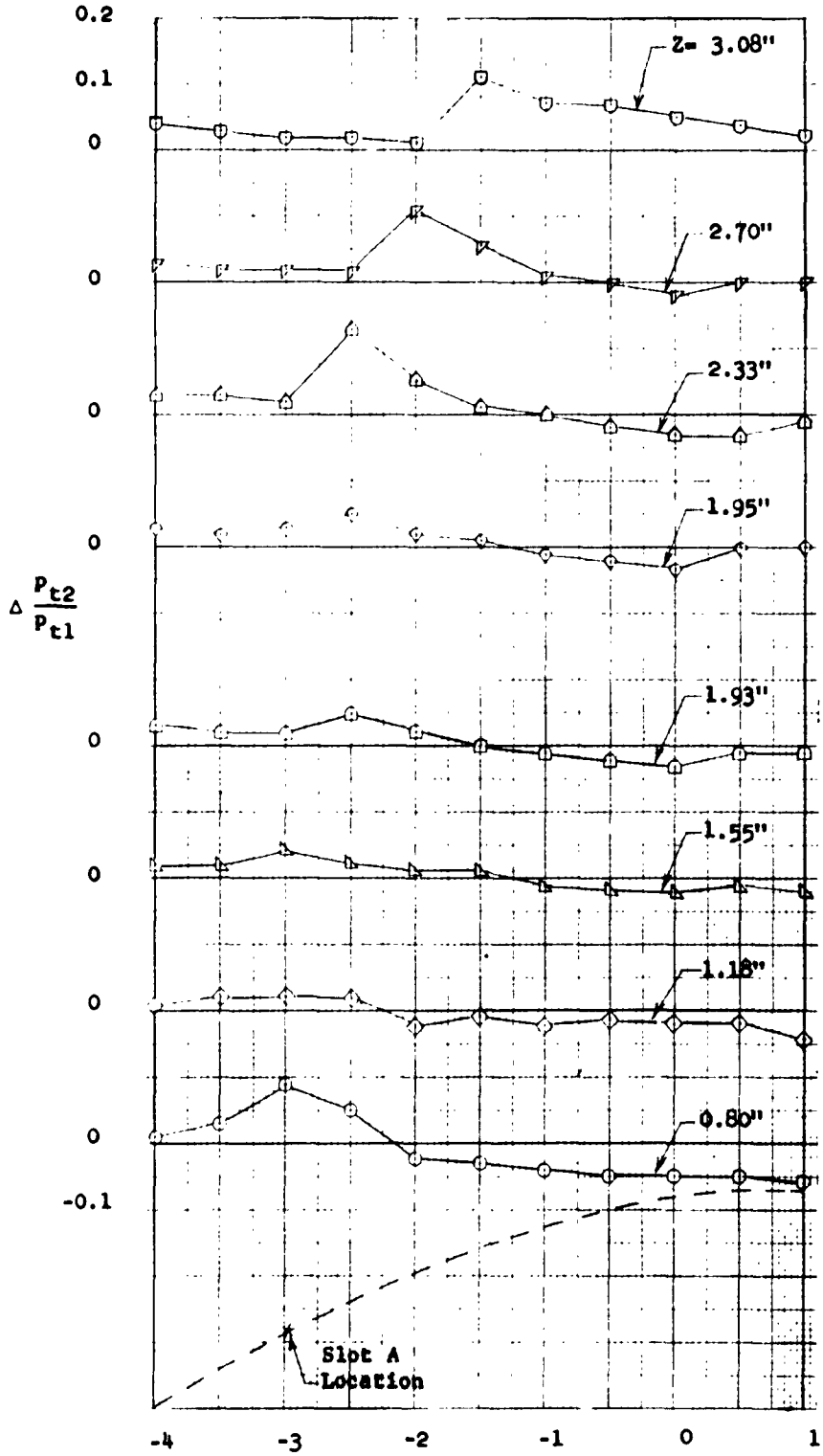

Figure 7 (Continued)

(b) p_j/p_∞ = 1174; Slot A

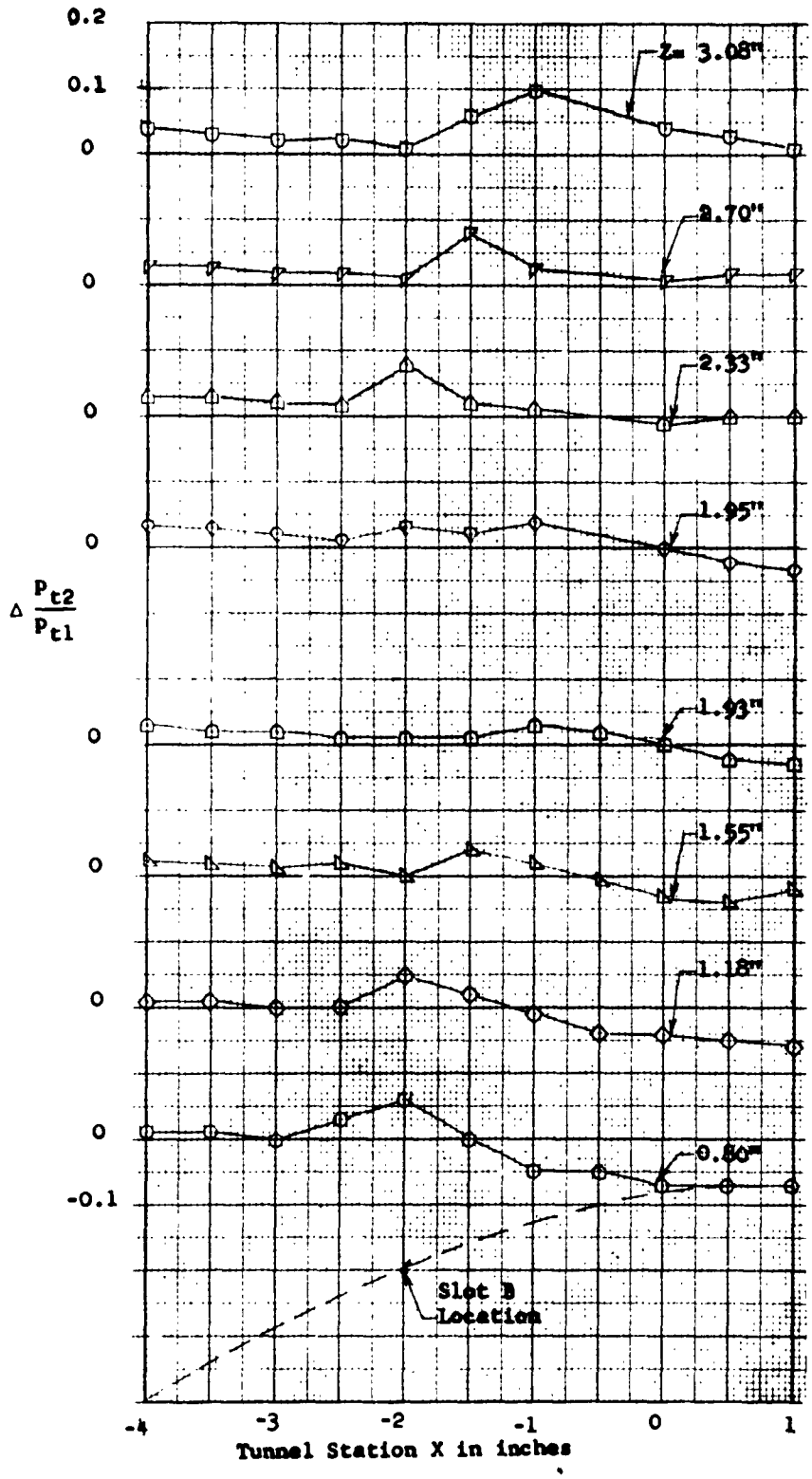

Figure 7 (Continued)

(c) p_j/p_∞ = 1153; Slot B

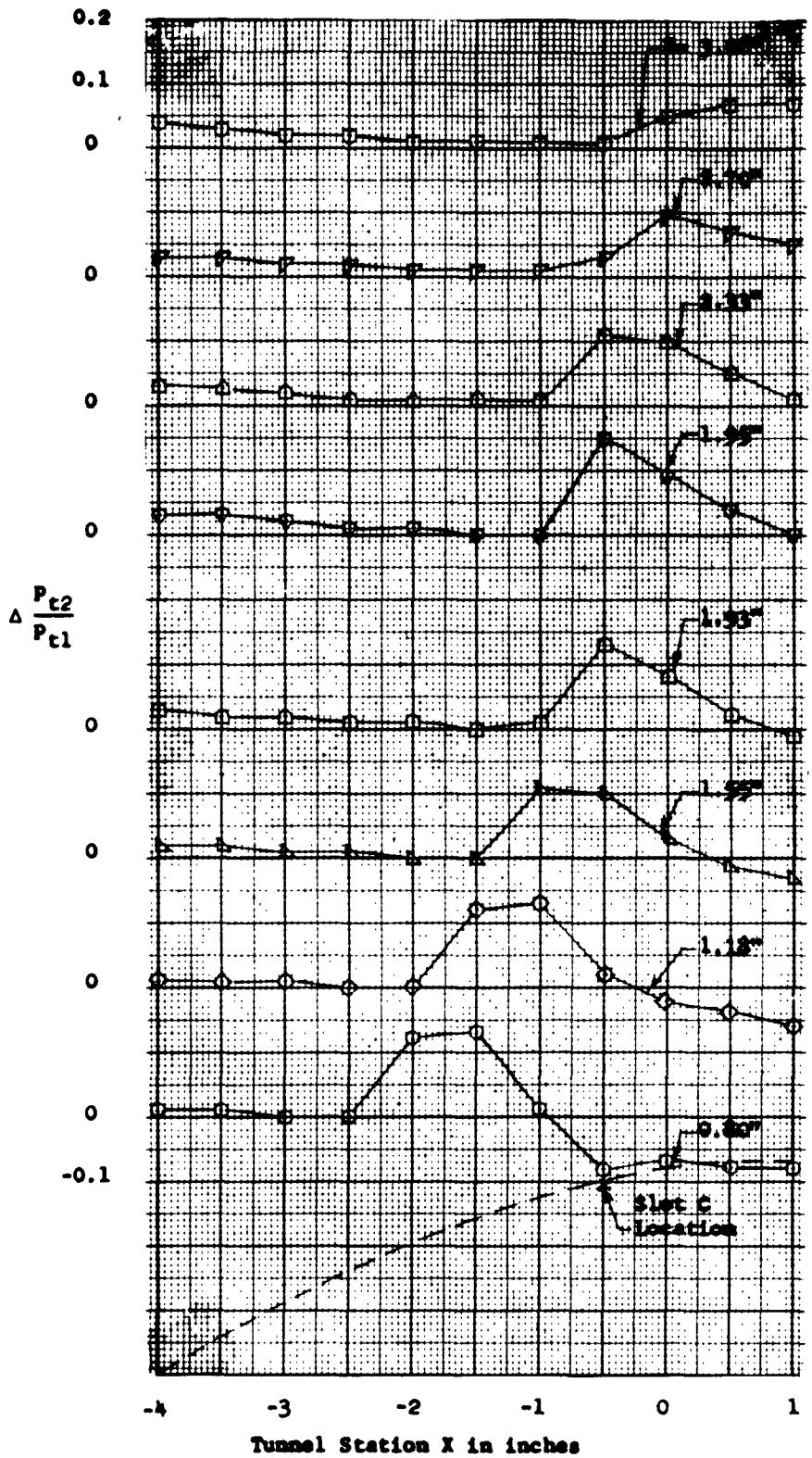

Figure 7 (Continued)

(d) p_j/p_∞ = 1171; Slot C

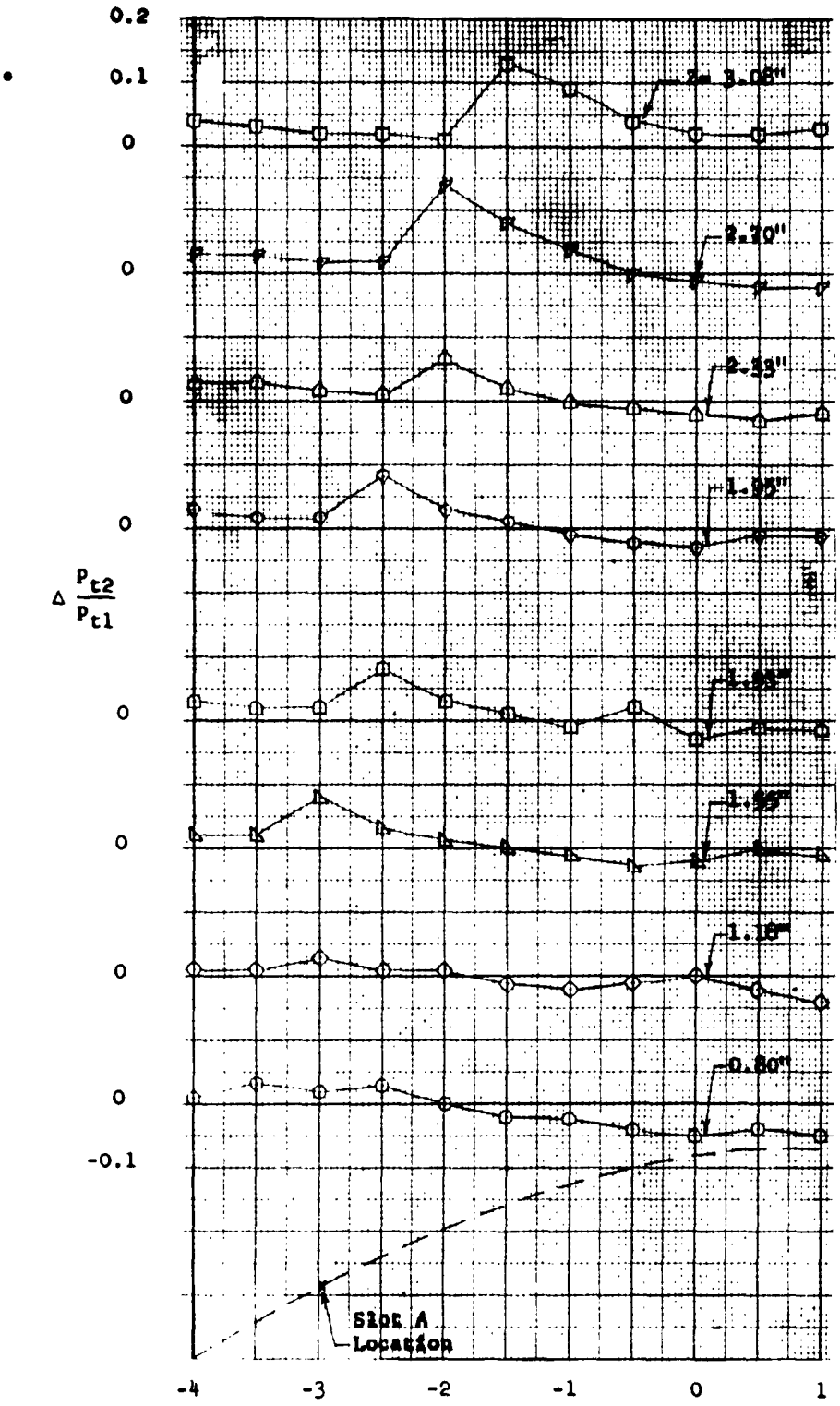

Figure 7 (Continued)

(e) p_j/p_∞ = 977; Slot A

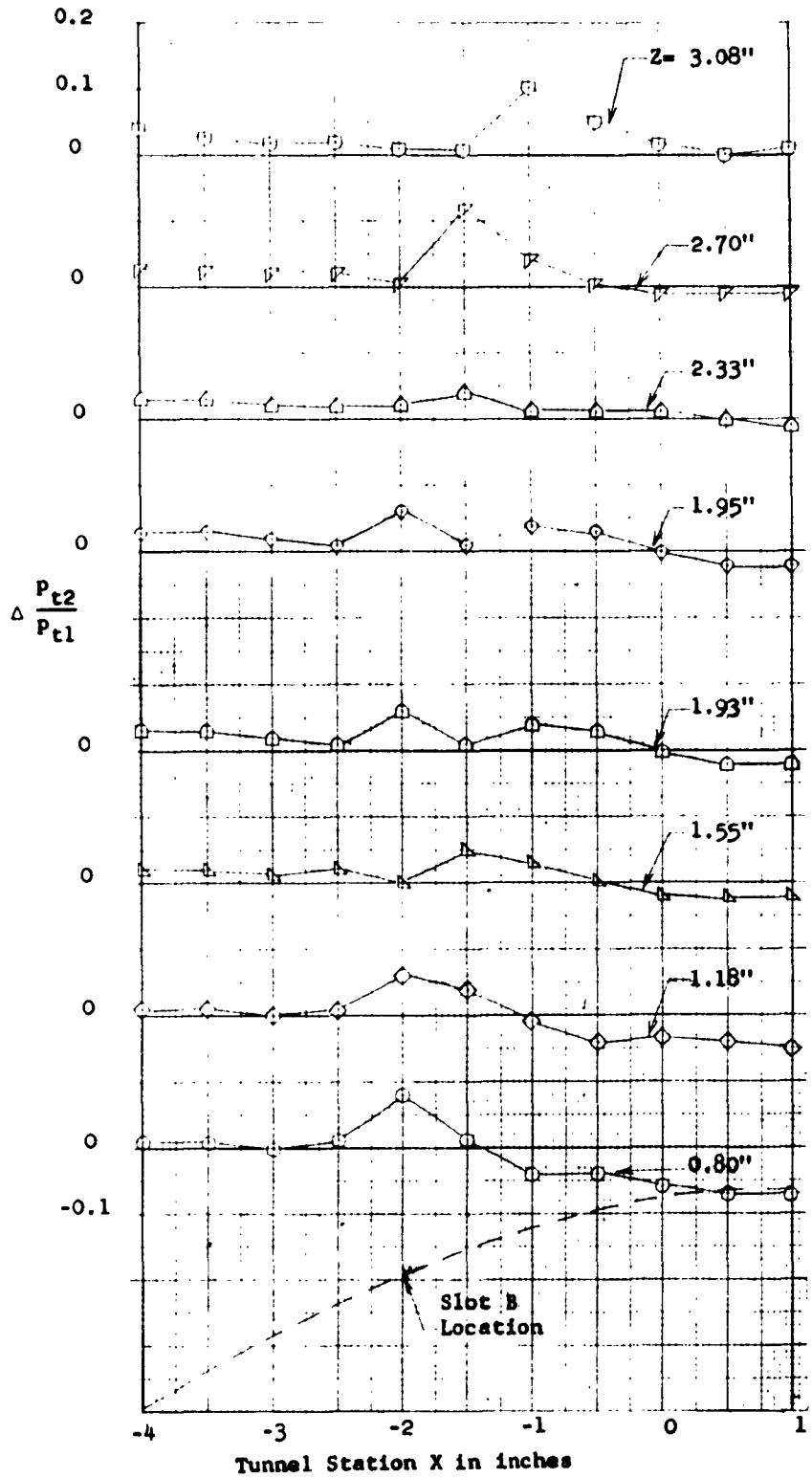

Figure 7 (Continued)

(f) p_j/p_∞ = 960; Slot B

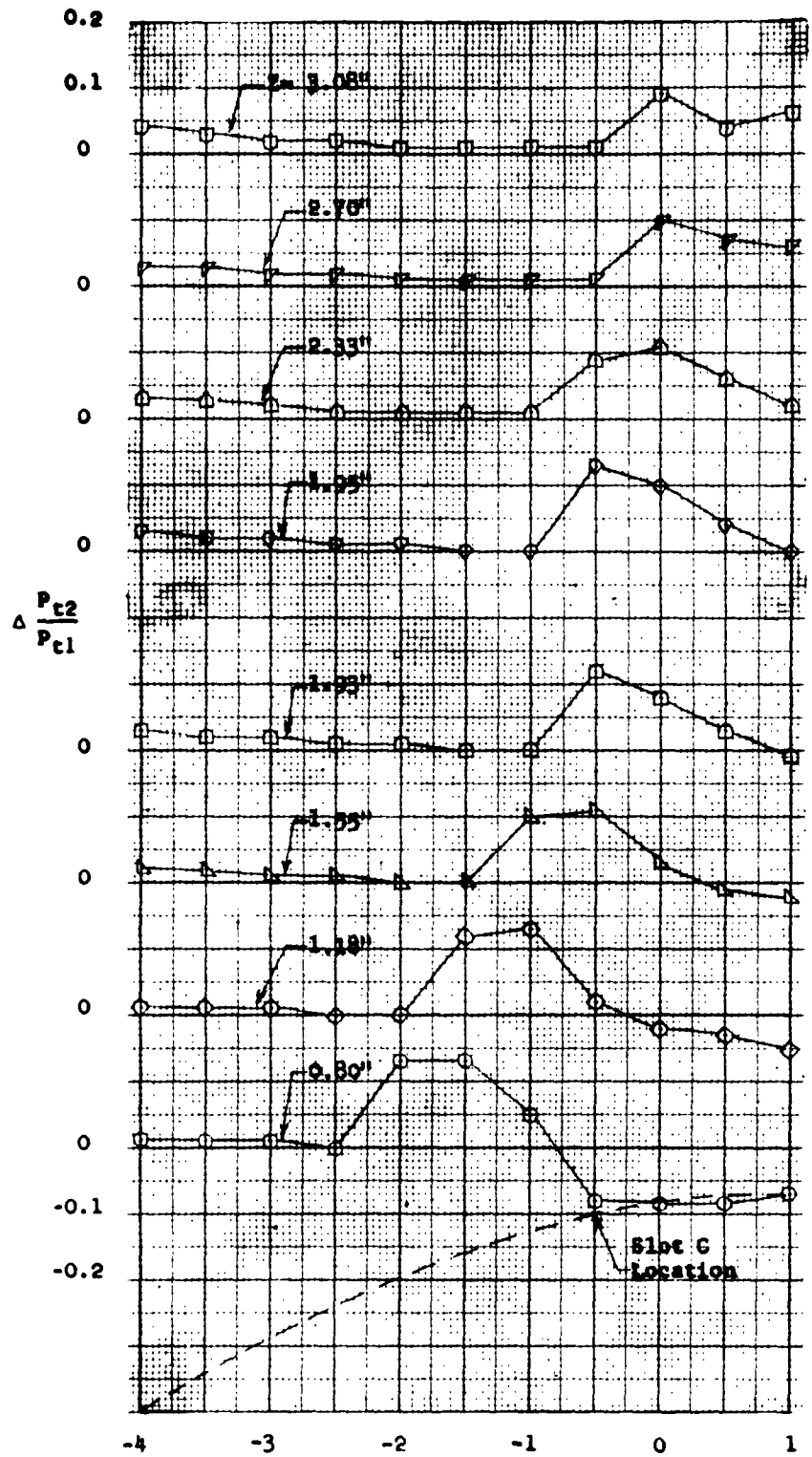

Figure 7 (Continued)

(g) P_j/P_∞ = 975; Slot C

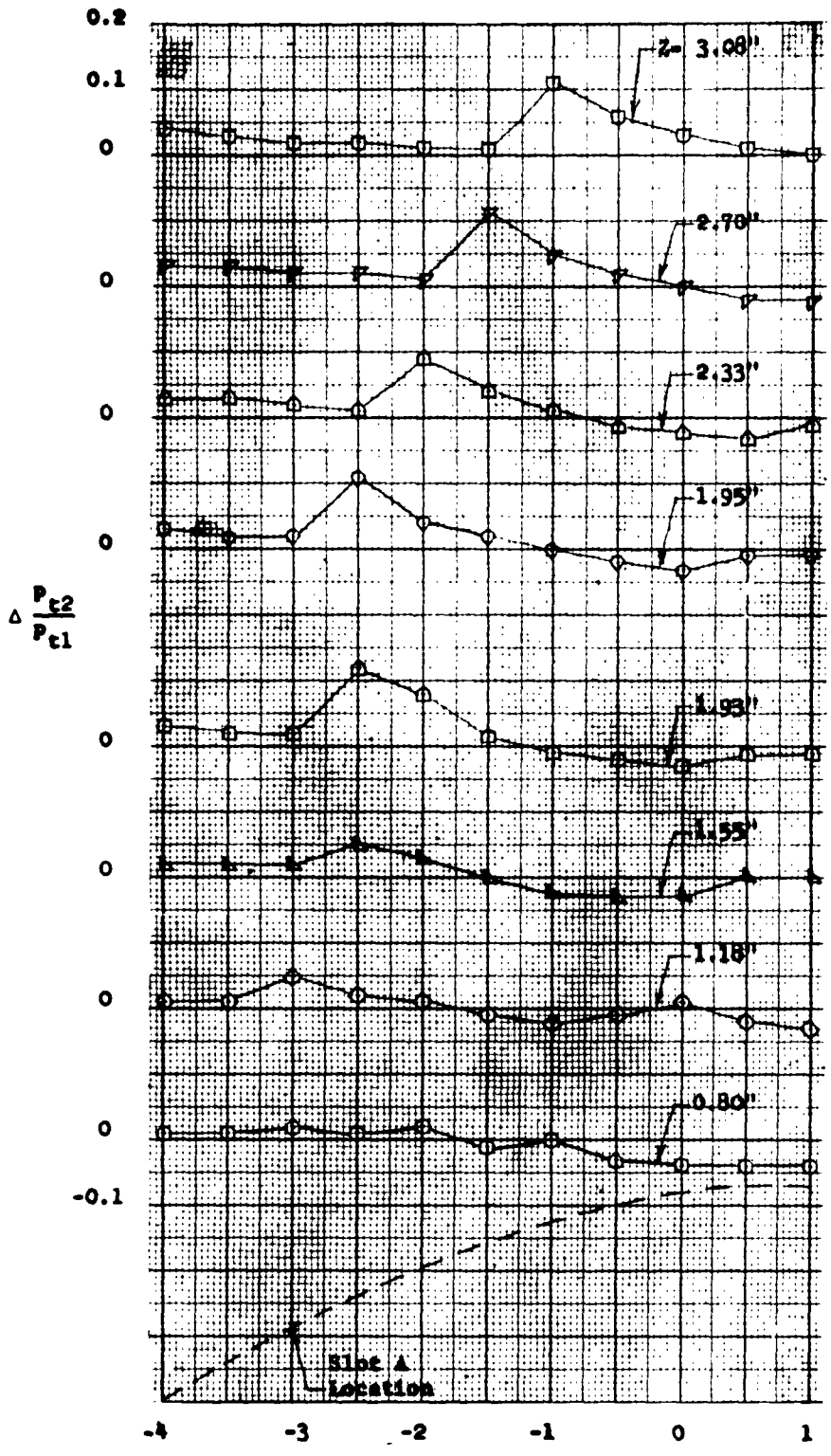

Figure 7 (Continued)

(h) p_j/p_∞ = 781; Slot A

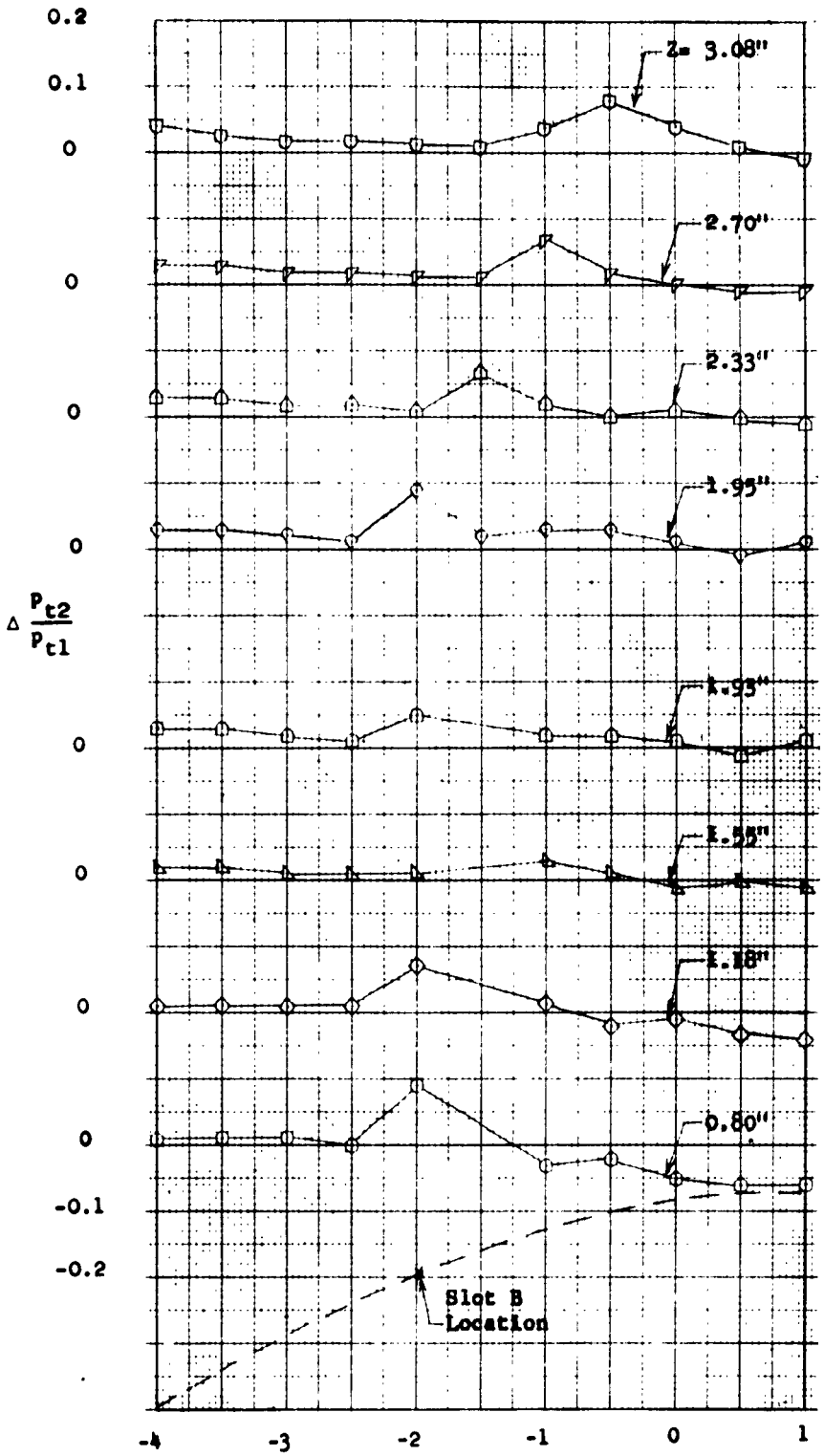

Figure 7 (Continued)

(1) p_j/p_∞ = 768; Slot B

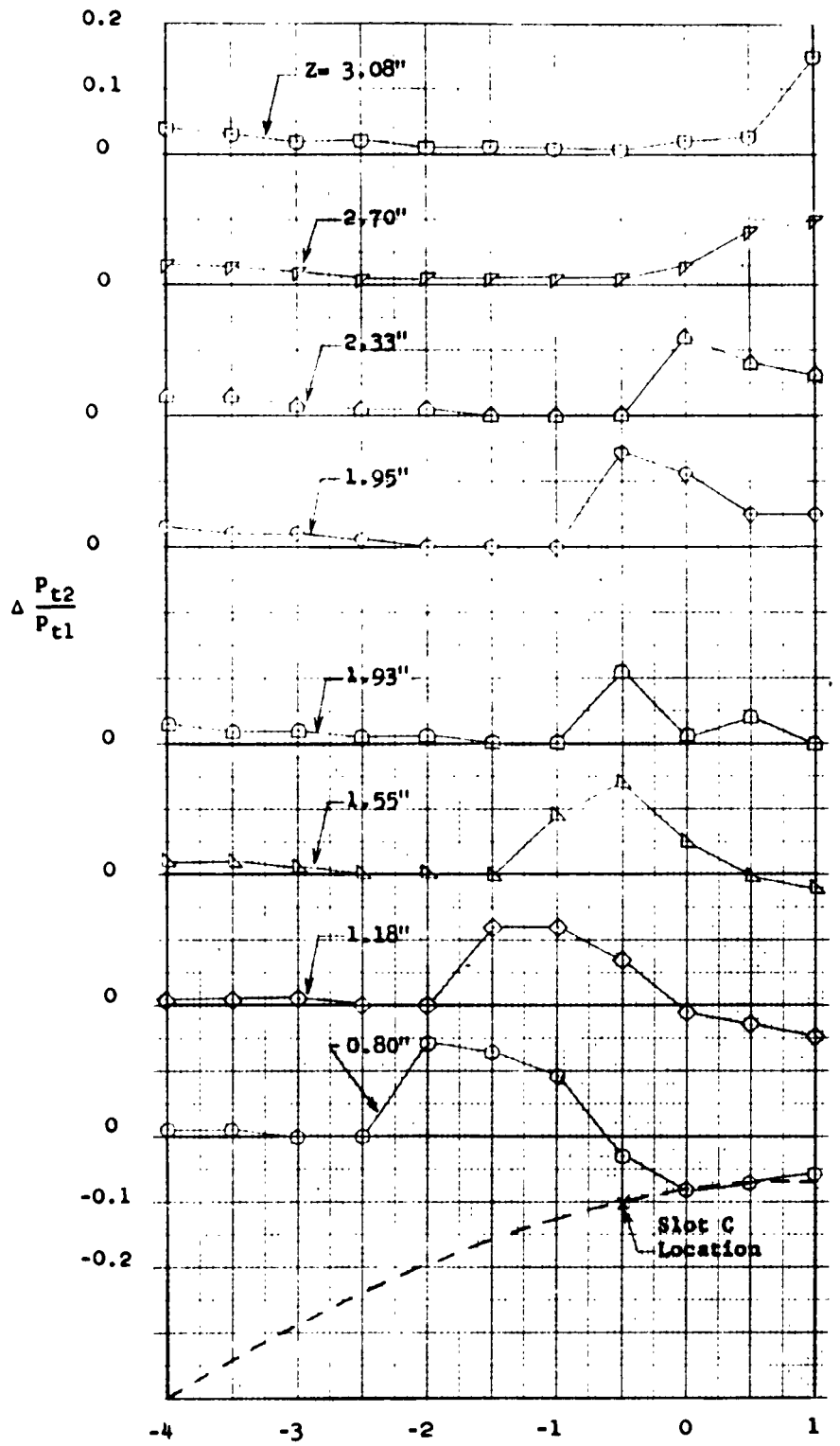

Figure 7 (Concluded)

(j) p_j/P_∞ = 779; Slot C

S-4624 19 Feb 1962
Model 1
(a) M = 2.48

S-4625 23 Mar 1962
Model 2
(b) M = 3.73

S-4626 3 Apr 1962
Model 3
(c) M = 4.50

Figure 8 - Schlieren Photographs of Models 1, 2, and 3 With No Jet Exhausting

S-4607 $p_j/p_\infty = 126$

S-4618 $p_j/p_\infty = 114$

S-4621 $p_j/p_\infty = 103$

Figure 9 - Schlieren Photographs of Model 1 With Jet Exhausting. Main Stream Mach Number = 2.48

(a) Slot A

S-4616

P_j/P_∞ = 124

S-4619

P_j/P_∞ = 112

S-4622

P_j/P_∞ = 101

Figure 9 (Continued)
(b) Slot B

S-4617
$P_j/P_\infty = 126$

S-4620
$P_j/P_\infty = 114$

S-4623
$P_j/P_\infty = 103$

Figure 9 (Concluded)

(c) Slot C

S-4627

$p_j/p_\infty = 784$

S-4628

$p_j/p_\infty = 712$

S-4629

$p_j/p_\infty = 641$

Figure 10 - Schlieren Photographs of Model 2 With Jet Exhausting. Main Stream Mach Number = 3.73

(a) Slot A

S-4630

P_j/P_∞ = 788

S-4631

P_j/P_∞ = 717

S-4632

P_j/P_∞ = 645

Figure 10 (Continued)
(b) Slot B

S-4633

$P_j/P_\infty = 789$

S-4634

$P_j/P_\infty = 717$

S-4635

$P_j/P_\infty = 645$

Figure 10 (Concluded)

(c) Slot C

S-4636 $p_j/p_\infty = 1174$

S-4637 $p_j/p_\infty = 977$

S-4638 $p_j/p_\infty = 781$

Figure 11 - Schlieren Photographs of Model 3 With Jet Exhausting. Main Stream Mach Number = 4.50

(a) Slot A

S-4639

P_j/P_∞ = 1153

S-4640

P_j/P_∞ = 960

S-4641

P_j/P_∞ = 768

Figure 11 (Continued)
(b) Slot B

S-4642

p_j/p_∞ = 1171

S-4643

p_j/p_∞ = 975

S-4644

p_j/p_∞ = 779

Figure 11 (Concluded)
(c) Slot C

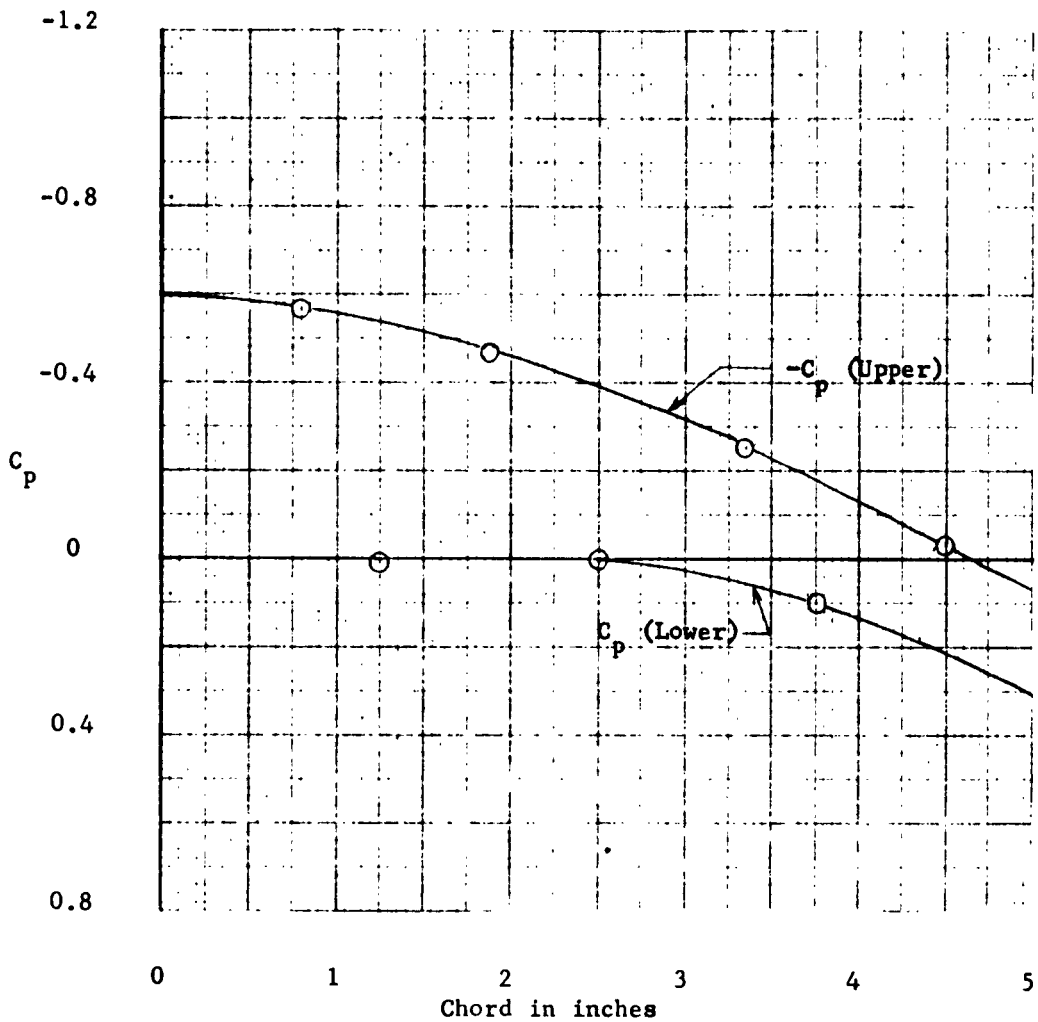

Figure 12 - Pressure Distribution on the Upper and Lower Surfaces of Model 1 (M = 2.48)

(a) $p_j/p_\infty = 0$

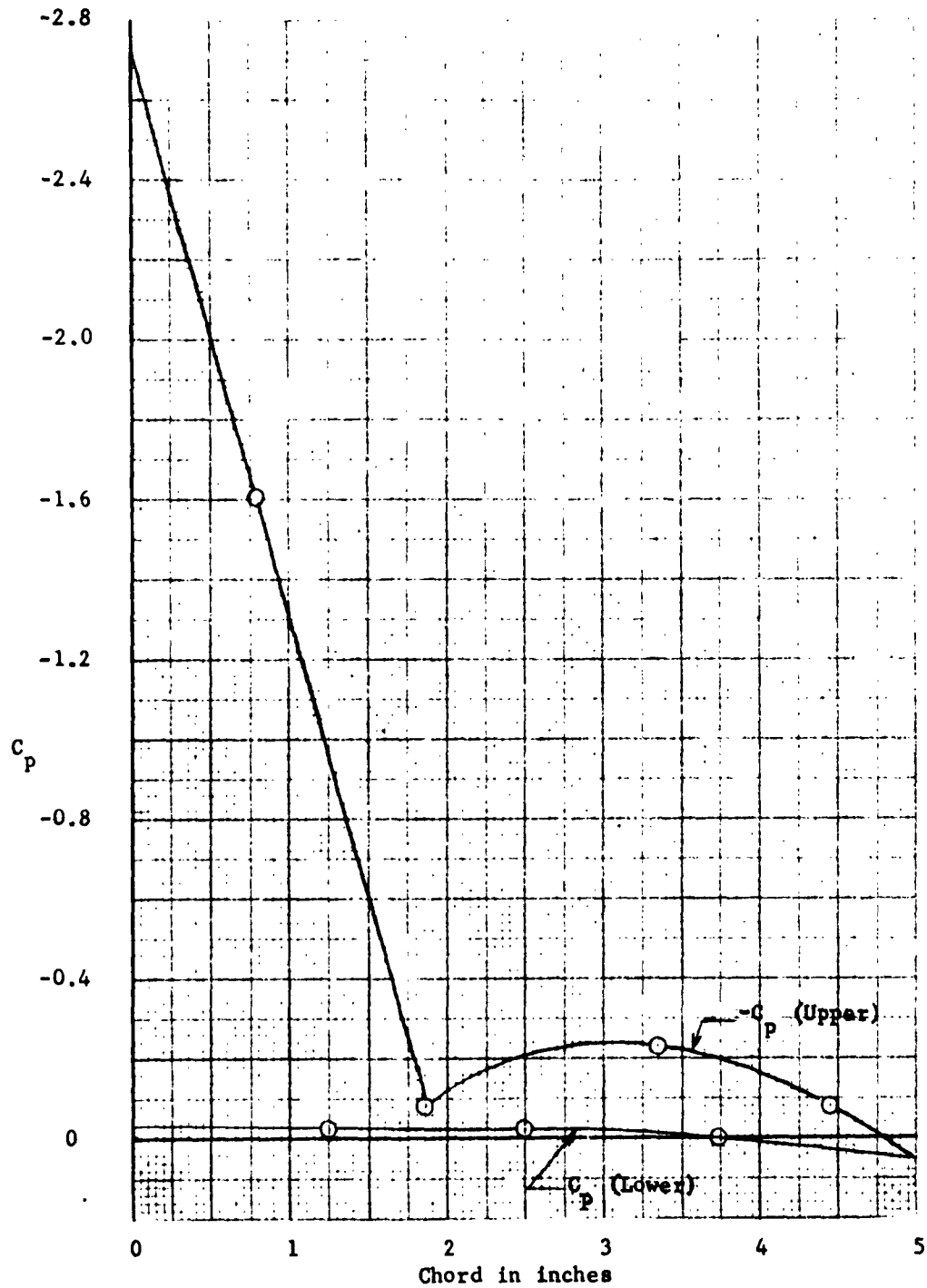

Figure 12 (Continued)

(b) p_j/p_∞ = 114 and 126; Slot A

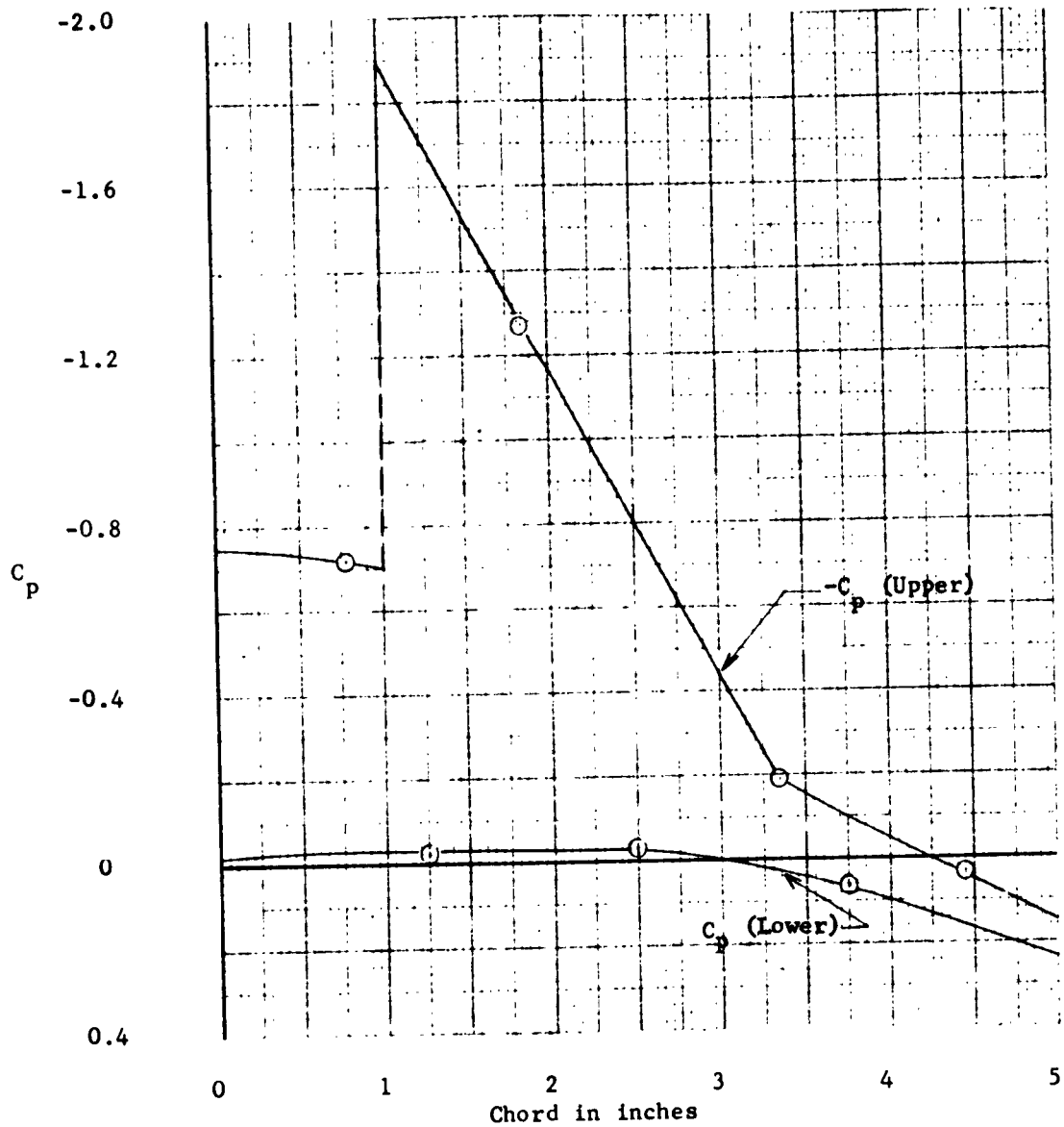

Figure 12 (Continued)
(c) p_j/p_∞ = 124; Slot B

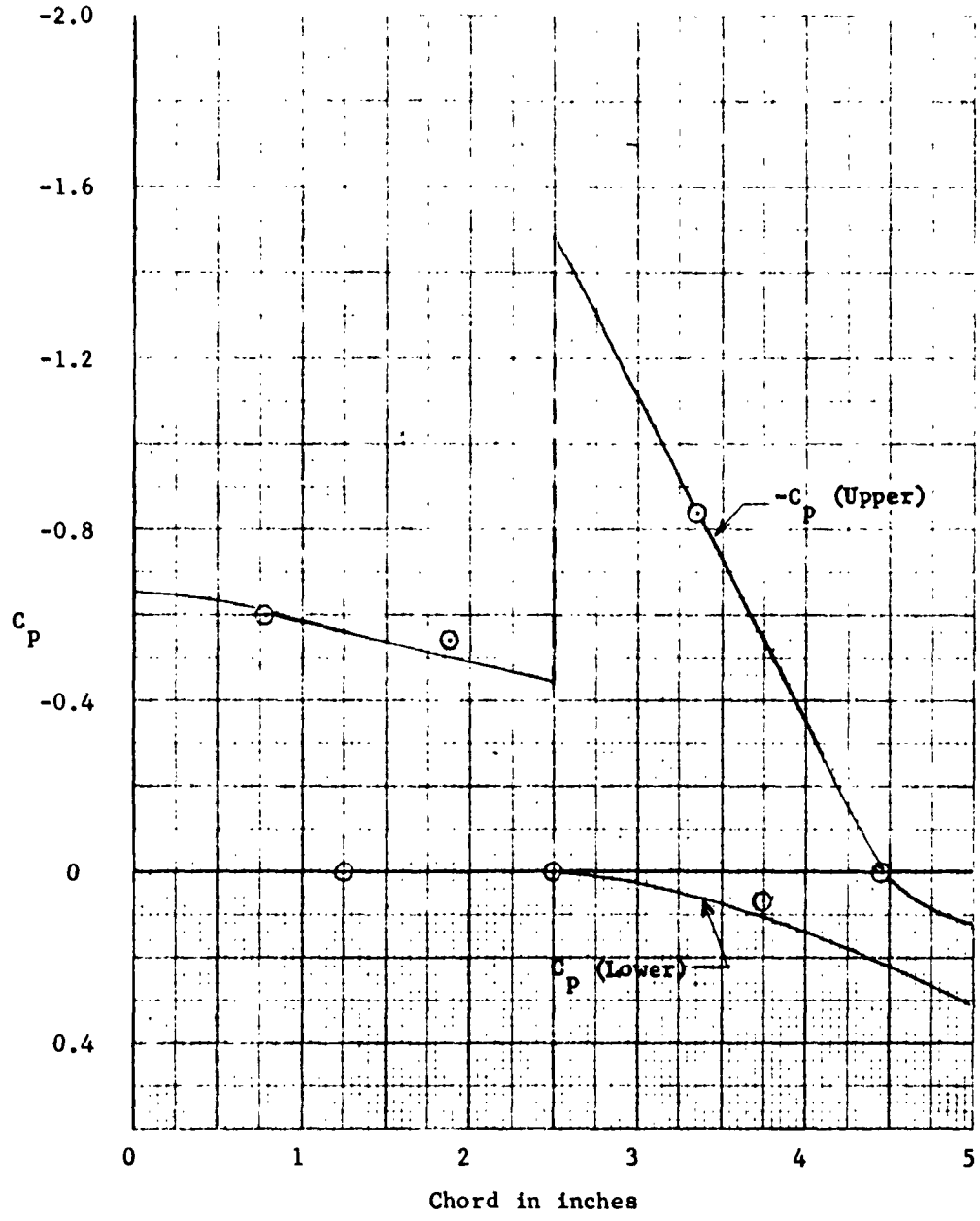

Figure 12 (Continued)

(d) P_j/P_∞ = 103 and 126; Slot C

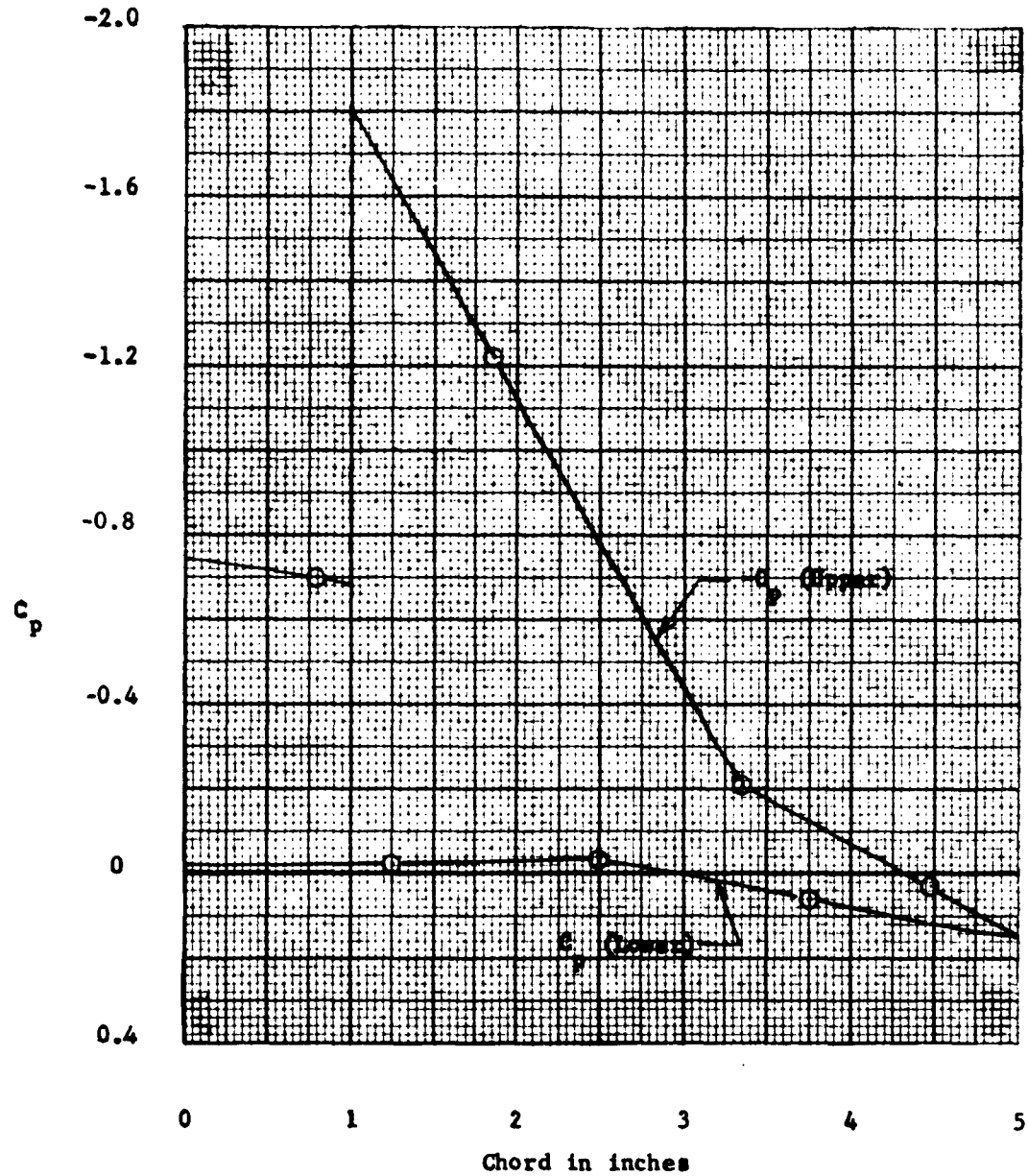

Figure 12 (Continued)
(e) p_j/p_∞ = 112; Slot B

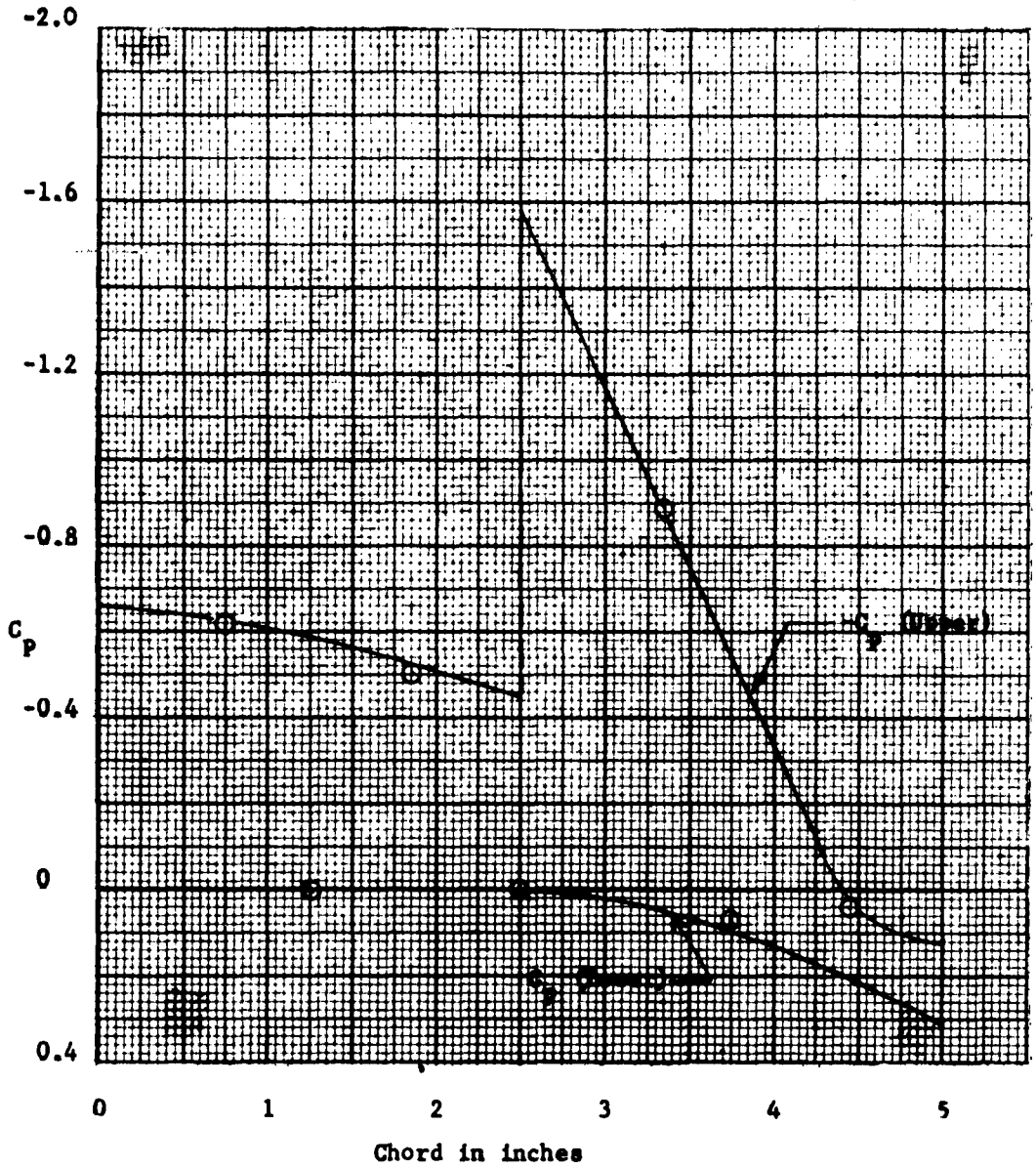

Figure 12 (Continued)
(f) p_j/p_∞ = 114; Slot C

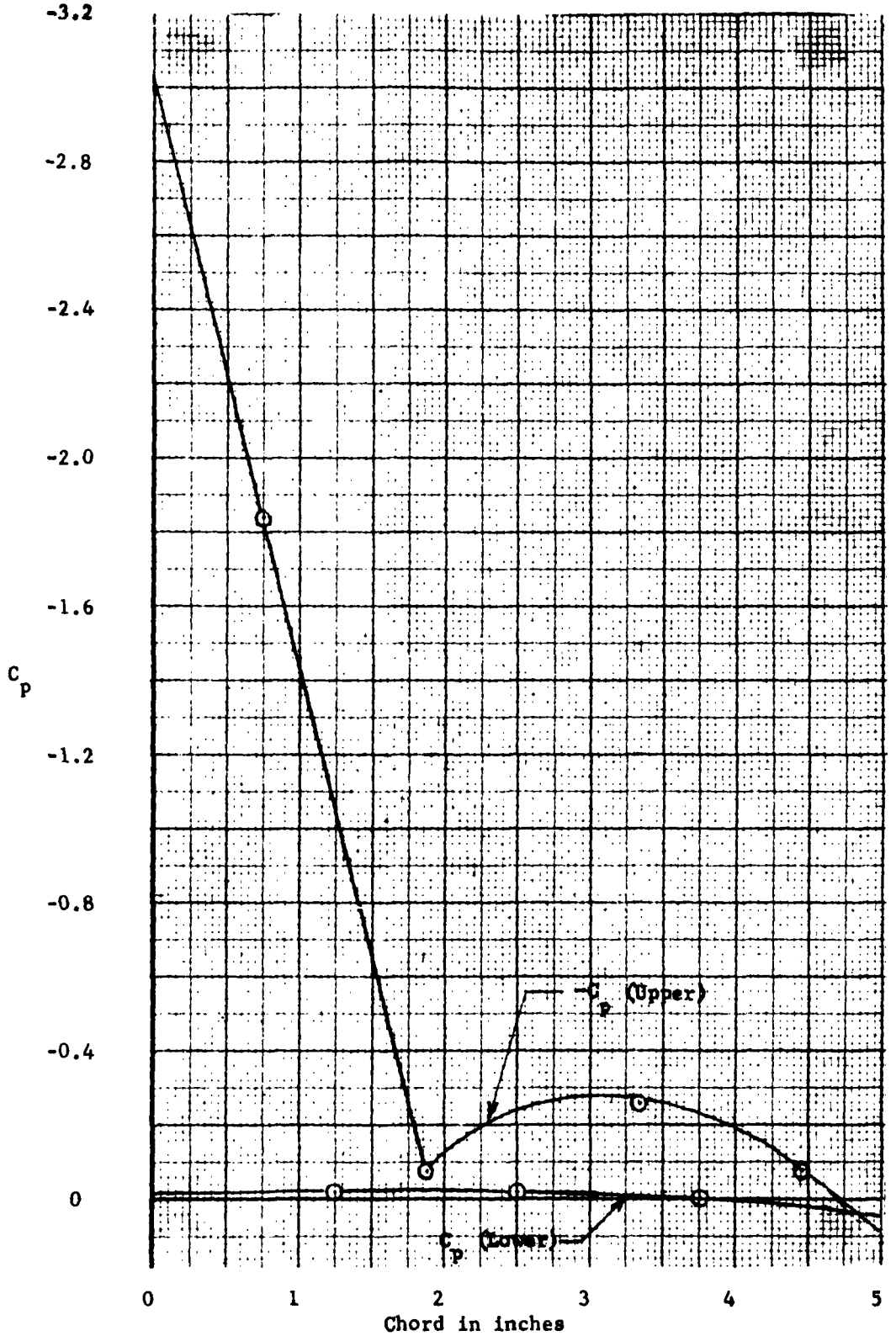

Figure 12 (Continued)

(g) p_j/p_∞ = 103; Slot A

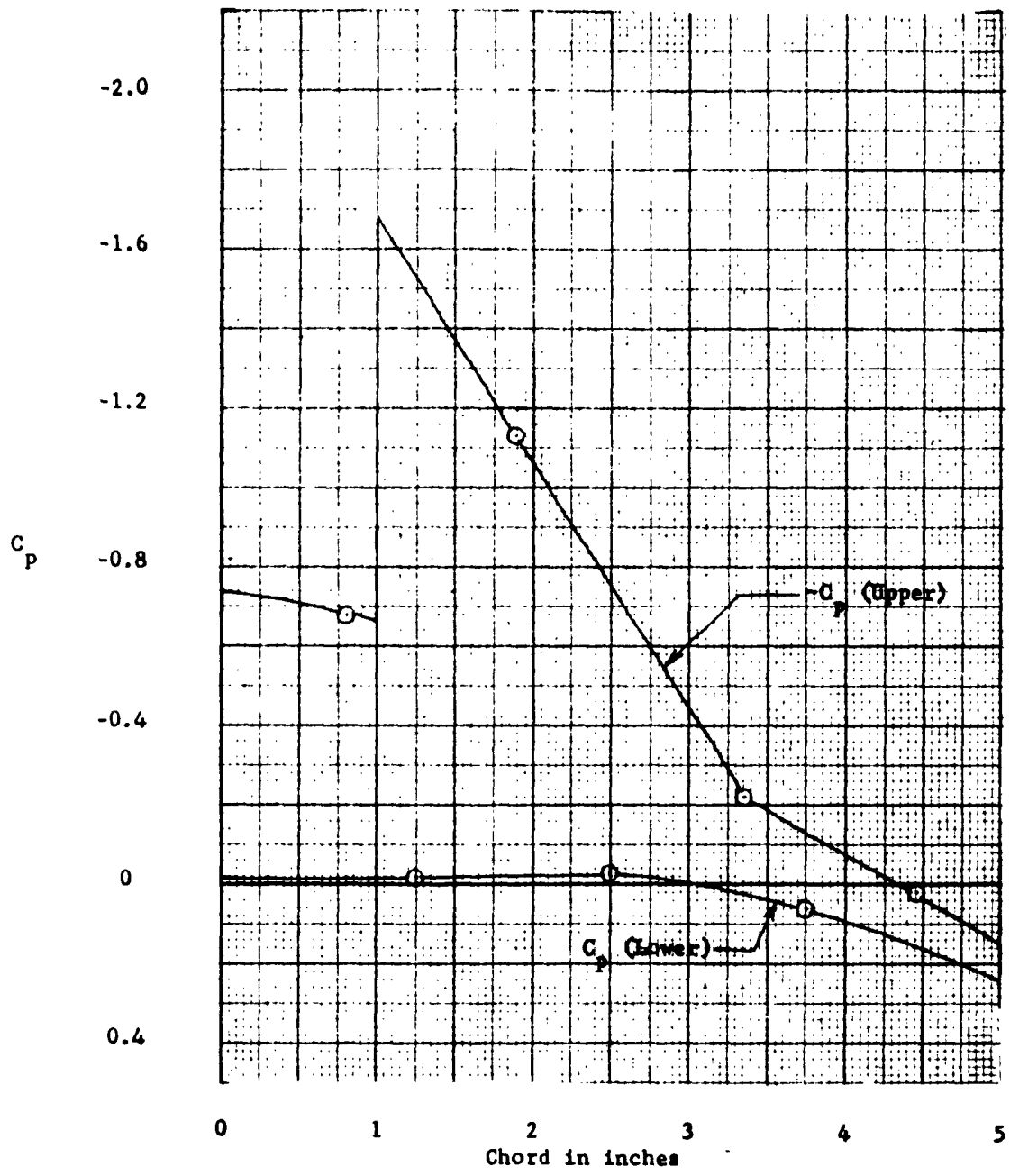

Figure 12 (Concluded)
(h) p_j/p_∞ = 101; Slot B

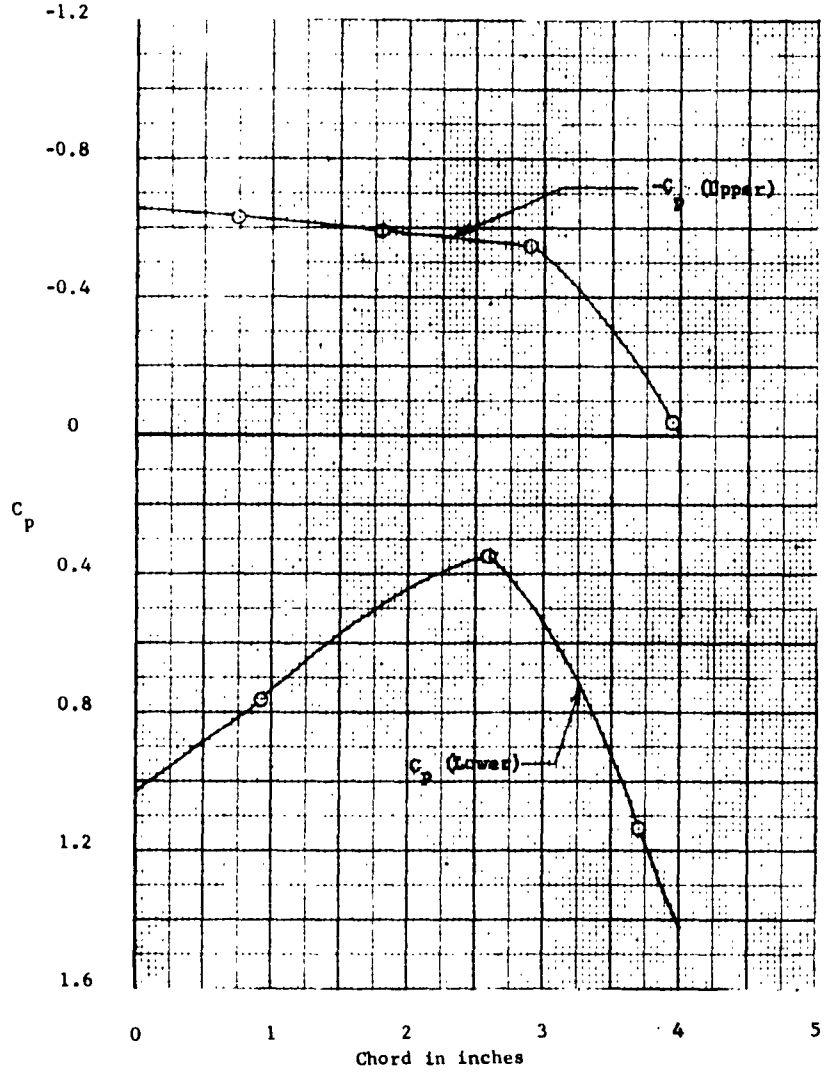

Figure 13 - Pressure Distribution on the Upper and Lower Surfaces of Model 2 (M = 3.73)

(a) $p_j/p_\infty = 0$

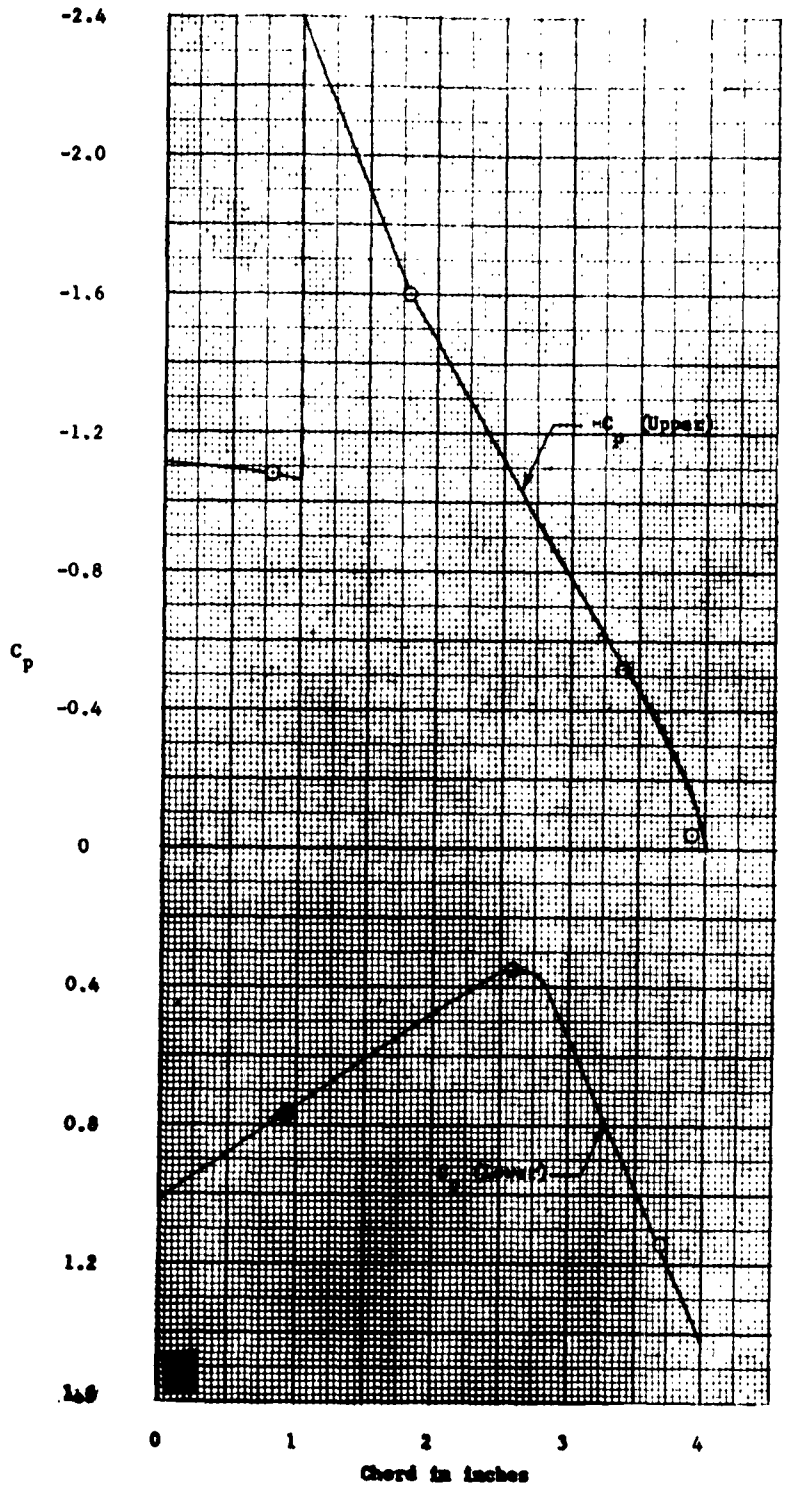

Figure 13 (Continued)

(b) p_j/p_∞ = 641, 712, and 784; Slot A

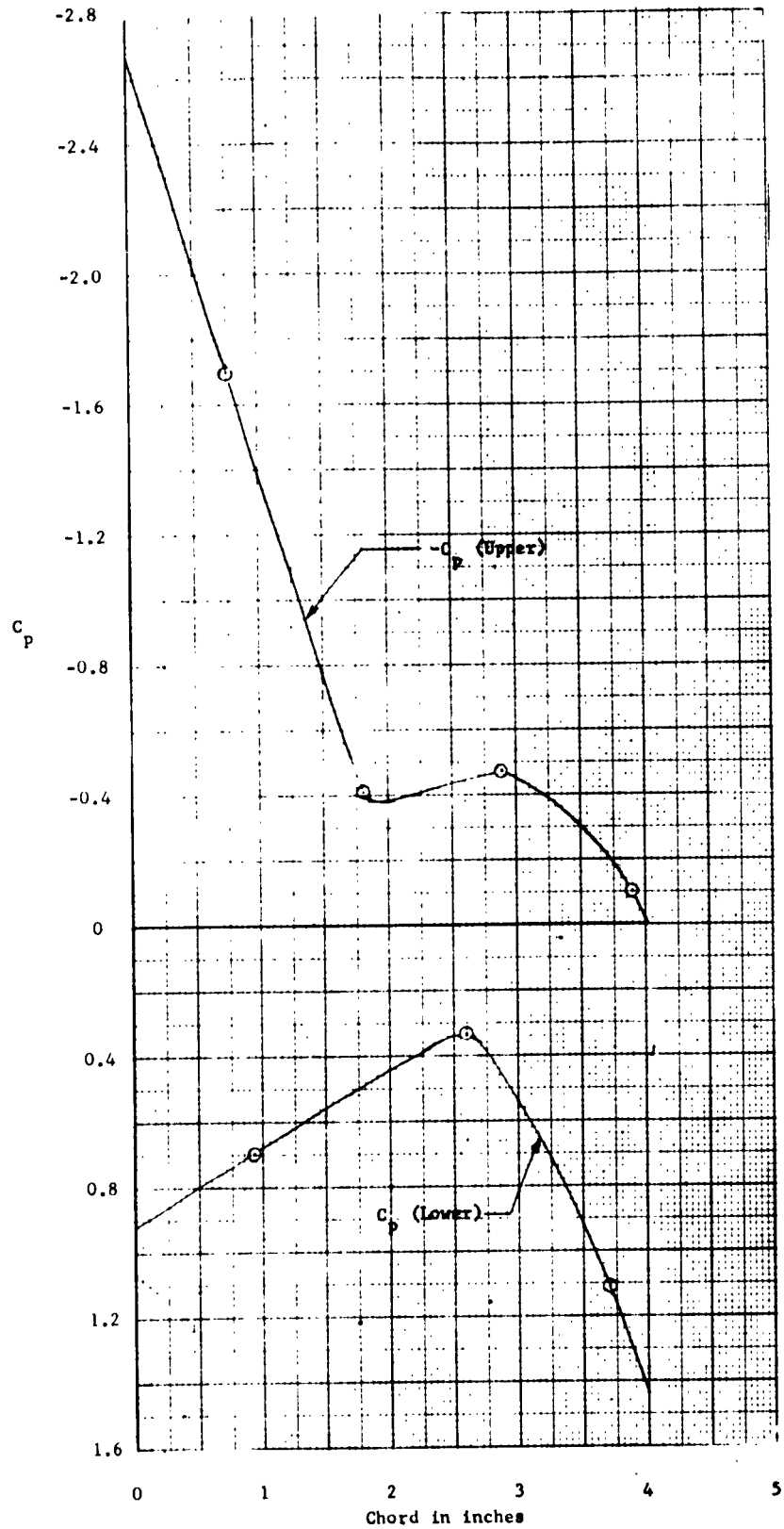

Figure 13 (Continued)

(c) p_j/p_∞ = 788; Slot B

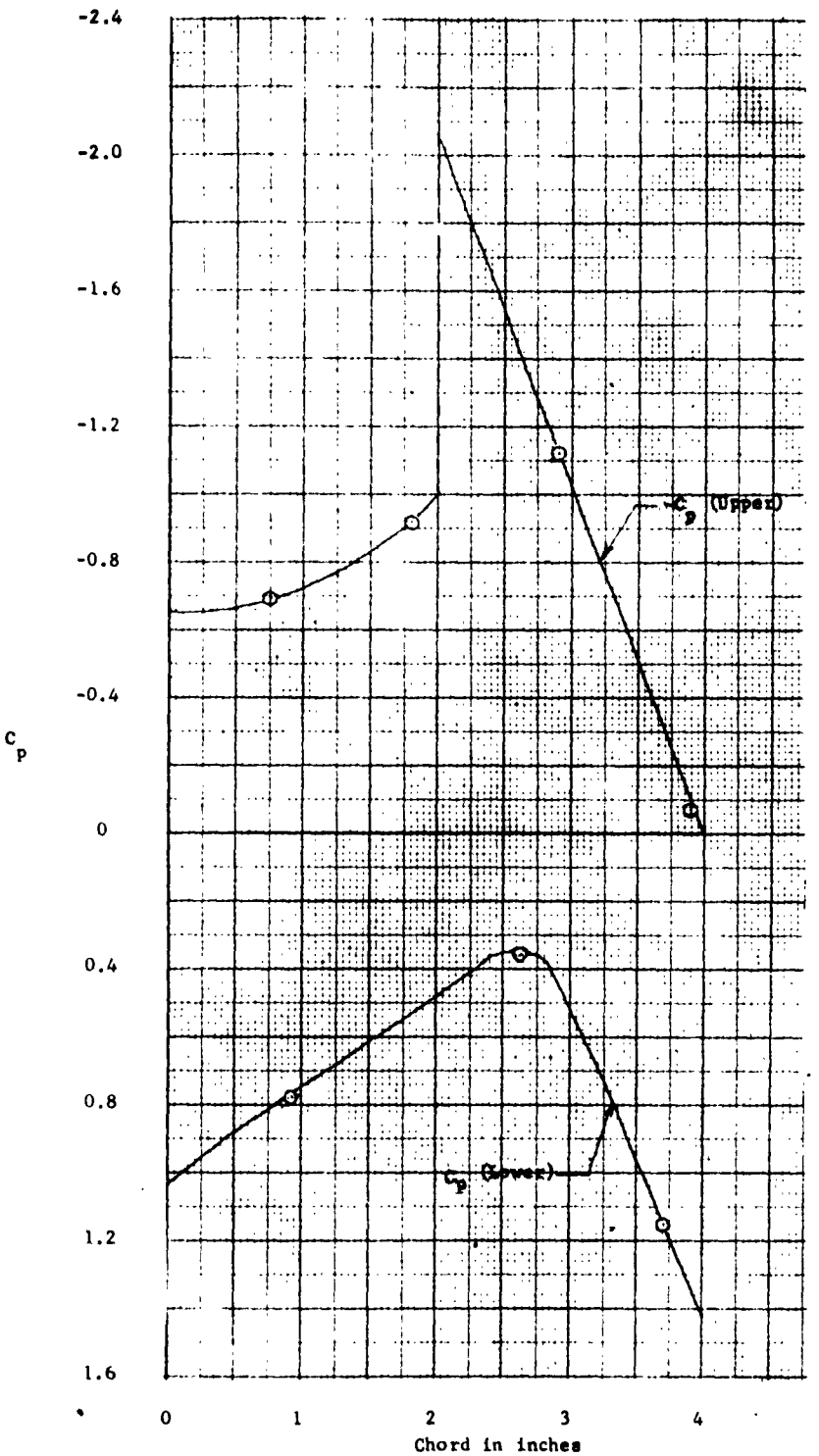

Figure 13 (Continued)
(d) p_j/p_∞ = 789; Slot C

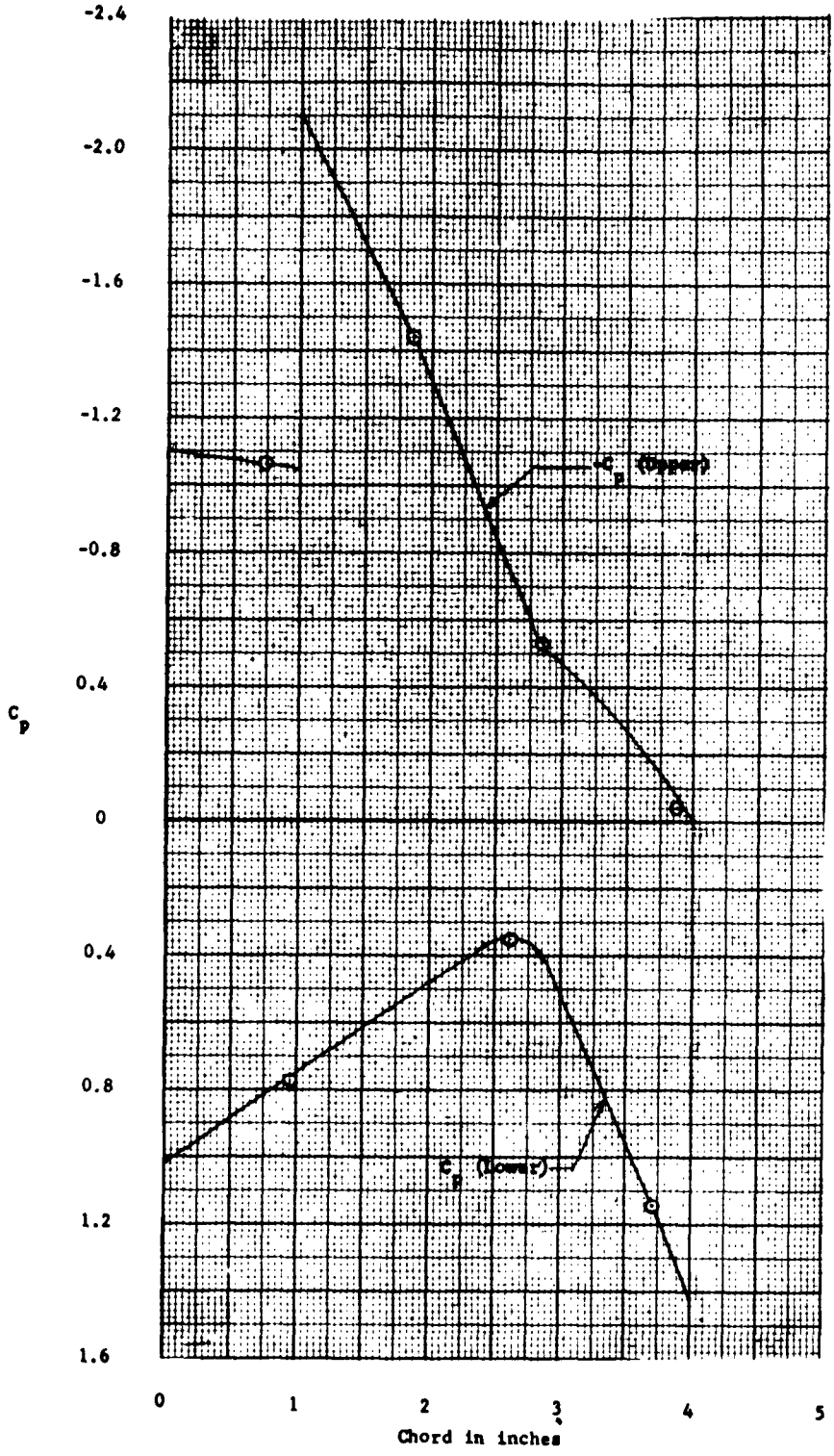

Figure 13 (Continued)
(e) P_j/P_∞ = 717; Slot B

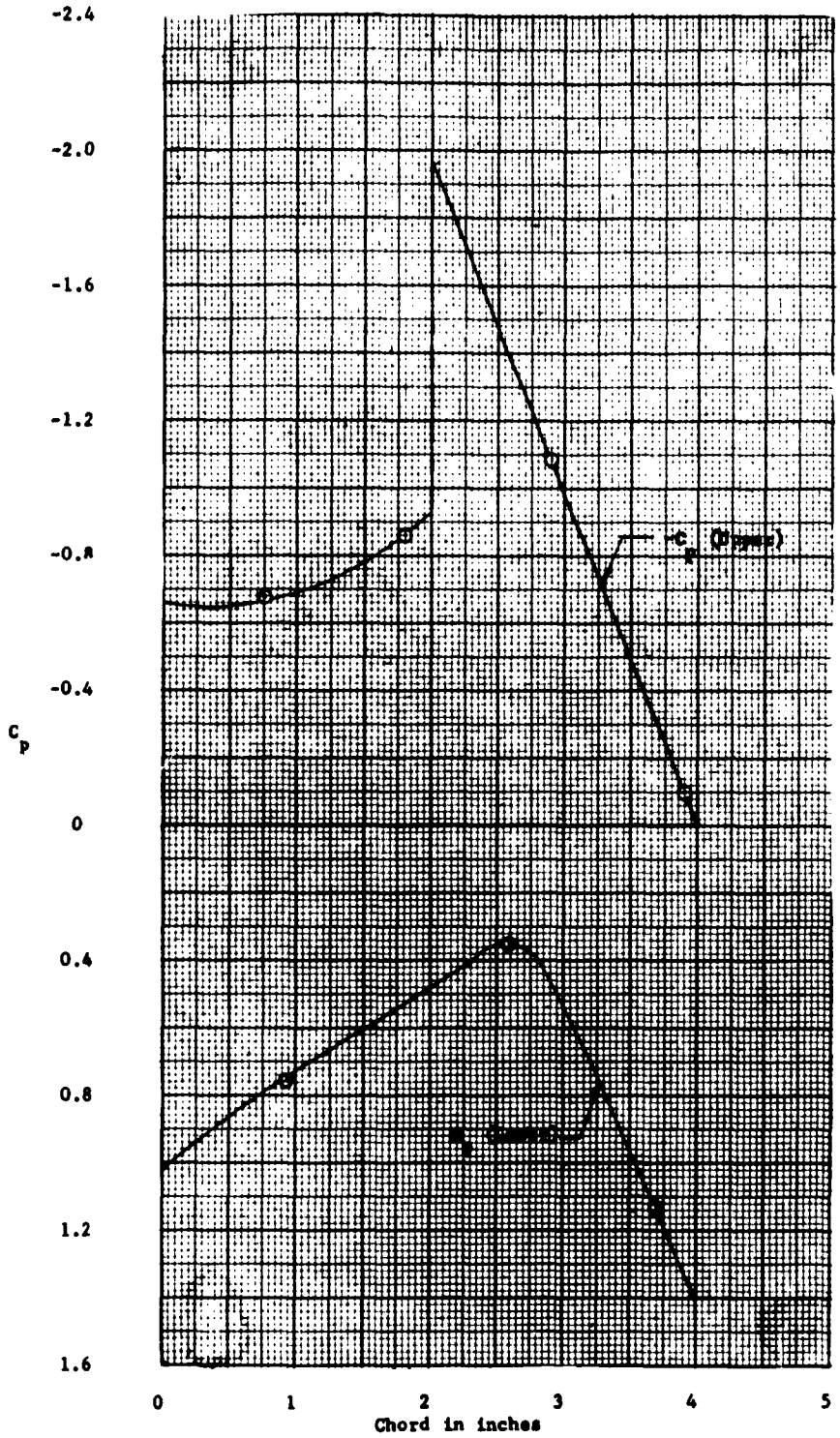

Figure 13 (Continued)
(f) p_j/p_∞ = 717, Slot C

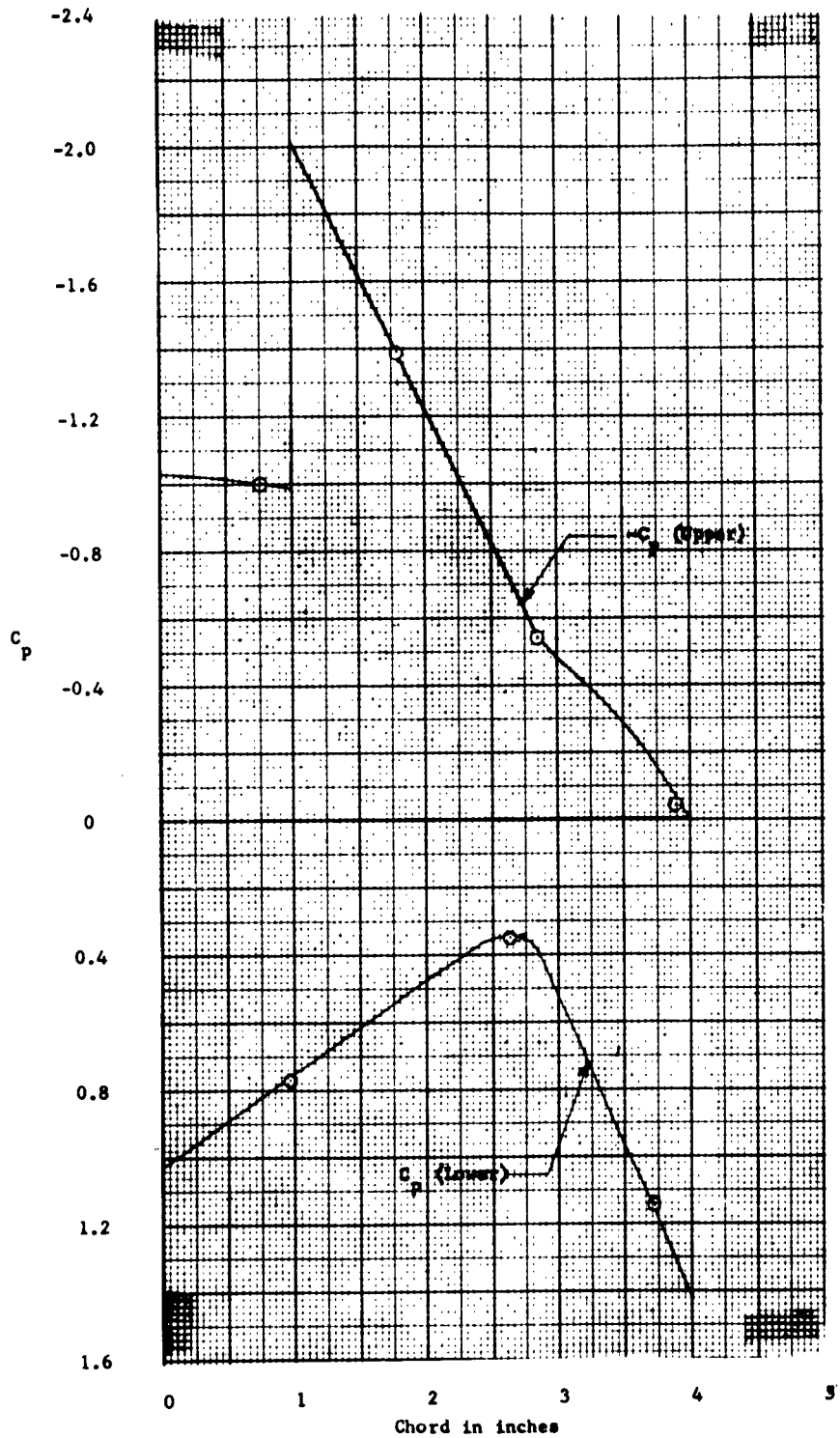

Figure 13 (Continued)
(g) $p_j/p_\infty = 645$; Slot B

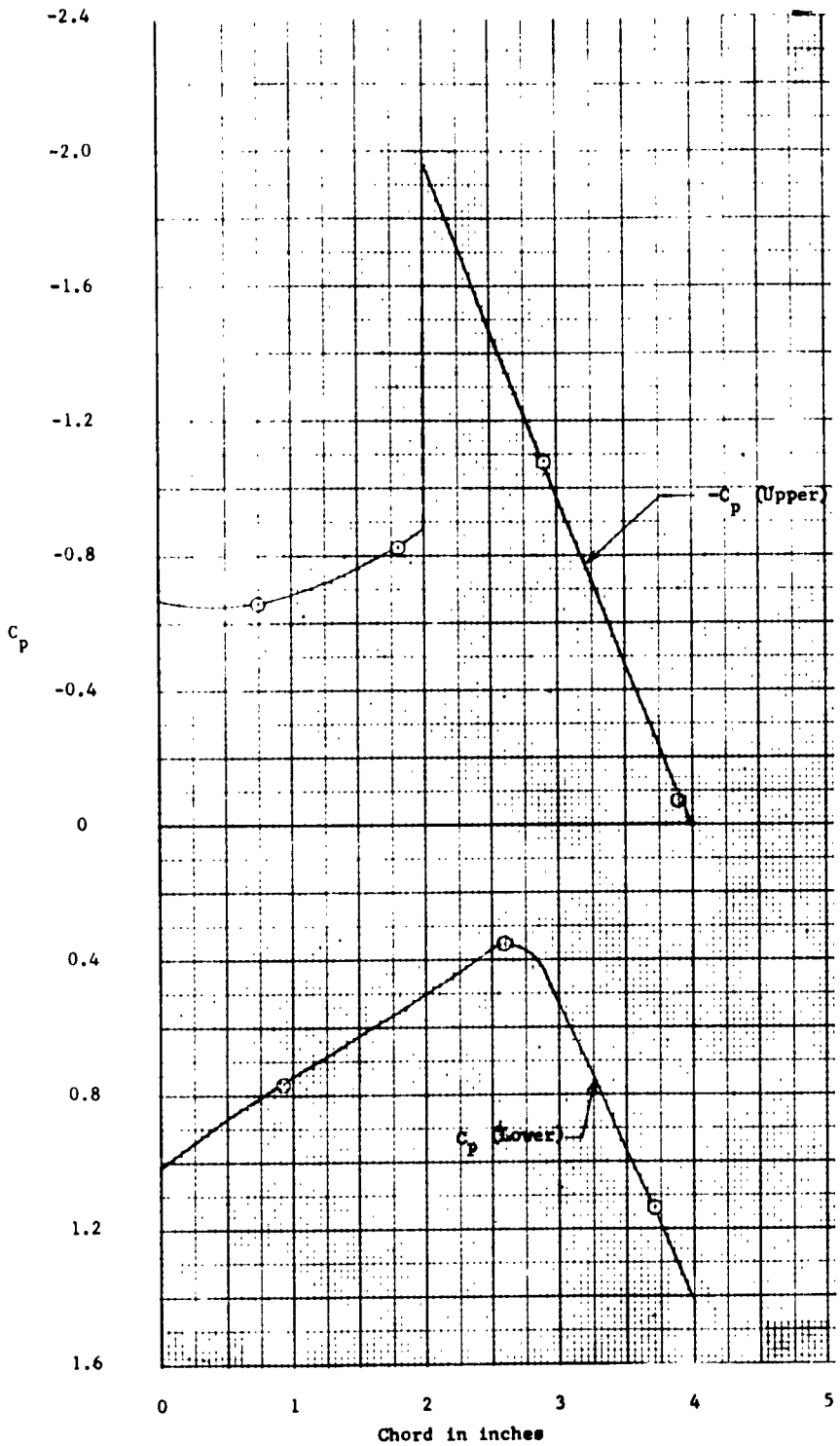

Figure 13 (Concluded)
(h) p_j/p_∞ =645; Slot C

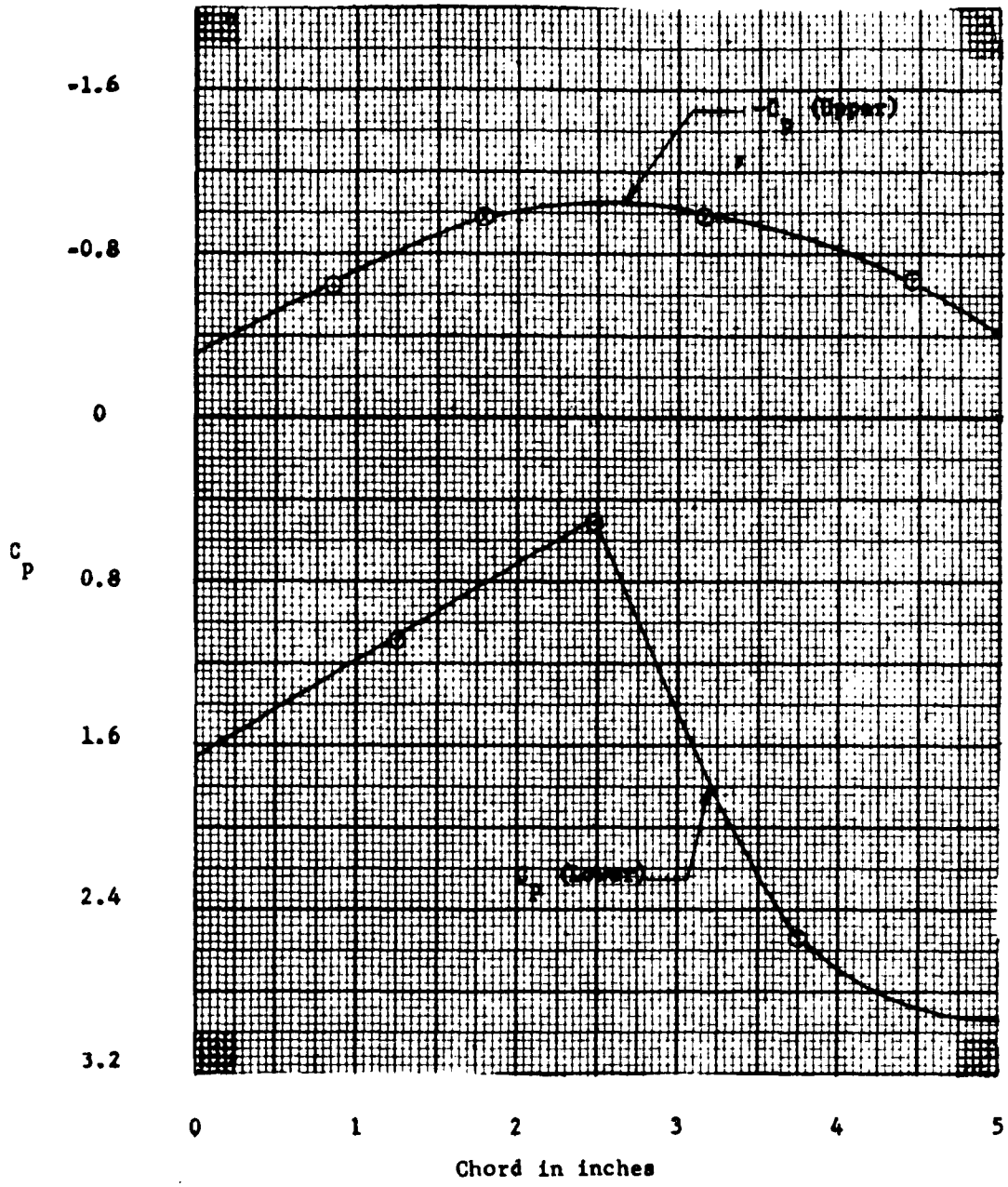

Figure 14 - Pressure Distribution on the Upper and Lower Surfaces of Model 3 (M = 4.50)

(a) $p_j/p_\infty = 0$

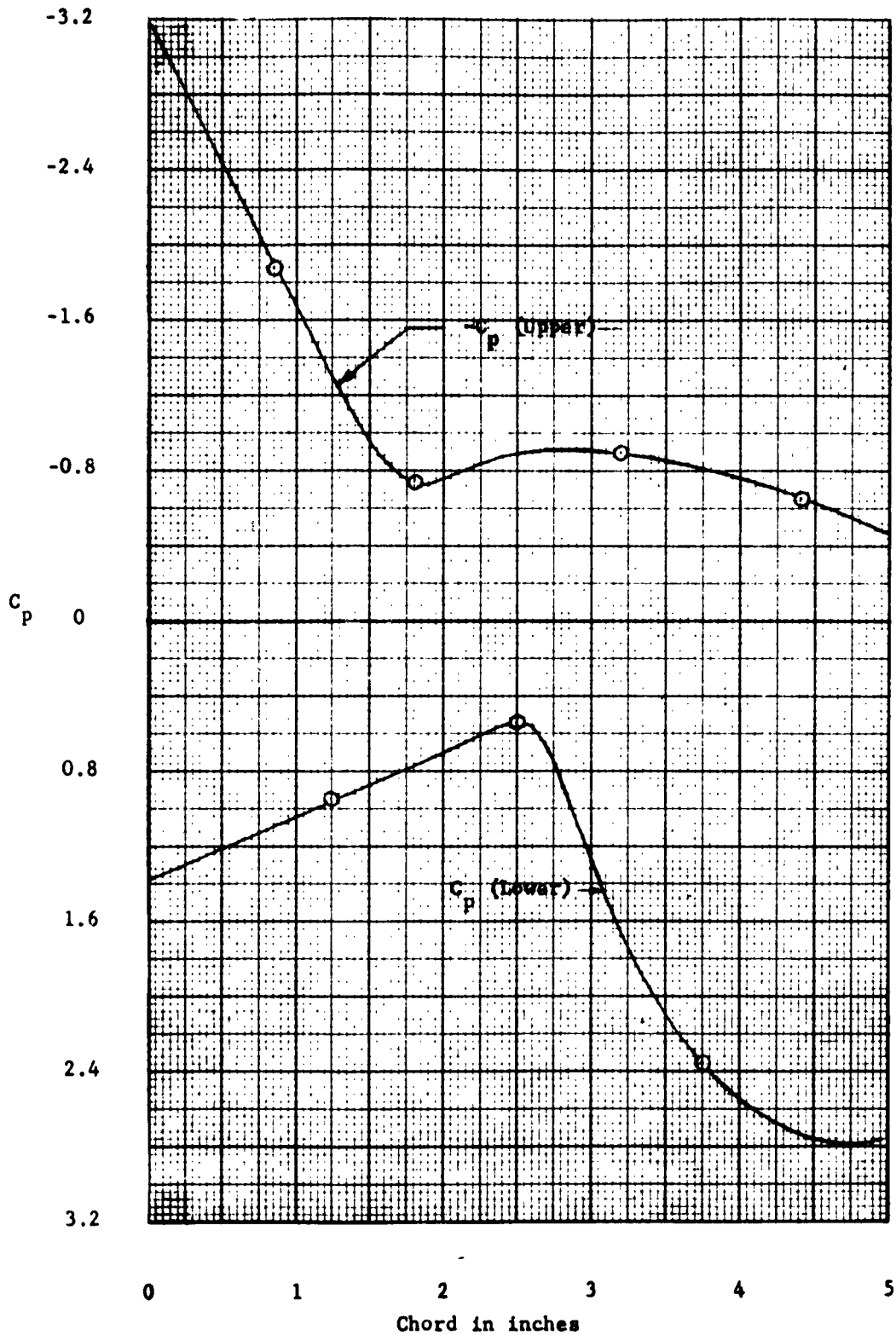

Figure 14 (Continued)

(b) p_j/p_∞ = 977 and 1174; Slot A

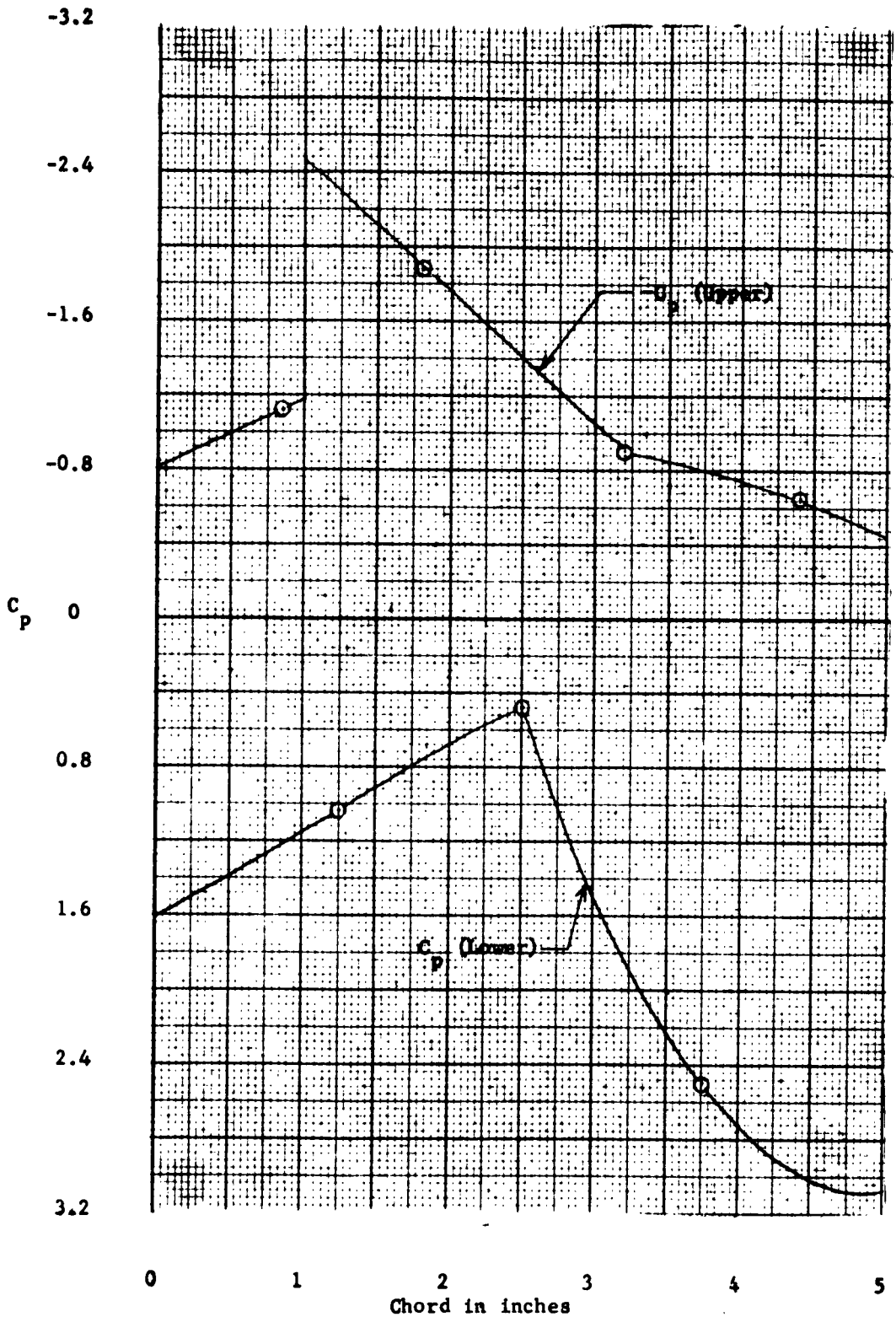

Figure 14 (Continued)
(c) p_j/p_∞ = 1153; Slot B

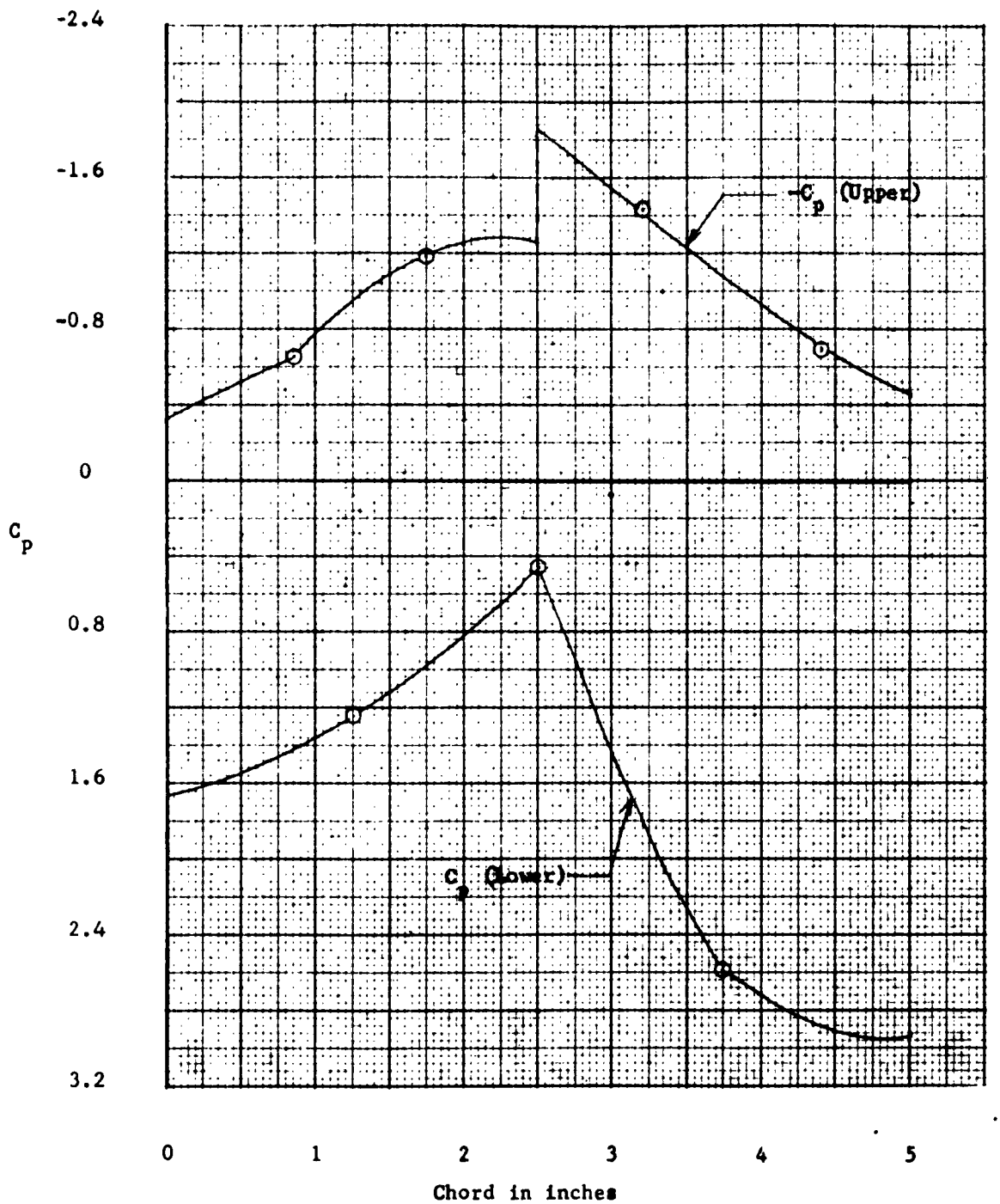

Figure 14 (Continued)
(d) p_j/p_∞ = 1171; Slot C

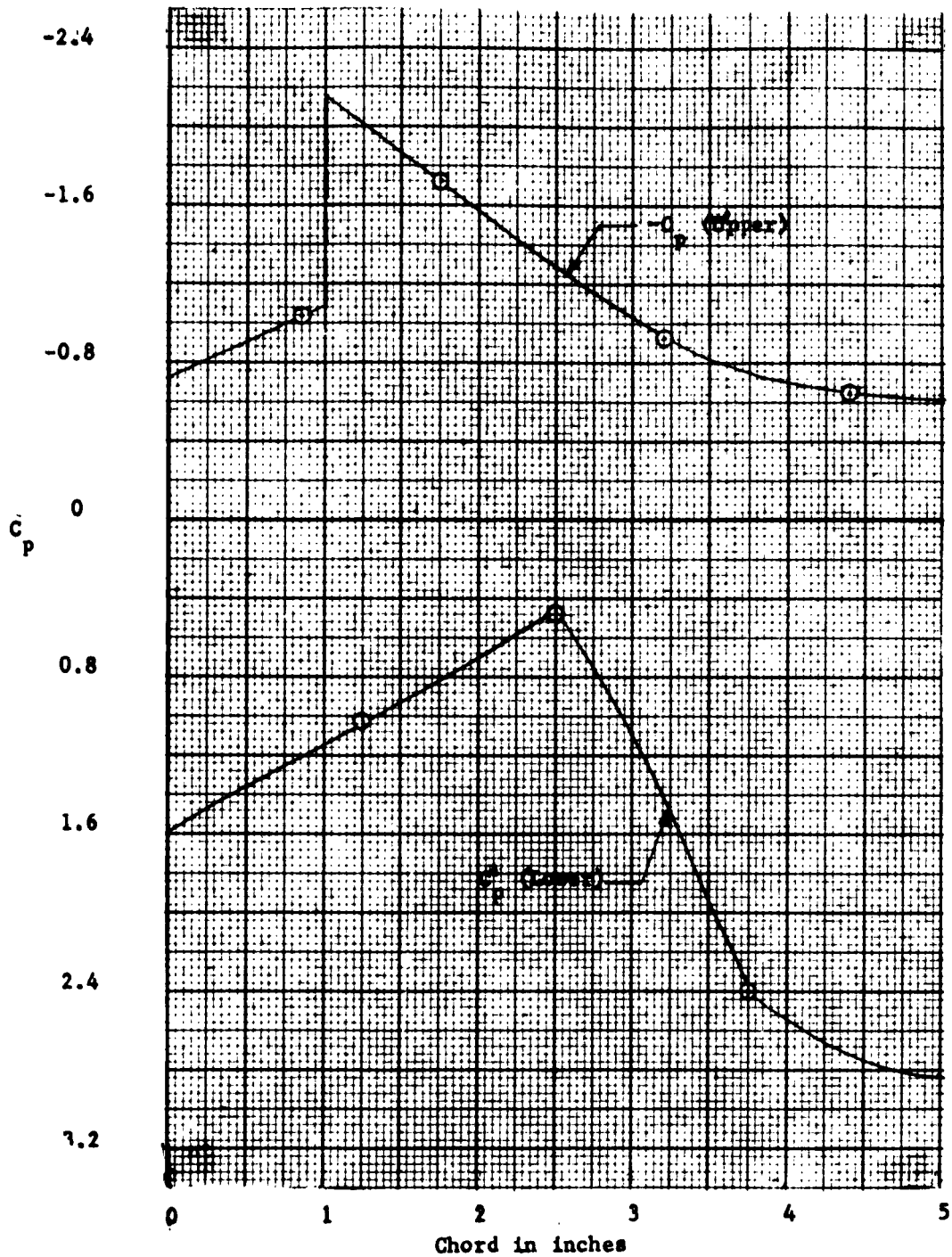

Figure 14 (Continued)

(e) p_j/p_∞ = 960; Slot B

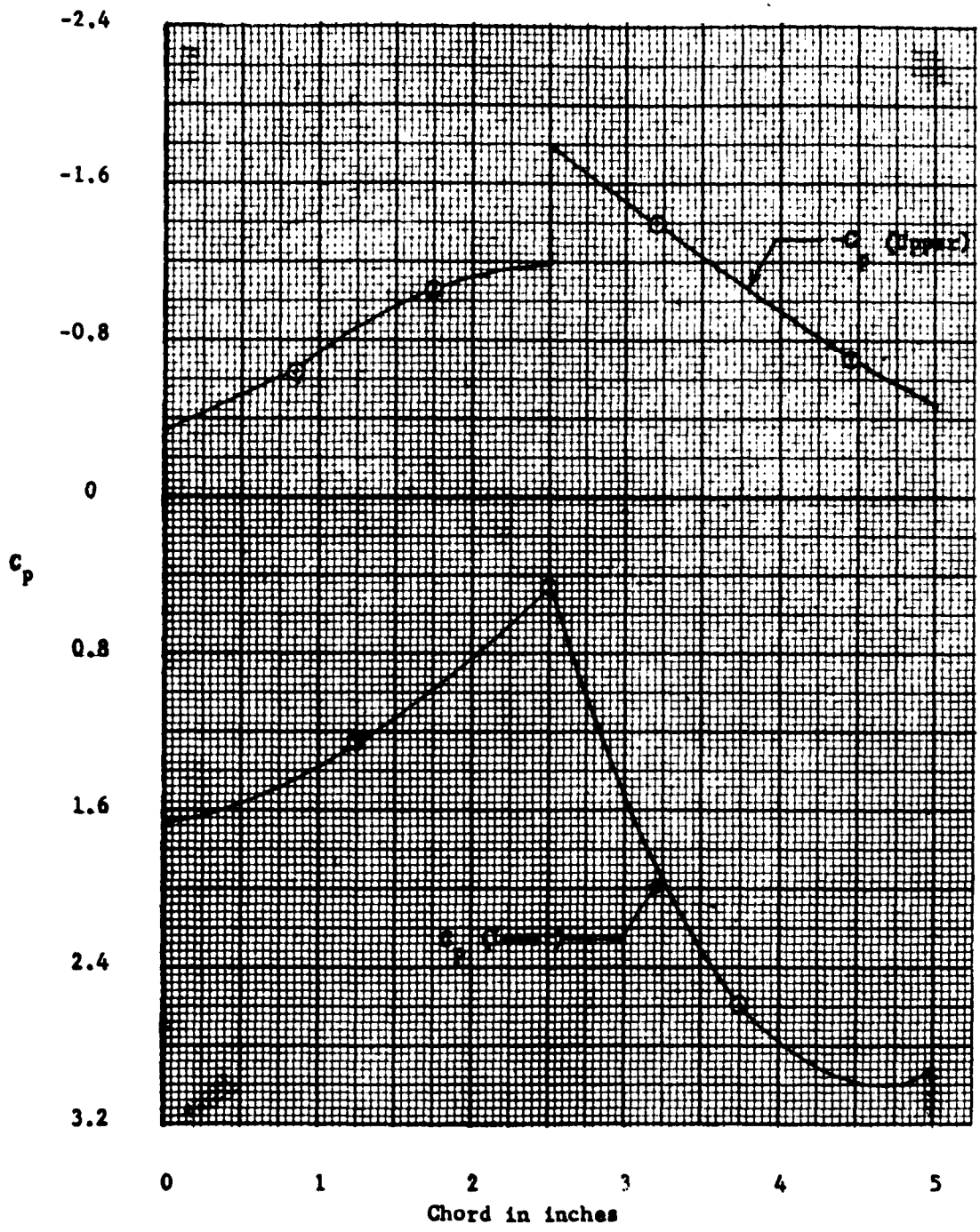

Figure 14 (Continued)

(f) p_j/p_∞ = 975; Slot C

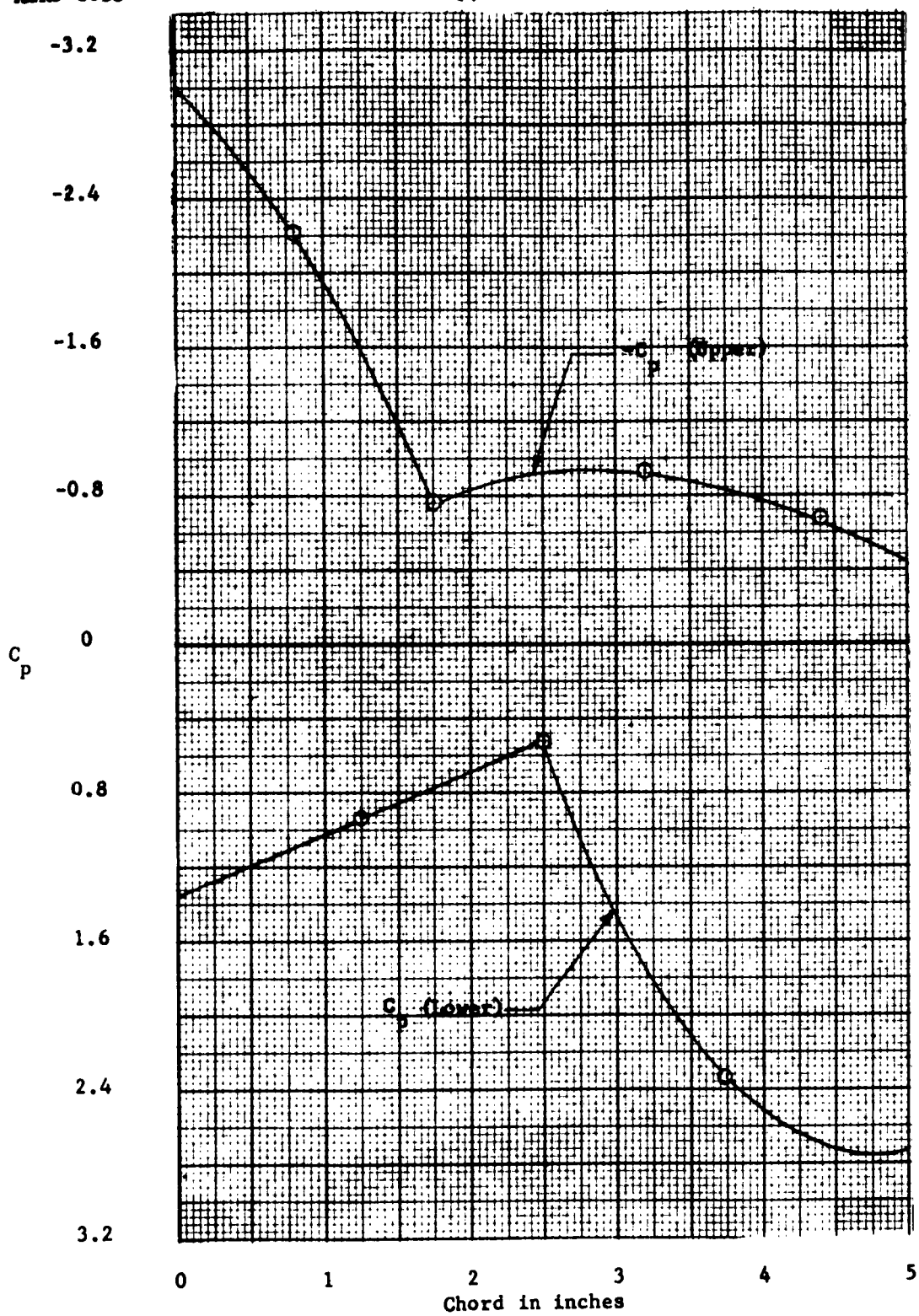

Figure 14 (Continued)

(g) p_j/p_∞ = 781; Slot A

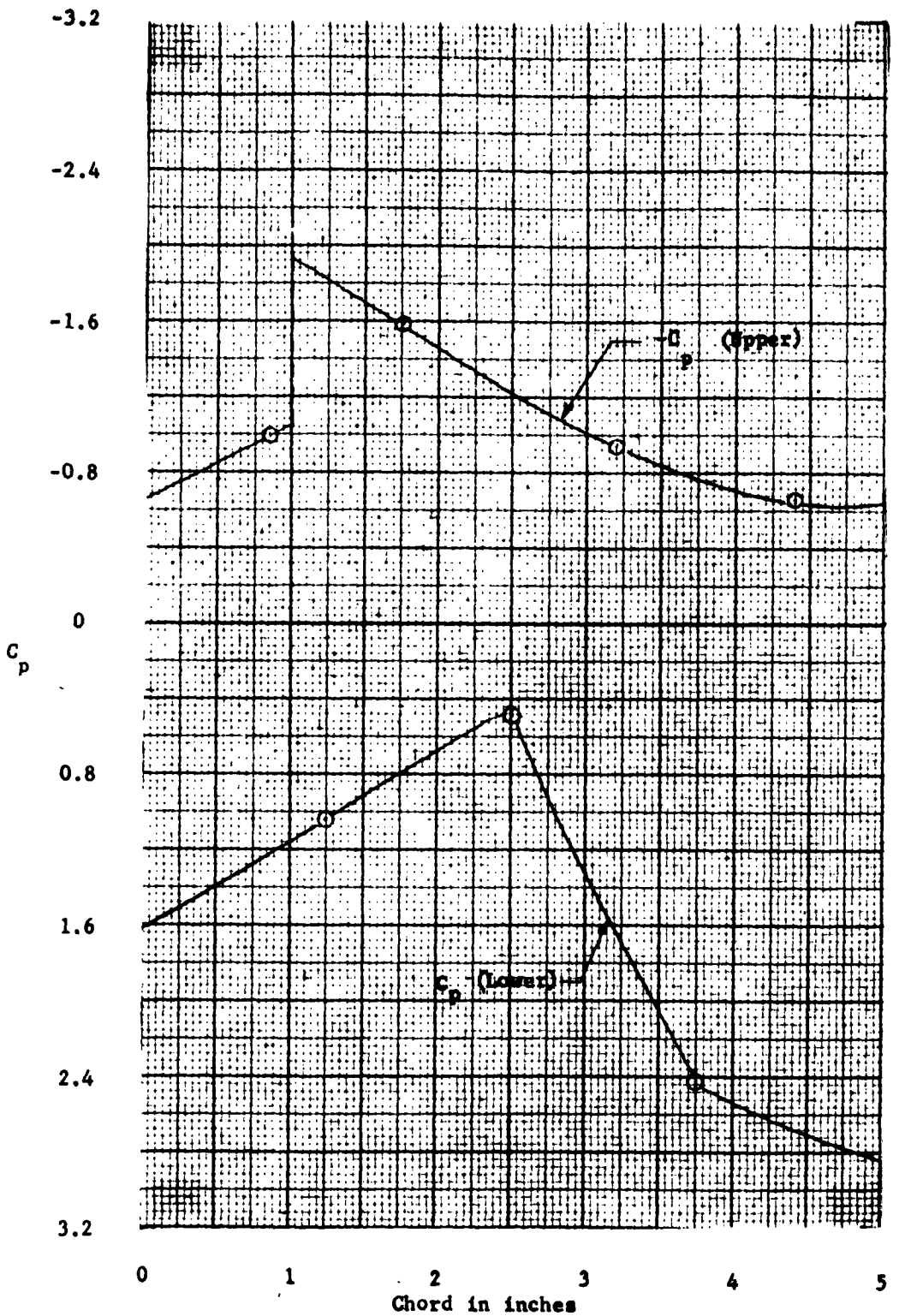

Figure 14 (Continued)

(h) p_j/p_∞ = 768; Slot B

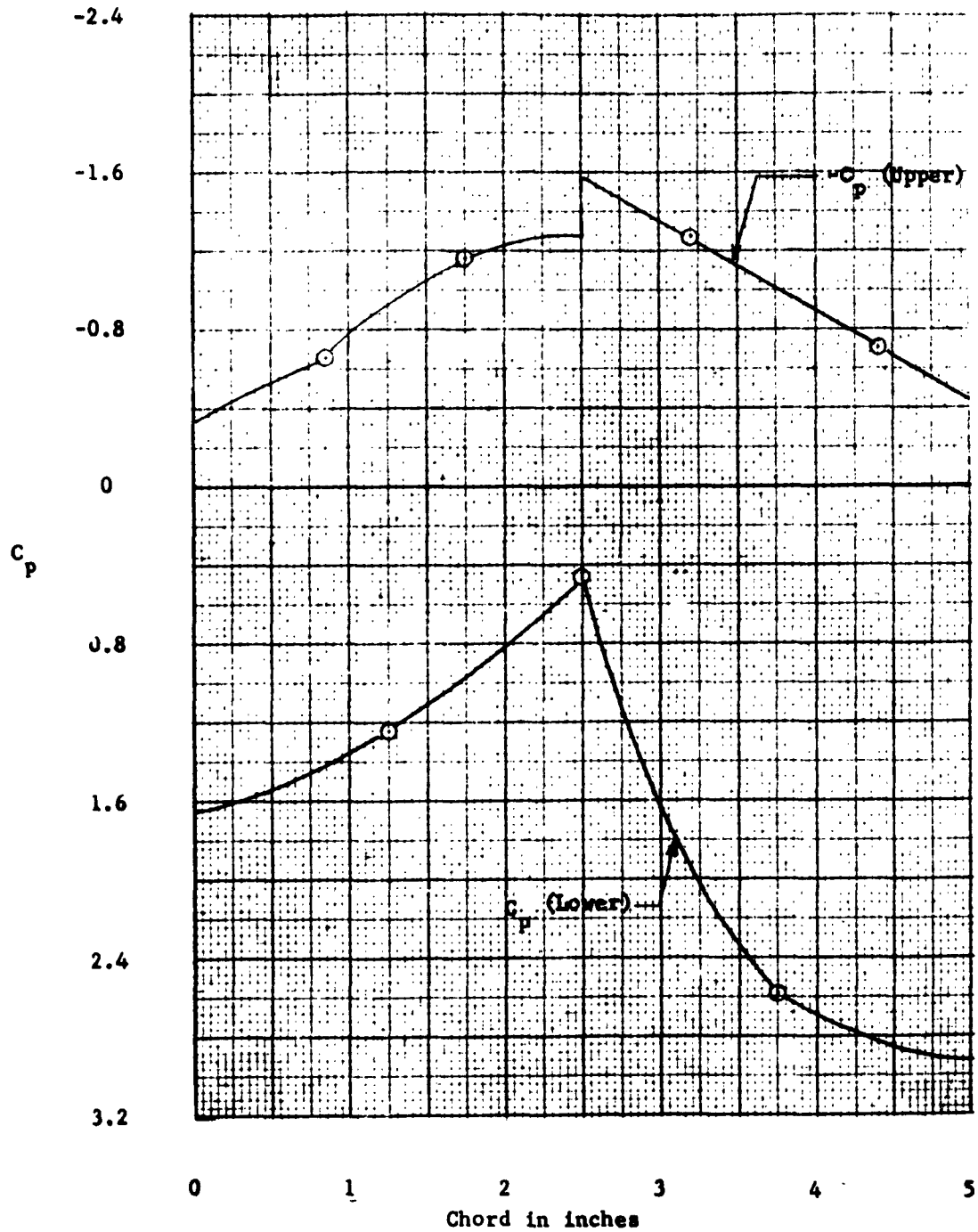

Figure 14 (Concluded)

(i) p_j/p_∞ = 779; Slot C

DISTRIBUTION LIST

Copies	
1	Chief, BUWEPS (RAAD-34) Navy Dept., Wash., D. C.
4	Chief, BUWEPS (DLI-3) Navy Dept., Wash., D. C.
10	ASTIA Arl., Va.
1	CDR, NATC (Dir., TPS) Patuxent River, Md.
1	CO, NADC Johnsville, Pa. (Attn: Tech. Lib.)
5	Scientific & Technical Information Facility Bethesda, Md. (Attn: NASA Rep. (S-AK/DL))

DTMB Aero Rpt 1053
David Taylor Model Basin
INTERACTION EFFECTS PRODUCED BY A SONIC JET EXHAUSTING FROM A CURVED TWO-DIMENSIONAL PLATE IN SUPERSONIC STREAM, by C. Carl Brindle and David W. Moxley, Jr. Wash., Apr 1963. [3]86 l. incl. illus [7]refs. (Aerodynamics Lab. Aero Rpt 1053. Aero Problem 650-088)

On covers [BuWeps] Problem Assignment 1-3a-14.

Tests made in 9½" supersonic tunnel at Mach 2.48, 3.73, and 4.50 to determine effects of sonic jet with various slot locations, blowing perpendicularly from curved two-dimensional plate. Model represents jet reaction controls near nose of supersonic vehicle. Normal forces created by interaction of exhausting jet and main stream obtained from pressure measurements on model. Data report.

JET CONTROLS
JETS--MIXING
PLATES, CURVED--PRESSURE DISTRIBUTION
INTERFERENCE, JET
SHOCK WAVES, DETACHED
BOUNDARY LAYER--SEPARATION
PHOTOGRAPHY, SCHLIEREN
SLOTS, BLOWING
BODIES--NORMAL FORCES
Brindle, Clayton Carl
Moxley, David W., Jr.
DTMB Aero Test B-88
BuWeps Prob Assigt 1-3a-14

DTMB Aero Rpt 1053
David Taylor Model Basin
INTERACTION EFFECTS PRODUCED BY A SONIC JET EXHAUSTING FROM A CURVED TWO-DIMENSIONAL PLATE IN SUPERSONIC STREAM, by C. Carl Brindle and David W. Moxley, Jr. Wash., Apr 1963. [3]86 l. incl. illus [7]refs. (Aerodynamics Lab. Aero Rpt 1053. Aero Problem 650-088)

On covers [BuWeps] Problem Assignment 1-3a-14.

Tests made in 9½" supersonic tunnel at Mach 2.48, 3.73, and 4.50 to determine effects of sonic jet with various slot locations, blowing perpendicularly from curved two-dimensional plate. Model represents jet reaction controls near nose of supersonic vehicle. Normal forces created by interaction of exhausting jet and main stream obtained from pressure measurements on model. Data report.

JET CONTROLS
JETS--MIXING
PLATES, CURVED--PRESSURE DISTRIBUTION
INTERFERENCE, JET
SHOCK WAVES, DETACHED
BOUNDARY LAYER--SEPARATION
PHOTOGRAPHY, SCHLIEREN
SLOTS, BLOWING
BODIES--NORMAL FORCES
Brindle, Clayton Carl
Moxley, David W., Jr.
DTMB Aero Test B-88
BuWeps Prob Assigt 1-3a-14

DTMB Aero Rpt 1053
David Taylor Model Basin
INTERACTION EFFECTS PRODUCED BY A SONIC JET EXHAUSTING FROM A CURVED TWO-DIMENSIONAL PLATE IN SUPERSONIC STREAM, by C. Carl Brindle and David W. Moxley, Jr. Wash., Apr 1963. [3]96 l. incl. illus [7]refs. (Aerodynamics Lab. Aero Rpt 1053. Aero Problem 650-088)

On covers [BuWeps] Problem Assignment 1-3a-14.

Tests made in 9½" supersonic tunnel at Mach 2.48, 3.73, and 4.50 to determine effects of sonic jet with various slot locations, blowing perpendicularly from curved two-dimensional plate. Model represents jet reaction controls near nose of supersonic vehicle. Normal forces created by interaction of exhausting jet and main stream obtained from pressure measurements on model. Data report.

JET CONTROLS
JETS--MIXING
PLATES, CURVED--PRESSURE DISTRIBUTION
INTERFERENCE, JET
SHOCK WAVES, DETACHED
BOUNDARY LAYER--SEPARATION
PHOTOGRAPHY, SCHLIEREN
SLOTS, BLOWING
BODIES--NORMAL FORCES
Brindle, Clayton Carl
Moxley, David W., Jr.
DTMB Aero Test B-88
BuWeps Prob Assigt 1-3a-14

DTMB Aero Rpt 1053
David Taylor Model Basin
INTERACTION EFFECTS PRODUCED BY A SONIC JET EXHAUSTING FROM A CURVED TWO-DIMENSIONAL PLATE IN SUPERSONIC STREAM, by C. Carl Brindle and David W. Moxley, Jr. Wash., Apr 1963. [3]86 l. incl. illus [7]refs. (Aerodynamics Lab. Aero Rpt 1053. Aero Problem 650-088)

On covers [BuWeps] Problem Assignment 1-3a-14.

Tests made in 9½" supersonic tunnel at Mach 2.48, 3.73, and 4.50 to determine effects of sonic jet with various slot locations, blowing perpendicularly from curved two-dimensional plate. Model represents jet reaction controls near nose of supersonic vehicle. Normal forces created by interaction of exhausting jet and main stream obtained from pressure measurements on model. Data report.

JET CONTROLS
JETS--MIXING
PLATES, CURVED--PRESSURE DISTRIBUTION
INTERFERENCE, JET
SHOCK WAVES, DETACHED
BOUNDARY LAYER--SEPARATION
PHOTOGRAPHY, SCHLIEREN
SLOTS, BLOWING
BODIES--NORMAL FORCES
Brindle, Clayton Carl
Moxley, David W., Jr.
DTMB Aero Test B-88
BuWeps Prob Assigt 1-3a-14